ISSN 0083-7903, 55 (Print)
ISSN 2538-1016; 55 (Online)

New Zealand Oceanographic Institute

Memoir No. 55

OCEANIC CIRCULATION OFF THE EAST COAST OF NEW ZEALAND

by

R.A. HEATH

1975

NEW ZEALAND

DEPARTMENT OF SCIENTIFIC AND INDUSTRIAL RESEARCH

OCEANIC CIRCULATION OFF THE EAST COAST OF NEW ZEALAND

by

R.A. Heath

New Zealand Oceanographic Institute

Memoir 55

Wellington

1975

Citation according to "World List of Scientific Periodicals" (4th edn)

Mem. N.Z. oceanogr. Inst. 55

ISSN 0083-7903

Received for Publication : August 1971

ISSN 0083 - 7903

A. R. SHEARER, GOVERNMENT PRINTER, WELLINGTON, NEW ZEALAND— 1975

CONTENTS

FIGURES

TABLES

OCEANIC CIRCULATION OFF THE EAST COAST OF NEW ZEALAND

by

R.A. Heath

ABSTRACT

The oceanic circulation off the east coast of New Zealand south of East Cape is examined mainly by the geostrophic method, other techniques being used where the geostrophic method is not applicable.

The East Cape Current is formed by part of the Subtropical eastward-flowing East Auckland Current being diverted southwards around East Cape by the bottom topography of the Ranfurly Bank, East Cape Ridge and Kermadec Trench. At about $41\frac{1}{2}^{\circ}$S, 178°E, the East Cape Current turns east then north, forming an anticyclonic eddy which has a radius of about 50-100 km and is developed to a depth of at least 1500 m.

Subtropical Water over the continental shelf and upper part of the continental slope off the south-east coast of the South Island meets the less saline Subantarctic Water further offshore on the slope in the Southland Front, a zone where the isolines of salinity, temperature and density slope downwards to the west. The water in this zone of large horizontal gradients, together with the coastal water further inshore, moves northwards as the Southland Current. The deeper water of the Southland Current is brought towards the surface in passing northwards through the Mernoo Gap at the western end of the Chatham Rise. Thus, at the surface the Southland Current is recognised south of the Rise by warm, saline water and north of the Rise by cool, low salinity water. Near Kaikoura part of the Southland Current turns offshore while the remainder continues northwards across Cook Strait and along the east coast of the North Island, before turning offshore near Cape Turnagain to combine with the East Cape Current. The offshore transport of the Southland Current near Kaikoura is increased when a small eddy, cast off from the East Cape Current, is present near Kaikoura. A new eddy is found about every two months and its formation appears to be closely linked with the circulation off the east coast of Australia.

In summer the current speeds off the east coast decrease with depth down to at least 1000 m whereas in winter they are nearly constant down to 300 m and decrease below this depth. This seasonal difference appears to be related to the development of the summer thermocline.

The Subtropical Convergence is situated along the Chatham Rise, which inhibits the southward movement of the East Cape Current. The seasonal change in the structure of this current is likely to be responsible for the slight southward movement of the Convergence which occurs in winter.

INTRODUCTION

Three currents* have been named off the east coast of New Zealand, East Cape, Southland and East Auckland Currents, but previous studies have considered these as separate entities while neglecting the continuity between them. The D'Urville Current, which enters Cook Strait from the west, also has some influence on the East Coast circulation. In this paper an examination is made of the East Cape Current followed by an analysis of the interaction between the East Cape, Southland and D'Urville Currents. The geographical extent of these three currents is shown in Fig. 1. An account of previous work on the individual currents follows.

*The term Canterbury Current has been used to define the northwards coastal flow north of Banks Peninsula, but this flow has been shown to be continuous with the Southland Current, and it has been suggested (Heath 1972a) that the term Canterbury Current be withdrawn and the term Southland Current be used for all the northward flow along the east coast of New Zealand.

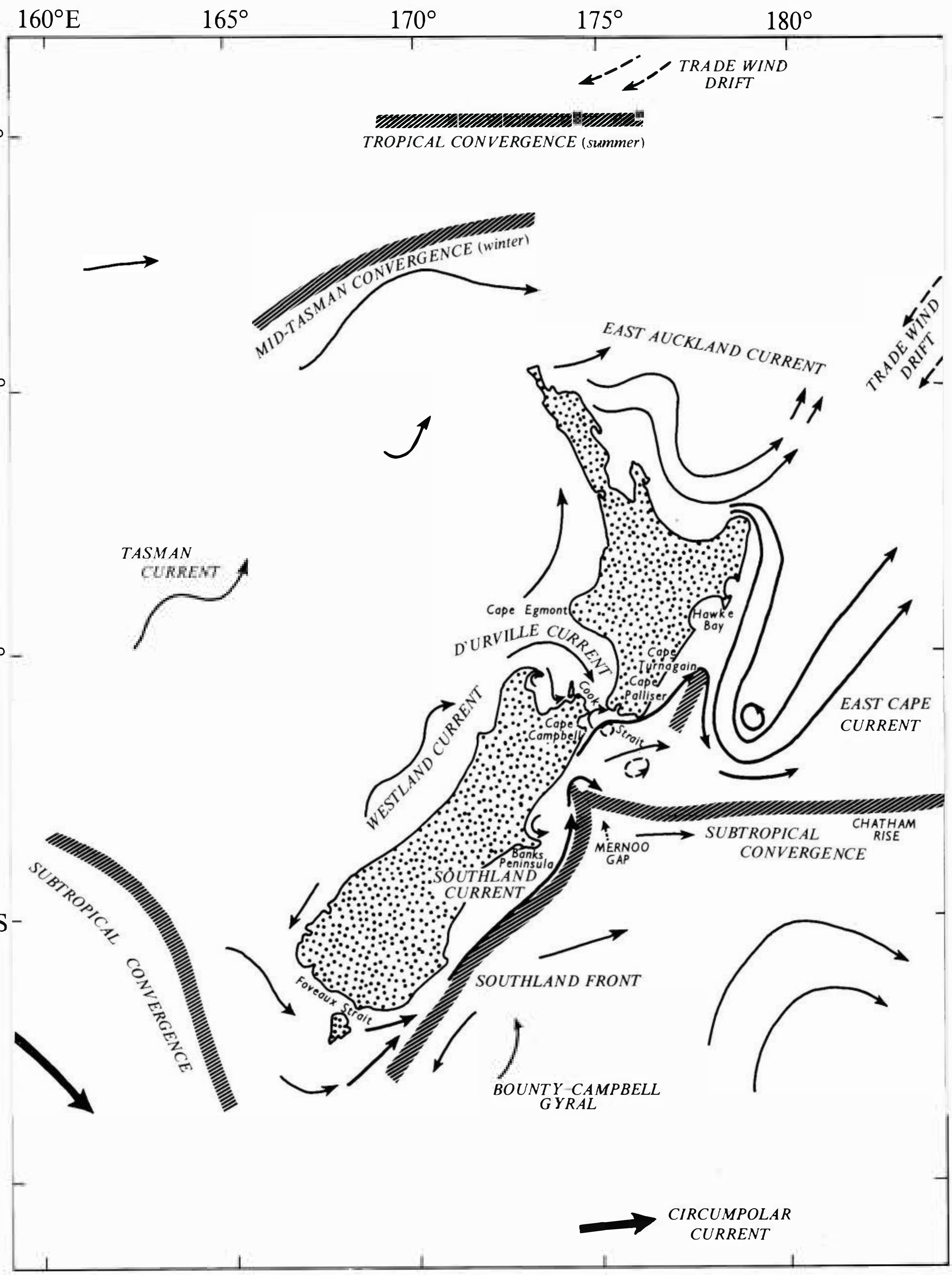

Fig. 1. Ocean currents around New Zealand as shown by Heath (1973).

EAST CAPE CURRENT

The presence of a surface tongue of Subtropical Water extending southwards along the east coast of the North Island was first reported by Fleming (1952) who assumed this feature indicated a southward movement of waters which he named the East Cape Current. Subsequent work off the east coast of New Zealand (Sdubbundhit and Gilmour 1964; Garner 1967a; Heath 1968) showed that seawards of the 1000 m isobath (approx.) the geostrophic current flows southwards down the east coast of the North Island to approximately the latitude of Cape Palliser where it turns north-eastwards.

The exact connection between the East Cape Current and the warm surface tongue has not previously been examined but it would be expected that the geostrophic currents create a warm tongue in the vertical water column by adjusting the mass field.

The possible origin of the water in the East Cape Current has been examined by Ridgway (1970a) who concluded that (anticyclonic) eddies are shed off from the main eastward flow of the East Auckland Current (Barker and Kibblewhite 1965) past East Cape.

EAST AUCKLAND CURRENT

Brodie (1960) found a southeasterly surface drift along the east coast of the North Island between North Cape and East Cape and named it the East Auckland Current. The surface geostrophic currents relative to 1000 decibars also show a general easterly movement in this area (Garner 1969).

SOUTHLAND CURRENT

Garner's (1961) view of the Southland Current as a branch of the 'Tasman Current' which flows eastwards through Foveaux Strait into the surface water off the Otago coast was supported by Brodie (1960) who found that drift cards released on the west coast of the South Island, south of latitude 45°S, were recovered on the east coast of the South Island. Burling (1961) suggested that the Southland Current originates southwest of Stewart Island and consists mainly of water from the Subtropical Convergence region with some admixture of Australasian Subantarctic Water. Thus water which passes through a wide range of latitude west of New Zealand may flow northwards in the Southland Current.

The mainly subtropical nature of the Southland Current in Foveaux Strait has been confirmed by Houtman (1966). Jillett (1969) showed that off the Otago Peninsula, the Subtropical Water in the Southland Current is located over the continental shelf and slope, bounded on the coastal side by low salinity shallow coastal water and on the seaward side by low salinity Subantarctic Surface Water.

The continuity of flow in the Southland Current on the east coast of New Zealand has been studied by Heath (1972a) whose analysis can be summarised as follows. The warm Subtropical Water on the continental shelf and upper part of the continental slope south of latitude 41°30'S on the east coast of the South Island, New Zealand meets the cooler, less saline Subantarctic Water in the Southland Front. Isolines slope sharply downwards towards the west in the Southland Front indicating that both the Subtropical and Subantarctic Water flows northwards as the Southland Current. South of Banks Peninsula the Southland Current is recognised at the surface by mainly warm, saline Subtropical Water but, in its passage northward through the western side of the Mernoo Gap, these characteristics are altered by cool, low-salinity Subantarctic Water being brought closer to the surface. North of Banks Peninsula the Southland Current is most easily recognised by cool, low salinity water. Where this cool, low salinity water meets the warmer, more saline water offshore, which is derived from the East Cape Current, the northern extension of the Subtropical Convergence is formed. The Southland Front extends northwards through the western side of the Mernoo Gap towards Kaikoura. The Southland Current branches near Kaikoura - one component meanders eastwards to combine with the East Cape Current; a second component diverges north-eastwards immediately north of Kaikoura, sweeping across the southern end of Cook Strait and continues northward along the east coast of the North Island; a further component flows northwards along the coast and enters the southwestern side of Cook Strait around Cape Campbell. The cool, low salinity water entering Cook Strait near Cape Campbell is mainly confined to the continental shelf. This water mixes with both the warmer, more saline surface and sub-surface Subtropical Water of the D'Urville Current which flows into Cook Strait from the north, and with the water in the Cook Strait Canyon which has its origin in the East Cape Current (Heath 1971). Mixed water derived from all three currents travels eastwards across Cook Strait and around Cape Palliser to meet the water of the Southland Current that has travelled north-eastwards from near Cape Campbell. In its passage northwards the water in the eastern margin of the Southland Current continually mixes with the water in the western margin of the East Cape Current and the transport of the Southland Current is generally offshore near Cape Turnagain (Heath 1972a).

D'URVILLE CURRENT

Brodie (1960) showed that there was a general surface drift of water from the west coast of the South Island into northern Cook Strait which he named the D'Urville Current. Heath (1969) found that the maximum average speed along drift card trajectories in the D'Urville Current was three-quarters of a knot ($0.39\ m\ s^{-1}$).

OBSERVATIONS

The present analysis is based mainly on temperature/salinity/depth data collected on three separate hydrological cruises. Some of these data have already been used in analyses of different features of the circulation (e.g. Heath 1971, 1972a, b) but the bulk are presented here with a synthesis of the circulation off the east coast.

Between 19 September and 11 October 1967, 87 hydrological stations were occupied in the region

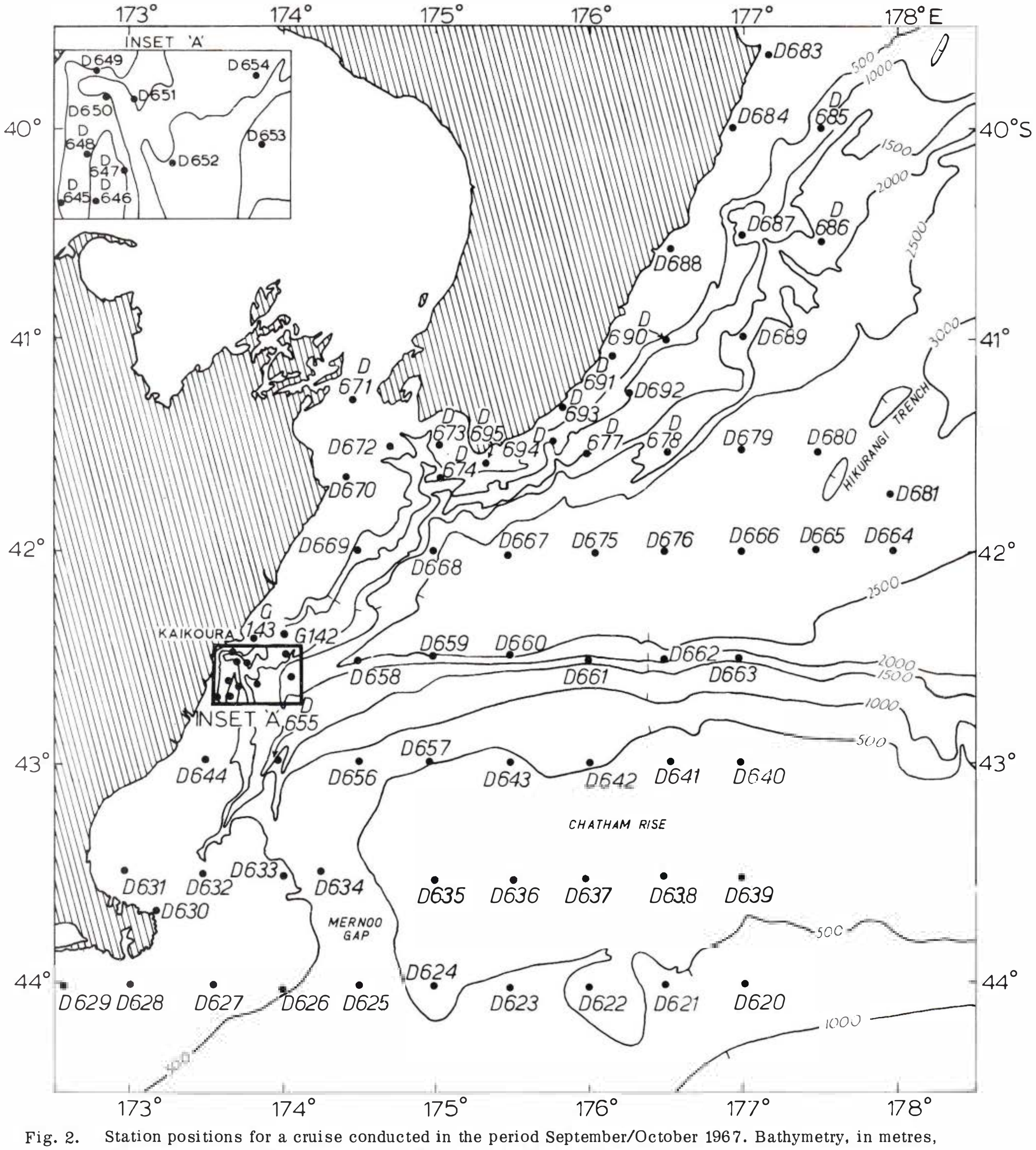

Fig. 2. Station positions for a cruise conducted in the period September/October 1967. Bathymetry, in metres, of the survey area from Lawrence (1967) (Fig. 1 of Heath 1972a).

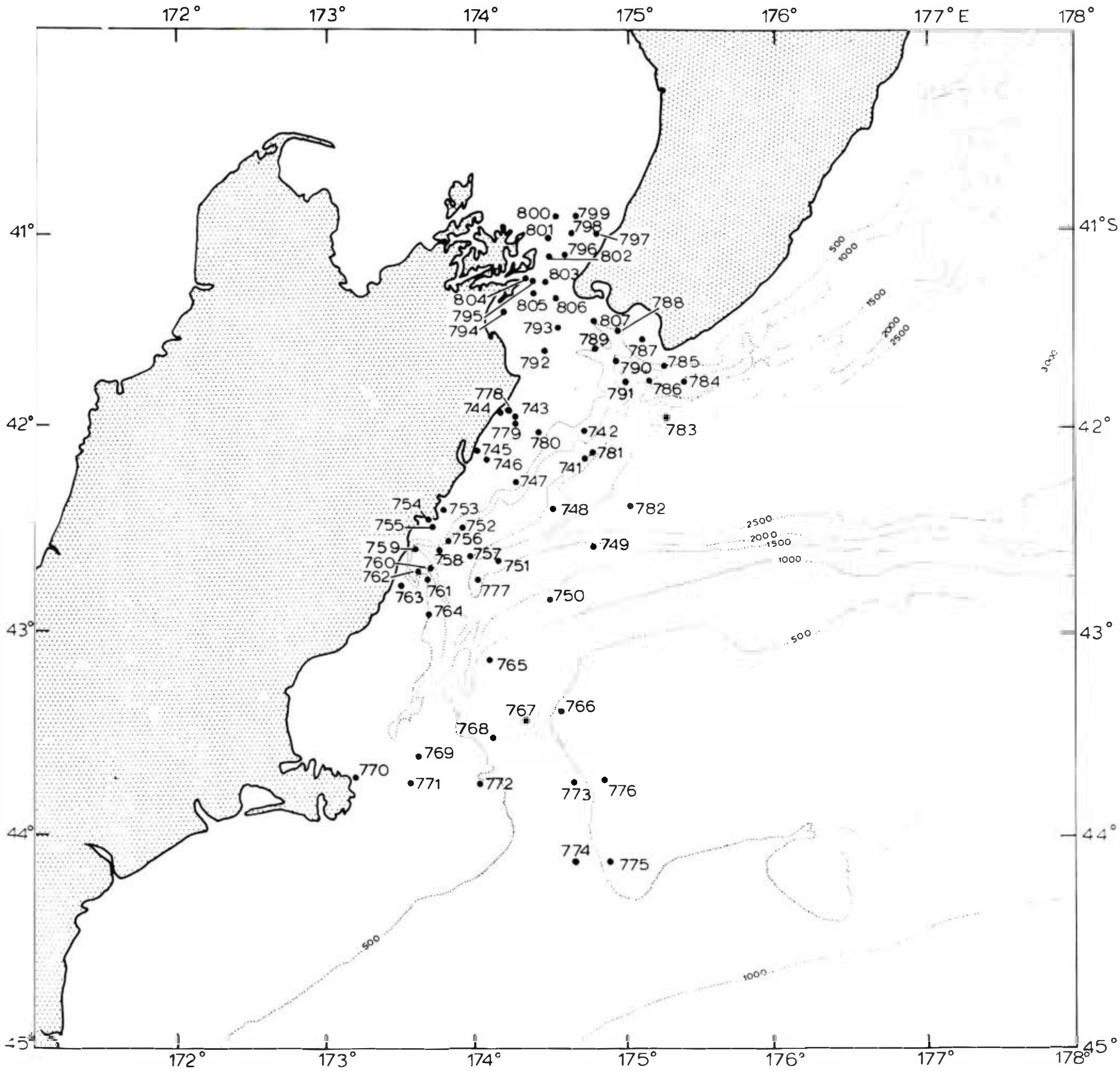

Fig. 3. Station positions for a cruise conducted between 26 November and 4 December 1968. The station numbers are to be prefixed by the letter D. The bathymetry, in metres, of the survey area is also shown. (Fig. 3 of Heath 1971).

from Hawke Bay to Banks Peninsula (Fig. 2). Most of these data (75 stations) have been used in an analysis of the Southland Current (Heath 1972a), the remainder (12 stations) are detailed in Appendix II. Some data from a cruise made between 26 November and 4 December 1968 in this area between Cook Strait and Banks Peninsula (Fig. 3) have been used in analyses of the circulation and hydrology in Cook Strait (21 stations, Heath 1971) and of coastal upwelling on the north Canterbury coast (9 stations, Heath 1972b) but the bulk of the data (37 stations) is given in Appendix II. The third cruise (57 stations) was conducted between 21 February and 14 March 1969 in the area from near East Cape to Kaikoura (Fig. 4). Station circumstances are given in Appendix I and the data are given in Appendix II. These data have been supplemented by temperatures and salinity data collected by Bradford (1972) at Kaikoura, surface hydrological data from the Union Steam Ship Company vessels T.E.V. *Maori* and M.V. *Hawea* and from airborne infrared radiation thermometer surveys.

2*

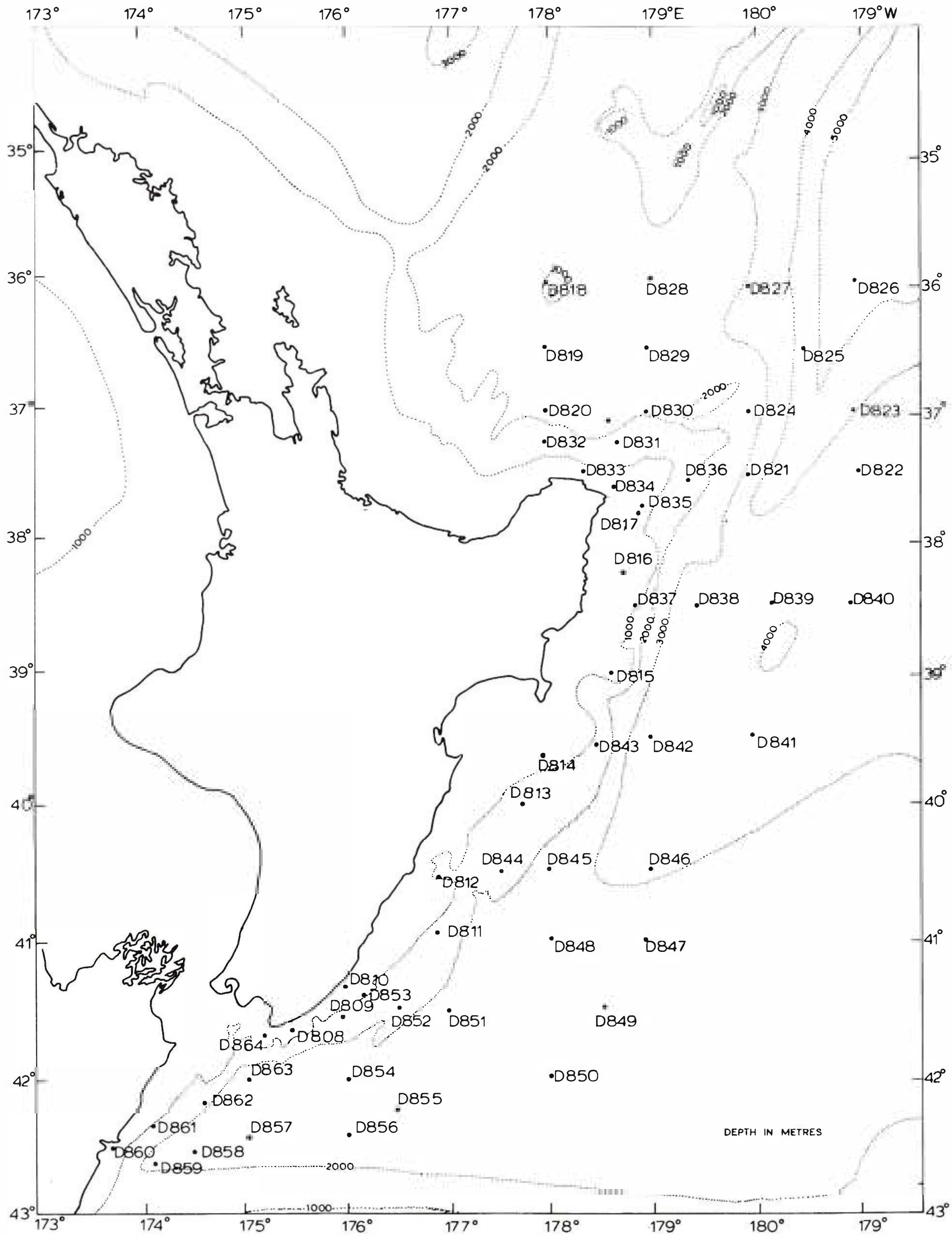

Fig. 4. Station positions for a cruise conducted between 21 February and 14 March 1969. The bathymetry, in metres, of the survey area is also shown.

COLLECTION OF DATA

Temperatures and water samples were obtained at each station by Negretti and Zambra reversing thermometers mounted on Knudsen sampling bottles. Thermometers were read after allowing time for stabilisation in an air-conditioned laboratory. Salinities were measured on board the ship with an inductive salinometer (Brown and Hamon 1961) using Copenhagen water as the standard. Bathythermograph casts to a depth of 270 m, where possible, and continuous surface thermograph records supplemented these temperature/salinity serial measurements. The corrected temperatures and salinities at the observed depths, the derived values of density, sound velocity, cumulative dynamic height anomalies and cumulative potential energy anomalies are given in Appendix II.

The airborne infrared radiation thermometer used was the model IT-3 manufactured by the Barnes Engineering Company (Instrument Division). The sensing head of this instrument was mounted in the body of a Piper *Aztec* aircraft and viewed the sea through a slot cut in the bottom of the aircraft fuselage. Flights were made at an altitude of 1000 feet. The relative accuracy of this method of measuring surface temperature is 0.5°C but drift within the instrument limits the minimum absolute accuracy to 1.2°C.

EAST CAPE CURRENT NEAR EAST CAPE

The Geostrophic Currents Near East Cape

Between 21 February and 14 March 1969 a hydrological cruise was conducted in the region bounded by 42°30'S and 36°S, longitude 179°W and the New Zealand coast (Fig. 4). The dynamic height anomaly contours at the surface relative to 500 dbars (0-500), 1000 dbars (0-1000) and 1500 dbars (0-1500) computed

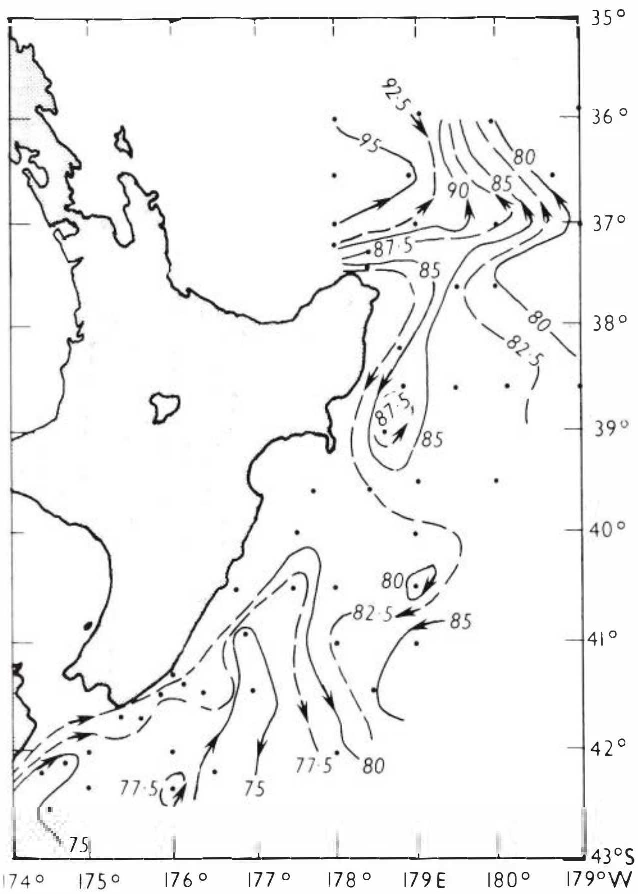

Fig. 5. Contours (dyn. cm) of the geopotential topography of the sea surface relative to 500 dbars for data collected in February/March 1969. Arrows show flow direction. (Fig. 25 of Heath 1972c).

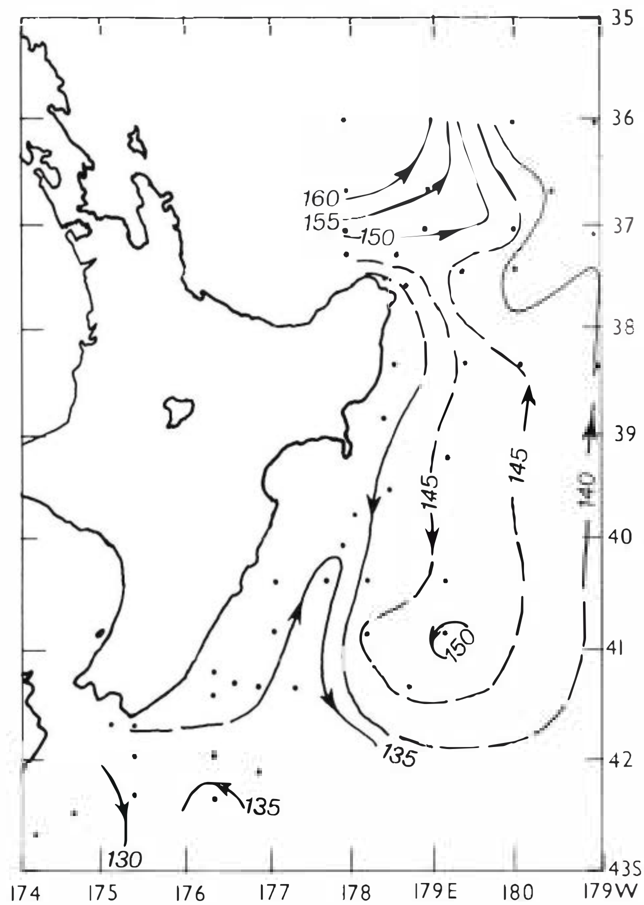

Fig. 6. Contours (dyn. cm) of the geopotential topography of the sea surface relative to 1000 dbars for data collected in February/March 1969. Arrows show flow direction.

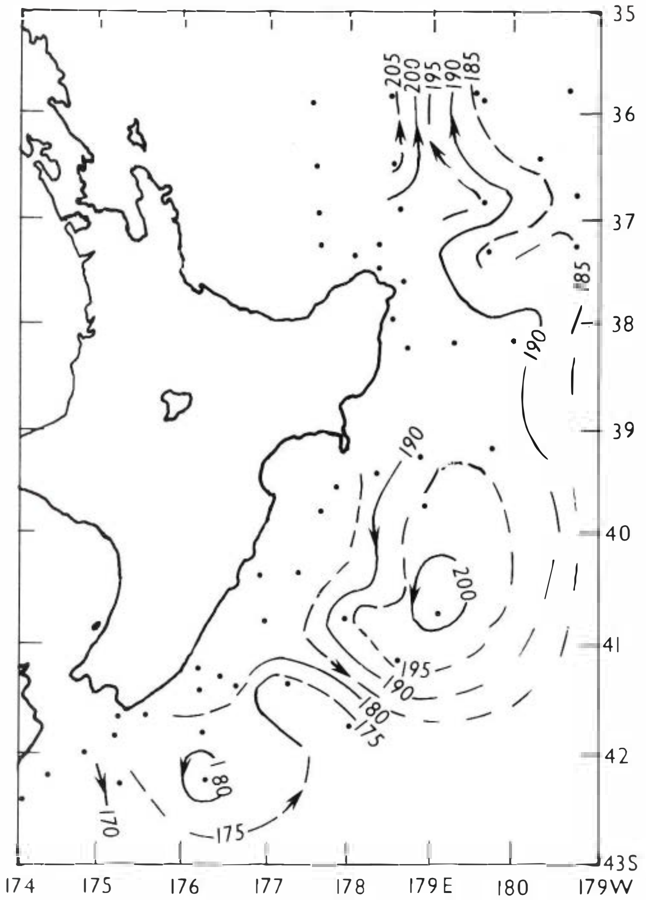

Fig. 7. Contours (dyn. cm) of the geopotential topography of the sea surface relative to 1500 dbars for data collected in February/March 1969. Arrows show flow direction.

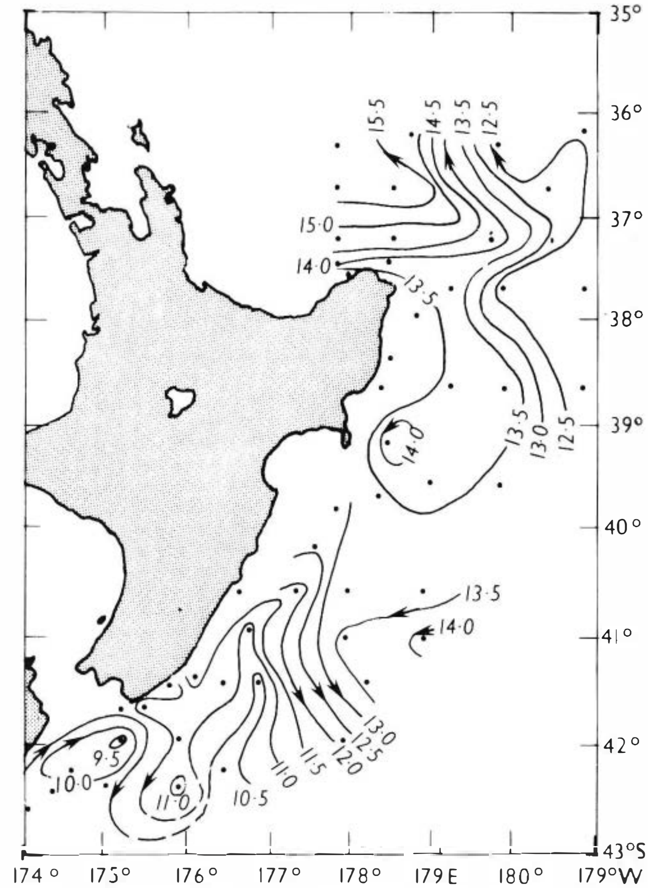

Fig. 8. Isotherms (°C) at a depth of 200 m for data collected in February/March 1969. Arrows show flow direction based on higher temperatures being on the left looking downstream. (Fig. 24 of Heath 1972c).

from these observations are shown in Figs 5-7 respectively. Heath (1972c) has shown that near East Cape both the Intermediate Water (defined by the salinity minimum in the vertical water column and found at approximately 1000 m near East Cape, the direction of flow being inferred from the direction of increasing salinity) and the water above it flow in the same direction with no zero level in this portion of the water column, i.e. all the water above approximately 1500 m flows in the same direction. Therefore the geostrophic currents (Figs 5-7) give a true indication of the direction of the absolute currents.

The geostrophic currents were strongly deflected towards the north in the area north of approximately 37°S. South of 37°S, near East Cape, they were deflected towards the south between East Cape and approximately longitude 179°30'E. East of 179°30'E, at the latitude of East Cape, there was a northwards movement of water from the Hikurangi Trench. Interpolated temperatures at 200 m depth and upper mixed layer depths, taken from BT records, are contoured in Figs 8, 9 respectively. Both sets of contours are similar in shape to the geostrophic current streamlines, suggesting that the currents were sufficiently strong to set up the mass field such that the higher temperature and greater depth of the mixed layer were to the left of the current direction. A deflection to the south around East Cape was also shown by the surface isotherms (Fig. 10) and isohalines (Fig. 11) but south of East Cape the geostrophic streamline pattern was more similar to the 200 m isotherms and mixed layer isobaths than to the surface temperatures and salinities. This is expected as the surface temperature and salinity patterns are more affected by local weather than are the sub-surface patterns.

Near East Cape, the water is too shallow for the geostrophic method to be used effectively, but as the 200 m isotherms are deflected southwards around the Cape, the southwards deflection of the East Cape Current must continue into shallow waters. Evidence for this deflection is also given by the New Zealand Pilot (Hydrographic Department 1958, p.235) which states 'outside of a depth of 100 fathoms, [between East Cape and Gable End Foreland] a constant current sets southward at a rate of one knot, but depending greatly on the force and direction of the wind.' Indirect evidence for a clockwise circulation around East Cape can be deduced from the wind conditions in this

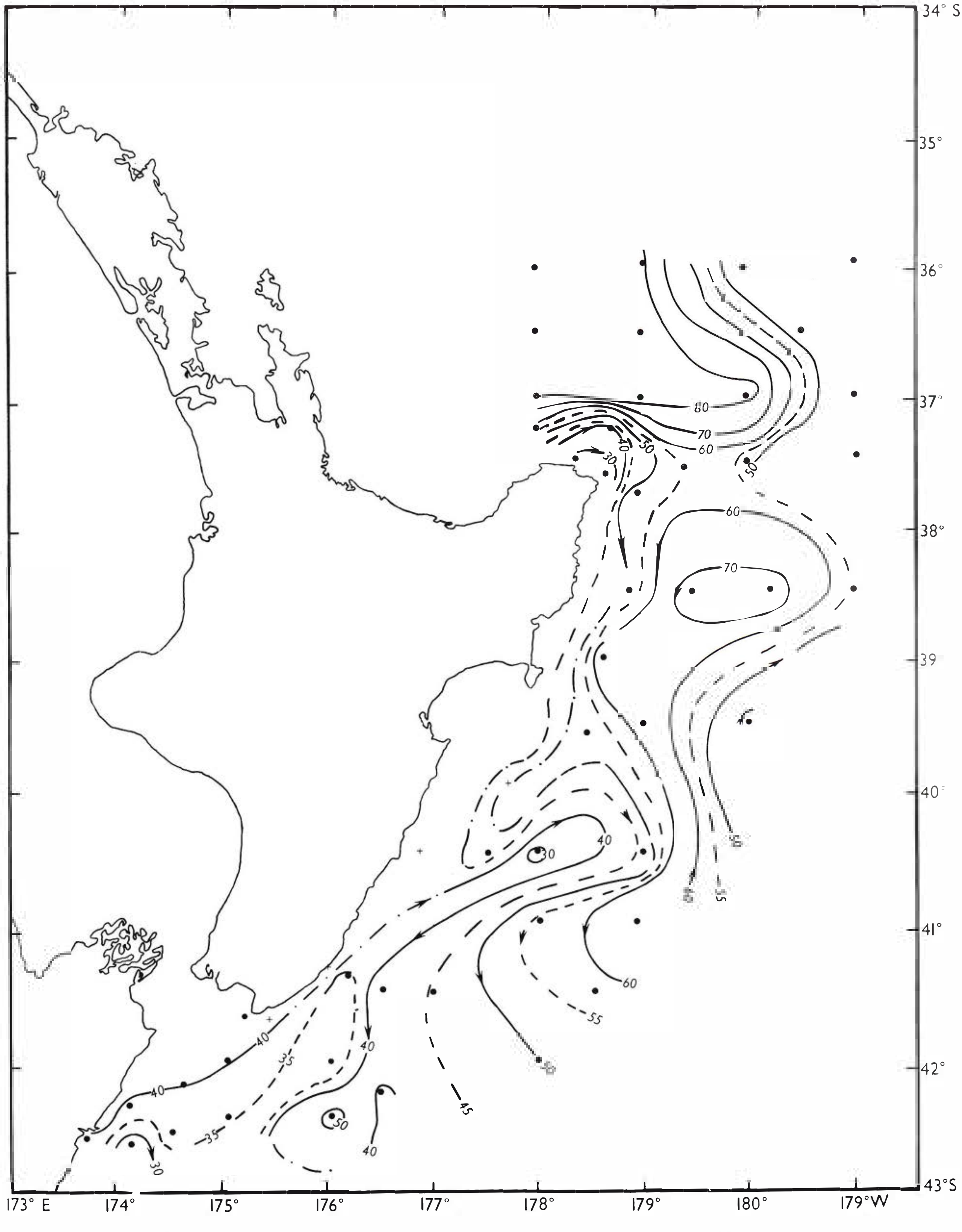

Fig. 9. Depth (m) of the upper mixed layer deduced from bathythermograph records collected in February/ March 1969.

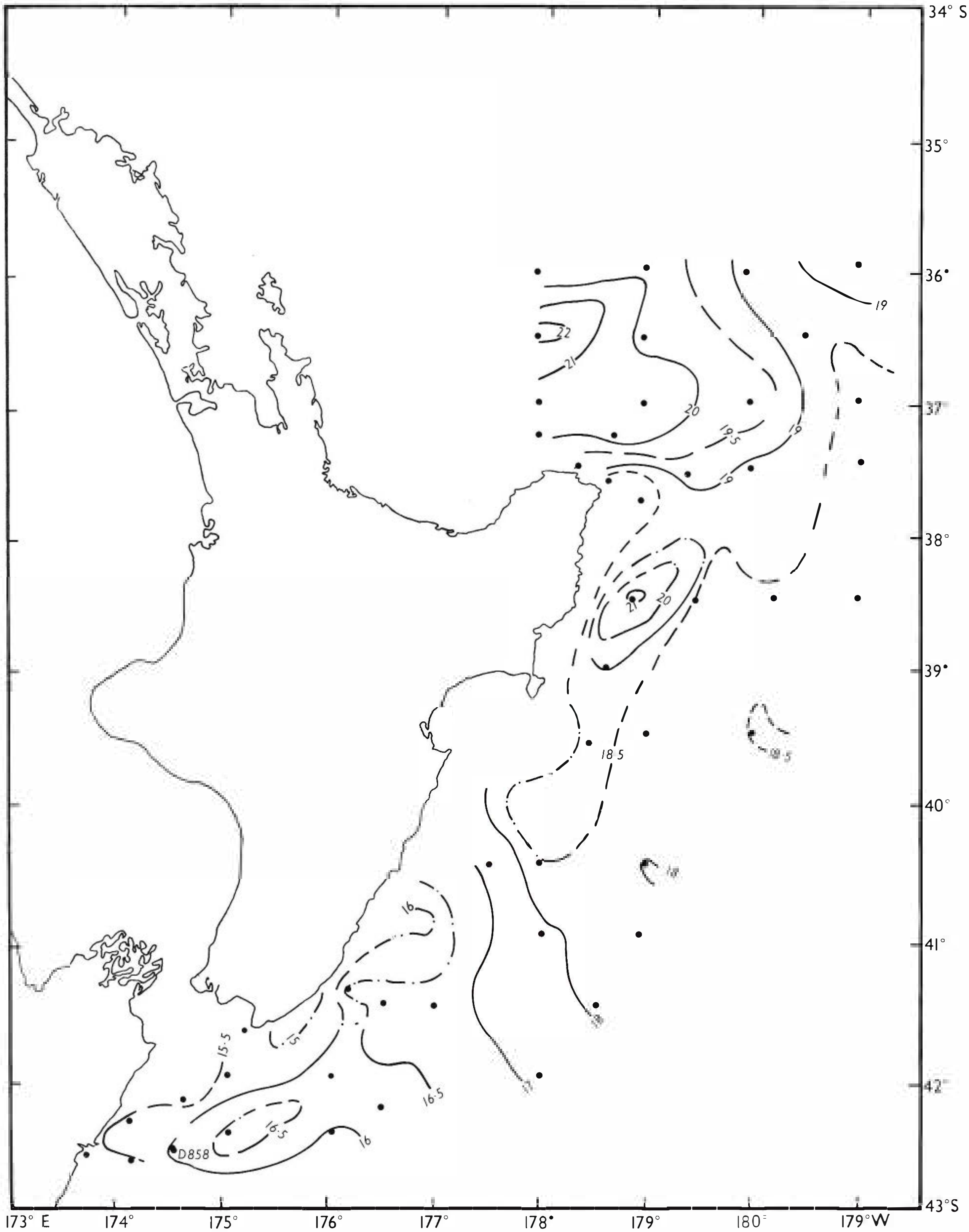

Fig. 10. Isotherms (°C) of the sea surface for data collected in February/March 1969.

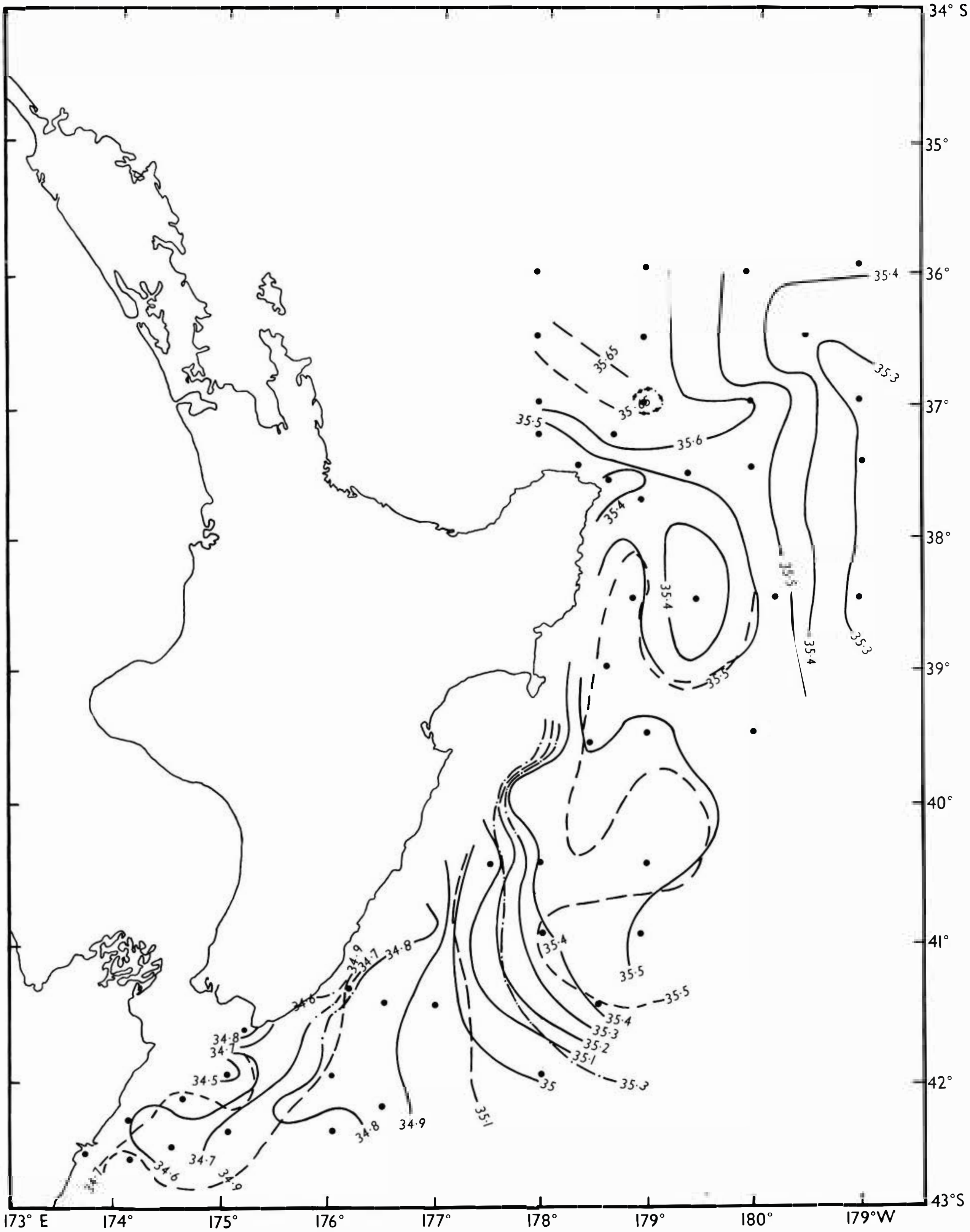

Fig. 11. Isohalines (‰) at the sea surface (full lines) for data collected in February/March 1969. Contours of the near-surface maximum salinity (‰) are shown by dashed lines.

Sig. 3

region. The New Zealand Pilot (1958, p.234) states 'Winds on either side of the East Cape are often very different, even when strong; when the wind is westerly in the Bay of Plenty and well out to seaward of East Cape, winds southward of the Cape, within about five miles of the shore, are probably north-easterly and light'. These winds give rise to a negative curl of the wind stress and, as can be seen from Equation 7 (p.22), this results in a decrease in the sum of the curl of the mass transport and the meridional transport. This decrease is equivalent to an increase in the clockwise circulation.

Dynamic height anomaly contours 0-500 dbars, 0-1000 dbars, 0-1500 dbars, derived from the two block surveys (Garner 1967a; Ridgway 1970a) are shown in Figs 12-14. The first survey was made in February/March 1963 and the second in February/March 1965. The one year difference between these observations limits their applicability to the study of only large features of the circulation, but, within this limitation, the data confirm the 1969 circulation pattern. From this analysis it appears that the East Cape Current is derived from a clockwise flow of Subtropical Water around East Cape south of latitude

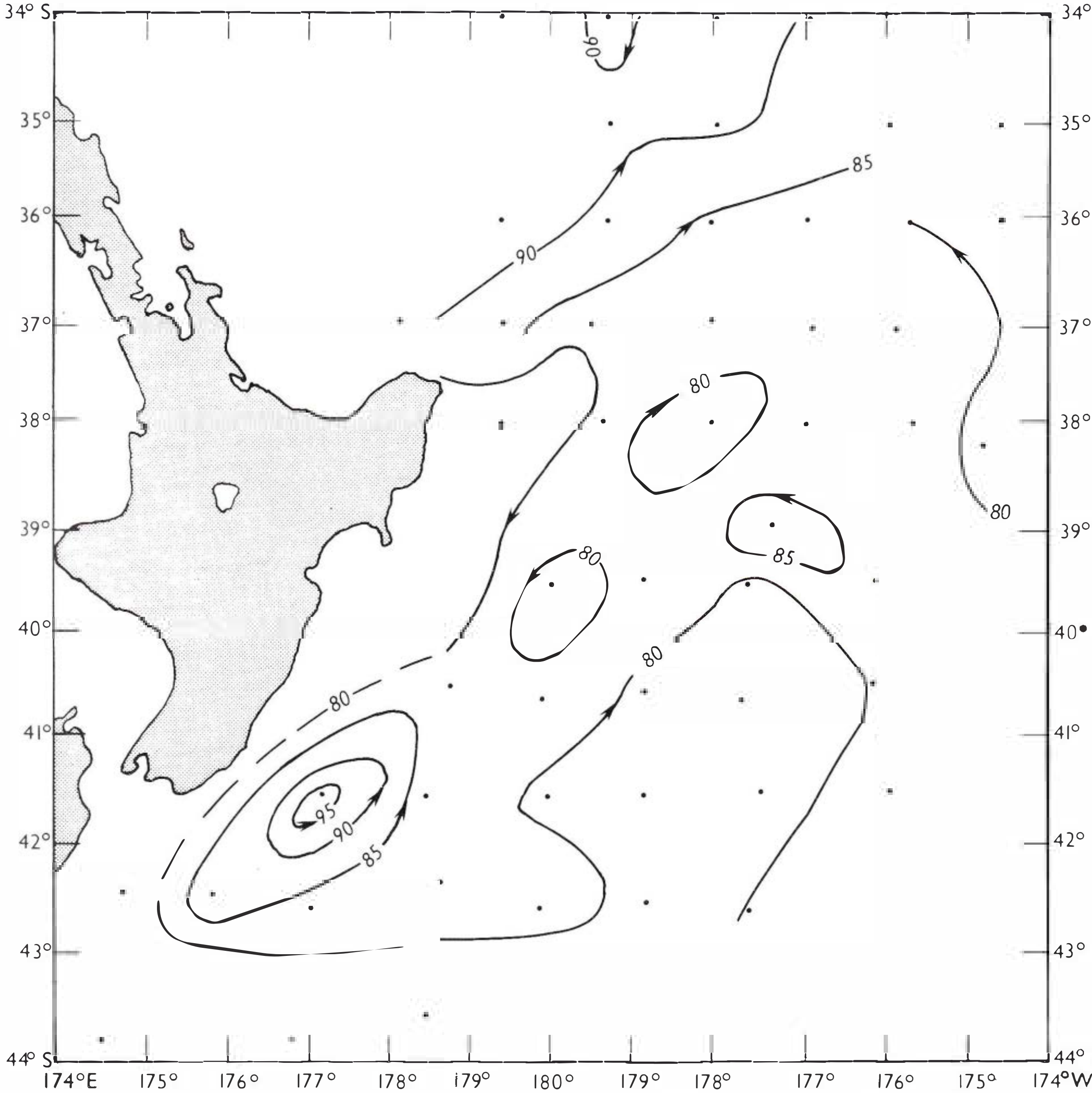

Fig. 12. Contours (dyn. cm) of the sea surface relative to a depth of 500 dbars for data collected in February/March 1963 (Garner 1967a) and February/March 1965 (Ridgway 1970a). Arrows show flow direction. (Fig. 21 of Heath 1972c).

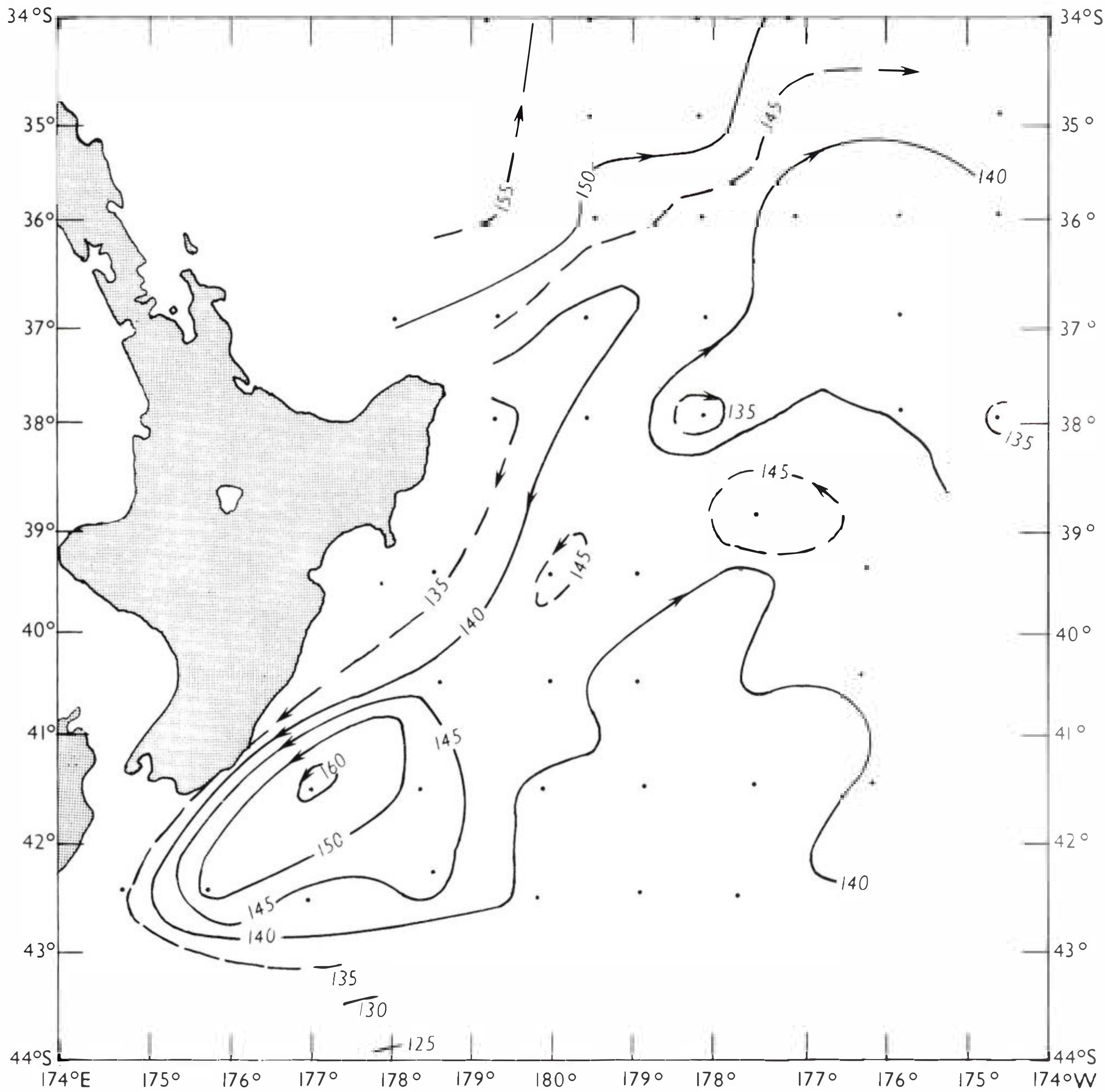

Fig. 13. Contours (dyn. cm) of the sea surface relative to a depth of 1000 dbars for data collected in February/ March 1963 (Garner 1967a) and February/March 1965 (Ridgway 1970a). Arrows show flow direction. (Fig. 22 of Heath 1972c).

37°S rather than a series of eddies formed at East Cape as postulated by Ridgway (1970a).

The Theoretical Influence of the Bottom Topography on the Circulation Near East Cape

Various authors have considered the effect that the bottom topography has on ocean currents by applying different approximations in the equations of motion. In the so-called Ekman type deflection (Ekman 1923) the change of the Coriolis parameter with latitude (β) is neglected and, in the Sverdrup type deflection (Sverdrup 1961) it has been shown by Neumann (1960) that the change in the Coriolis parameter is the significant parameter. The following analysis is similar to that given by Neumann (1960) except that here the bathymetric feature of interest is the western side of the Kermadec Trench (Fig. 15) whereas he considered a symmetrical rise.

We will consider the case with the ridge alone (i.e. with no land and therefore we need not be

3*

concerned about the boundary condition U=0 at the land boundary) to get an estimate of the deflection of the flow. The development of the basic equations has been included to allow the approximations made to be evident.

Basic Equations : The equations of motion in right-hand co-ordinate system (x to the east, y to the north and Z vertically upwards) neglecting the local change of the velocity with time and the spatial accelerations are :

$$f\rho v + A \frac{\partial^2 u}{\partial z^2} - \rho r u - \frac{\partial p}{\partial x} = 0 \qquad (1)$$

$$-f\rho u + A \frac{\partial^2 v}{\partial z^2} - \rho r v - \frac{\partial p}{\partial y} = 0 \qquad (2)$$

Here A is the coefficient of eddy viscosity, and is assumed to be constant, ρ the density, p the pressure, f the Coriolis Parameter, which is negative in the Southern Hemisphere, r the horizontal coefficient of internal friction, and u and v the horizontal velocity components in the x and y directions respectively. In these equations friction has been included as both a term which is a linear function of the speed (the Guldberg and Mohn (1876) approximation) and a newtonian stress term. When equations 1 and 2 are

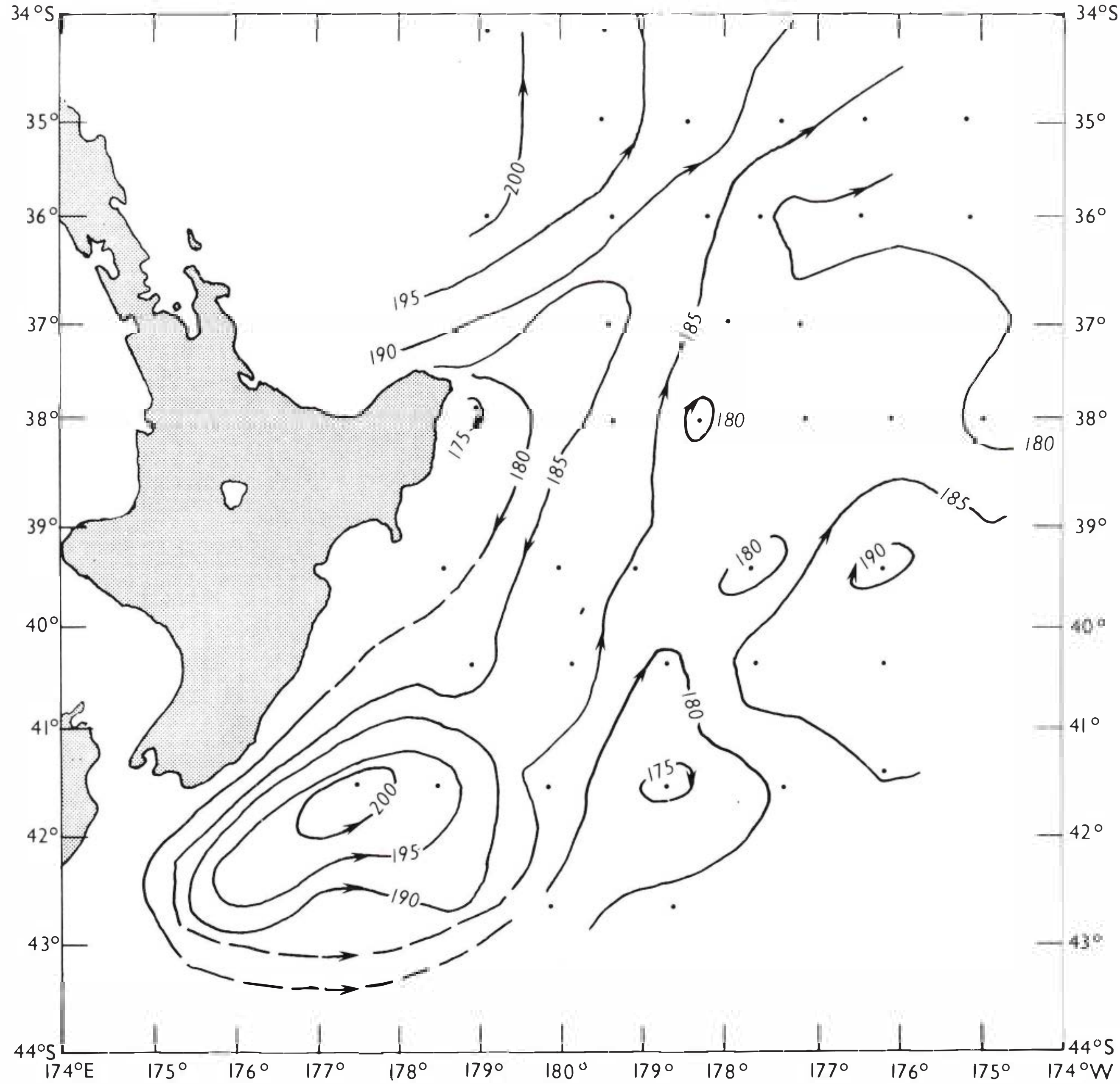

Fig. 14. Contours (dyn. cm) of the sea surface relative to a depth of 1500 dbars for data collected in February/ March 1963 (Garner 1967a) and February/March 1965 (Ridgway 1970a). Arrows show flow direction. (Fig. 23 of Heath 1972c).

integrated vertically the newtonian stress term reduces to a surface stress (wind effect), which will be neglected, and a bottom stress, which will be computed with the Guldberg and Mohn frictional term. Therefore the choice of frictional coefficient reduces to the choice of a suitable r which includes the effect of bottom friction.

Integrating the above equations from $Z = \xi(x, y)$ to $Z = D(x, y)$ gives

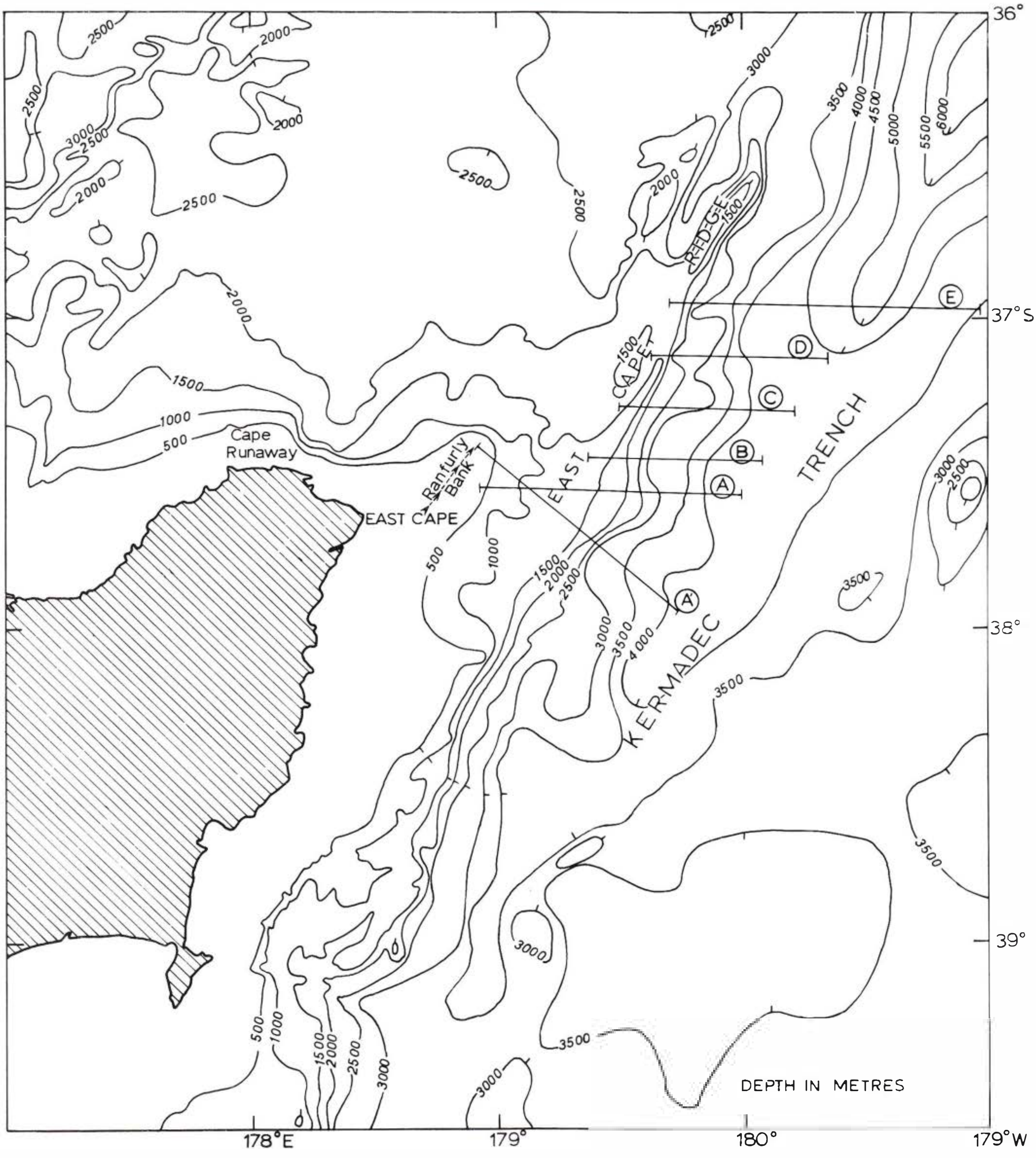

Fig. 15. The bathymetry (m) near East Cape. The positions of the lines described in the text are also shown and are labelled with the corresponding letters.

TABLE 1

The latitudinal and longitudinal variation on a transport streamline near East Cape for the boundary condition $V = 0$ at $x = \ell/4$. The transports used in the computation have been calculated from the product of an appropriate surface velocity and the depth at the top of the ridge (*see* note below). The depth variation from the top of the ridge to the bottom of the trench has been represented by half a cosine curve.

Latitude $\phi = 37°30'S$

Coriolis parameter $f = -8.8 \times 10^{-5}\ s^{-1}$;

$\beta = 1.8 \times 10^{-11}\ m^{-1}\ s^{-1}$; $\quad r = 3.3 \times 10^{-6}\ s^{-1}$

(Neumann 1955)

Line	Depth at top of ridge (m)	ℓ(m)	a(m)	Variation of $V = 0$ $= \ell/4$ x (m)	y (m)
A	500	185.4×10^3	2000	46×10^3	$+ 3.45 \times 10^7$
B	1250	118.6×10^3	1625	30×10^3	0.693×10^6
C	1250	122.3×10^3	1625	31×10^3	0.7373×10^6
D	1250	124.2×10^3	1625	31×10^3	0.729×10^6
E	1500	131.6×10^3	1687	33×10^3	0.672×10^6

NOTE : In the computation of the quantity S the surface geostrophic zonal current was taken at $1\ m\ s^{-1}$, but in calculating the value of y, the quantity S has to be divided by the zonal mass transport and, if the zonal current is the same over the entire vertical water column, the zonal velocities cancel. This assumption of a constant current over the entire vertical water column (i.e. homogeneous ocean) was made in the first part of the analysis (*see* this page).

$$fV + \tau_{xs} - \tau_{xb} - rU - p_D \frac{\partial D}{\partial x} + p_\xi \frac{\partial \xi}{\partial x} - \frac{\partial}{\partial x} \int_D^\xi p dz = 0 \qquad (3)$$

and

$$-fU + \tau_{ys} - \tau_{yb} - rV - p_D \frac{\partial D}{\partial y} + p_\xi \frac{\partial \xi}{\partial y} - \frac{\partial}{\partial y} \int_D^\xi p dz = 0 \qquad (4)$$

where

$$U = \int_D^\xi \rho u dz \qquad\qquad V = \int_D^\xi \rho v dz$$

τ_{xs}, τ_{ys}, are the wind stress components on the sea surface and τ_{xb}, τ_{yb}, are the bottom stress components.

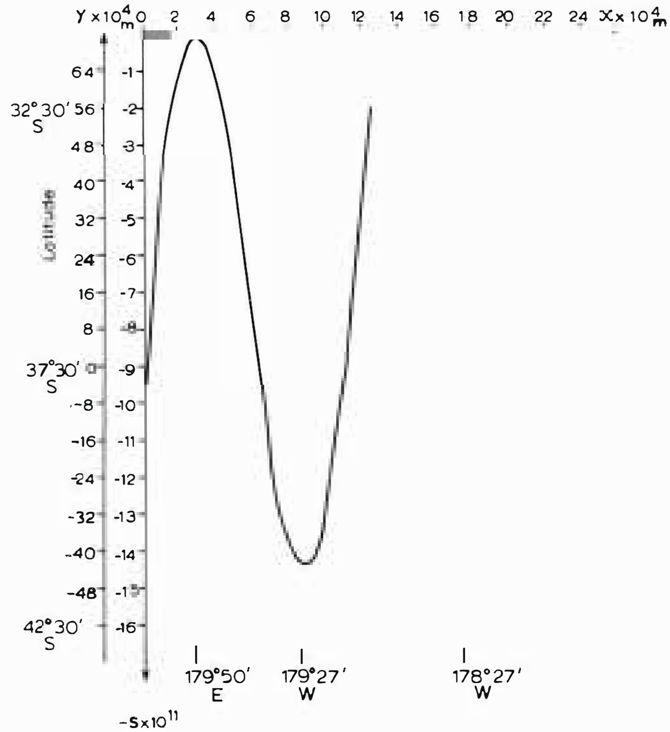

Fig. 16. Latitudinal (y) and longitudinal (x) variation of the streamline $\psi = 0$ for the boundary condition of no meridional flow ($V = 0$) at $x = \ell/4$ for the sinusoidal approximation to the bathymetry for line C in Fig. 15.

Cross-differentiating equations 3 and 4 and subtracting after absorbing the bottom stress in the internal friction terms gives

$$f\left(\frac{\partial U}{\partial x} + \frac{\partial V}{\partial y}\right) + V\frac{\partial f}{\partial y} + \frac{\partial \tau_{xs}}{\partial y} - \frac{\partial \tau_{ys}}{\partial x} + r\left(\frac{\partial V}{\partial x} - \frac{\partial U}{\partial y}\right) = \frac{\partial P_D}{\partial y}\frac{\partial D}{\partial x} - \frac{\partial P_D}{\partial x}\frac{\partial D}{\partial y} - \frac{\partial P_\xi}{\partial y}\frac{\partial \xi}{\partial x} + \frac{\partial P_\xi}{\partial x}\frac{\partial \xi}{\partial y} \qquad (5)$$

Using the continuity equation in the form

$$\frac{\partial U}{\partial x} + \frac{\partial V}{\partial y} = 0 \qquad (6)$$

and assuming that the horizontal gradient of the atmospheric pressure is zero, equation 5 becomes

$$V\beta + \frac{\partial \tau_{xs}}{\partial y} - \frac{\partial \tau_{ys}}{\partial x} + r\left(\frac{\partial V}{\partial x} - \frac{\partial U}{\partial y}\right) = \frac{\partial P_D}{\partial y}\frac{\partial D}{\partial x} - \frac{\partial P_D}{\partial x}\frac{\partial D}{\partial y} \qquad (7)$$

where $\beta = \partial f/\partial y$ is taken as constant (the Beta-plane approximation).

For a homogeneous ocean only the barotropic mode is present. Therefore

$$\frac{\partial P_D}{\partial y} = g\rho\left(\frac{\partial \xi}{\partial y} - \frac{\partial D}{\partial y}\right) \quad \text{and} \quad \frac{\partial P_D}{\partial x} = g\rho\left(\frac{\partial \xi}{\partial x} - \frac{\partial D}{\partial x}\right)$$

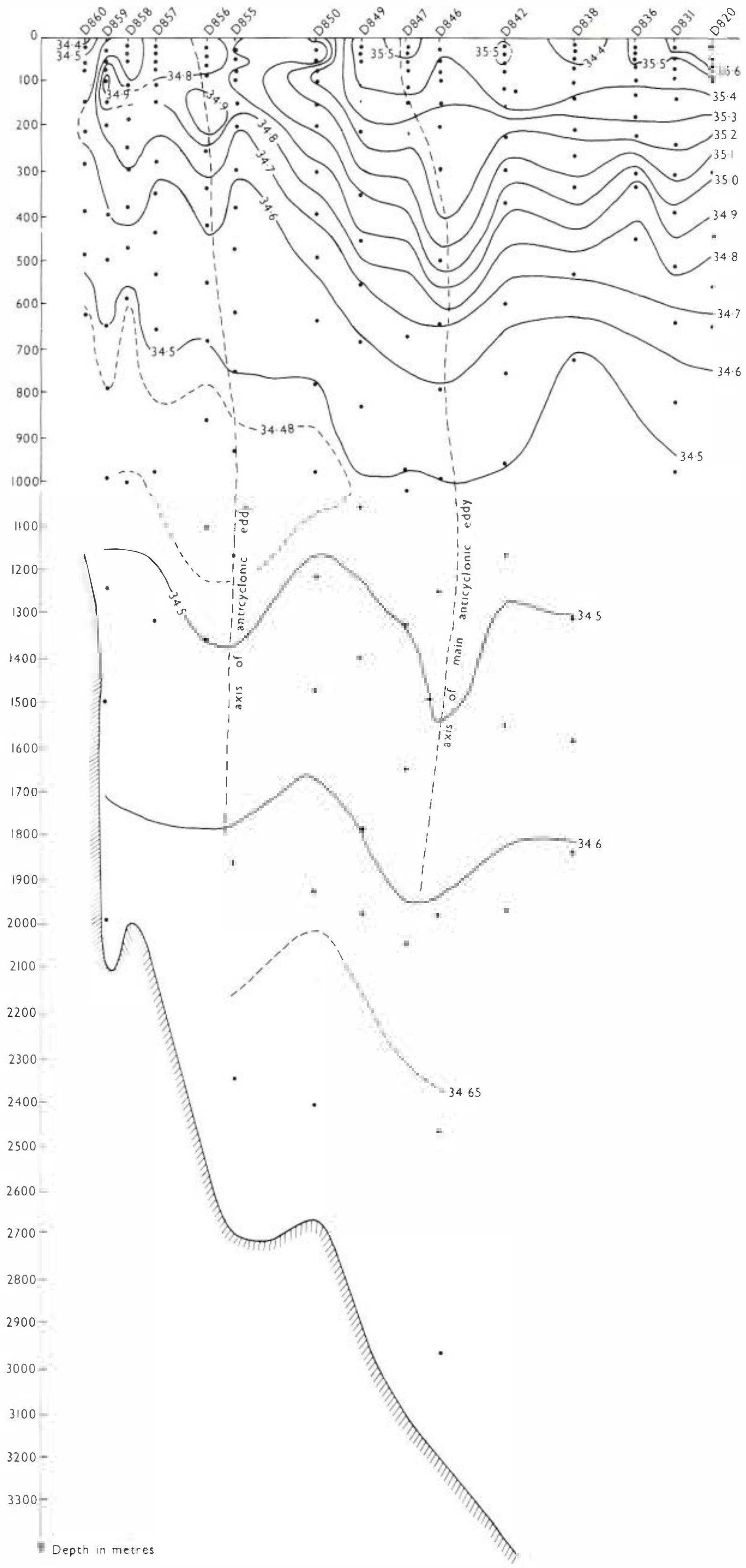

Fig. 17. Sectional salinity (‰) plot along the axis of the East Cape Current System from position 37°00'S, 178°00'E (Stn D820) to 42°30'S, 173°40'E (Stn D860).

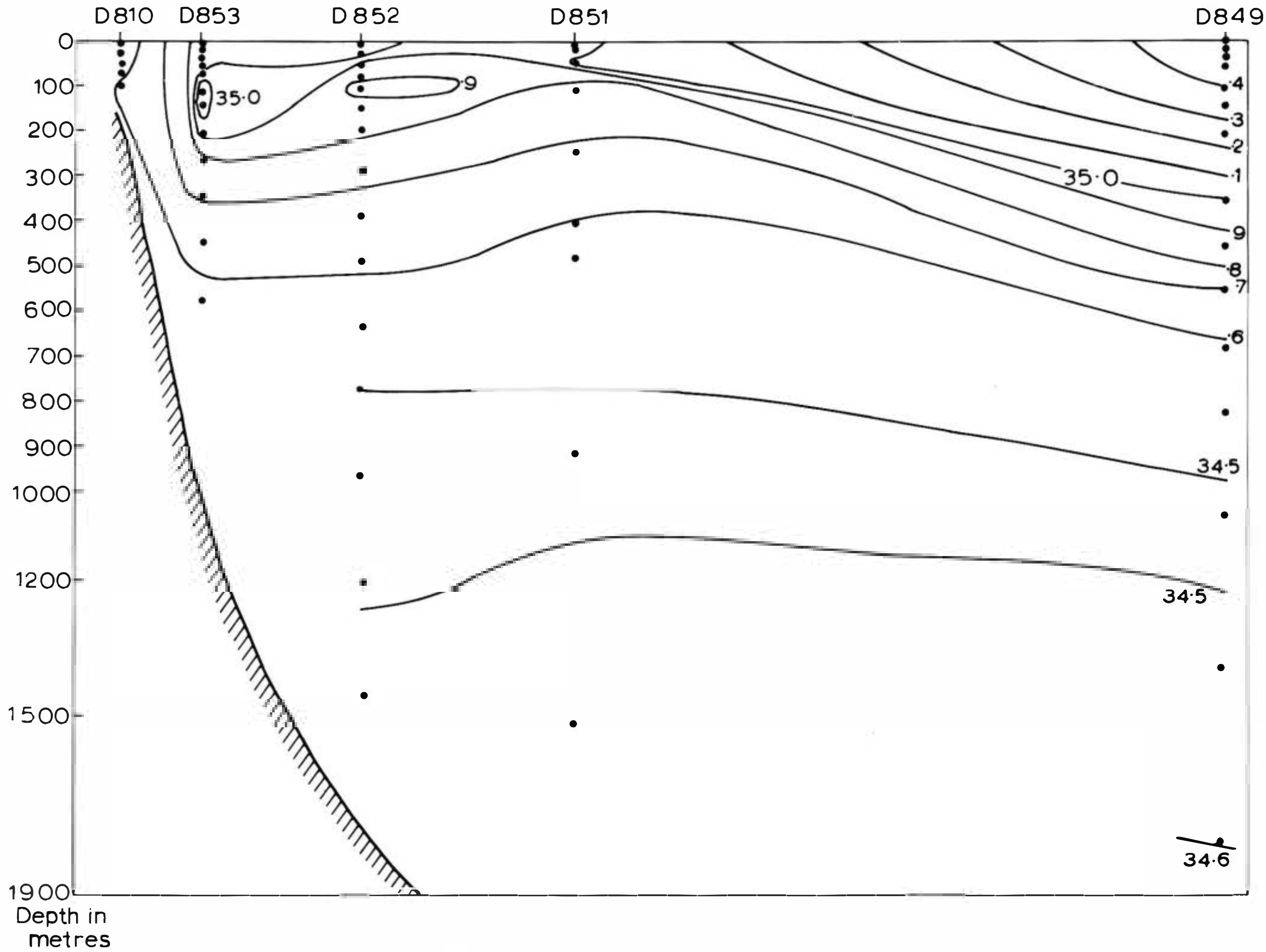

Fig. 18. Cross-sectional salinity (‰) profile in a zonal line extending from the east coast of the North Island, New Zealand at latitude 41°30'S from data collected in February/March 1969.

For the case of a homogeneous ocean and with the curl of the wind stress zero (the effect of the wind stress has been examined qualitatively on p. 18), equation 7 becomes

$$V\beta + r\left(\frac{\partial V}{\partial x} - \frac{\partial U}{\partial y}\right) = g\rho\left(\frac{\partial \xi}{\partial y}\frac{\partial D}{\partial x} - \frac{\partial \xi}{\partial x}\frac{\partial D}{\partial y}\right) \quad (8)$$

Using the continuity equation 6 a transport stream function ψ can be defined where

$$\frac{\partial \psi}{\partial x} = V \qquad \frac{\partial \psi}{\partial y} = -U \quad (9)$$

In the region of interest the slope of the bottom topography is greatest in the zonal direction, consequently we may assume that $\partial D/\partial y = 0$. Also, we may assume that $\partial U/\partial y = \Delta U/\Delta y \approx 0$ because the latitudinal range in which we are interested, Δy, is small (equivalent to neglecting $\partial^2 f/\partial y^2$). With these conditions after substituting for the stream function ψ, equation 8 becomes

$$\frac{\partial \psi}{\partial x}\beta + r\frac{\partial^2 \psi}{\partial x^2} = g\rho\frac{\partial \xi}{\partial y}\frac{\partial D}{\partial x} \quad (10)$$

TABLE 2

Position of the large anticyclonic eddy in the head of the Hikurangi Trench during the cruises conducted in this area.

Period	Reference	POSITION Lat. ° ' S	Long. ° E
September 1962	Sdubbundhit and Gilmour 1964	40 30	178
February-March 1963	Garner 1967a	41 30	178
April 1967	Heath 1968	42 00	179
October 1967	Heath 1972a	42 00	178
March 1969	Appendix II	41 00	179

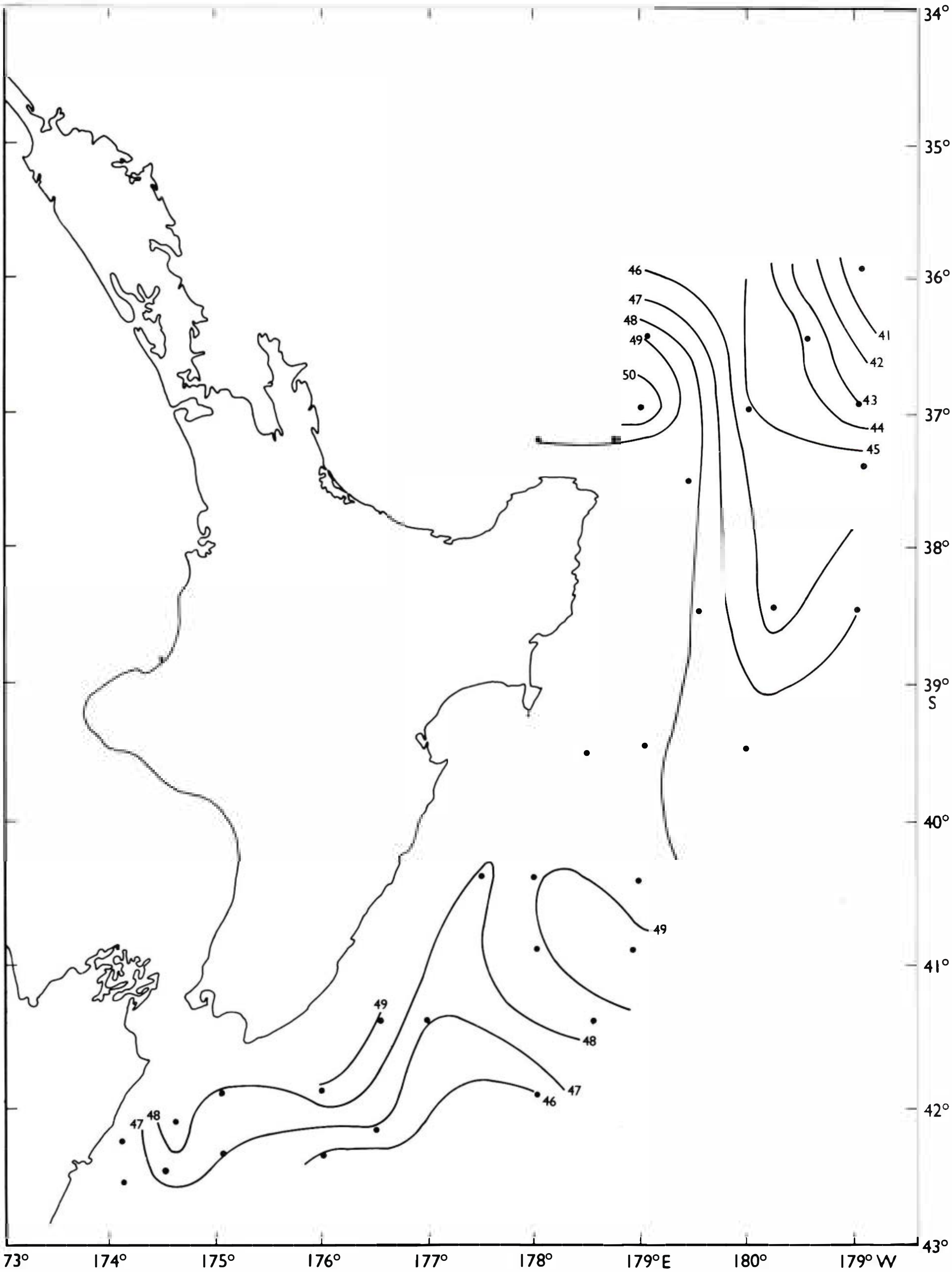

Fig. 19. Isohalines (‰) of the surface minimum salinity for data collected in February/March 1969. The quantities shown are the decimal values less than 34.00‰.

For the case $\partial\xi/\partial y$ = constant, and with the approximation of a bottom topography in the form of a sinusoidal wave

$$D(x) = D_0 + a\cos\left(\frac{2\pi x}{\ell}\right) \tag{11}$$

of which, however, only part of a wave length will be considered, equation 10 becomes

$$\frac{\partial^2\psi}{\partial x^2} + E\frac{\partial\psi}{\partial x} = -B\frac{2\pi a}{\ell}\sin\frac{2\pi x}{\ell} \tag{12}$$

where

$$E = \frac{\beta}{r} \qquad\qquad B = \frac{g\rho}{r}\frac{\partial\xi}{\partial y}$$

The transport in the zonal direction at x = 0 is U, therefore from equation 9 the stream function is seen to be of the form

$$\psi = -Jy + k(x) \tag{13}$$

where J = U and is constant.

The x dependent solution of equation 12 can be broken up into a complementary function which satisfies

$$\frac{\partial}{\partial x}\left(\frac{\partial}{\partial x} + E\right)\psi = 0 \tag{14}$$

and has a solution

$$\psi = C_1 e^{-Ex} + C_2 \tag{15}$$

and the particular solution which satisfies

$$\frac{\partial}{\partial x}\left(\frac{\partial}{\partial x} + E\right)\psi = -B\frac{2\pi a}{\ell}\sin\frac{2\pi x}{\ell}$$

and has a solution

$$\psi = C_3\sin\frac{2\pi x}{\ell} + C_4\cos\frac{2\pi x}{\ell} \tag{16}$$

where $E\,C_3 = \frac{2\pi}{\ell}C_4$ and $\frac{2\pi}{\ell}C_3 + E\,C_4 = Ba$

i.e. $C_4 = \dfrac{Ba}{E + \frac{1}{E}\left(\frac{2\pi}{\ell}\right)^2} = M$ $\qquad C_3 = \dfrac{2\pi M}{E\ell}$

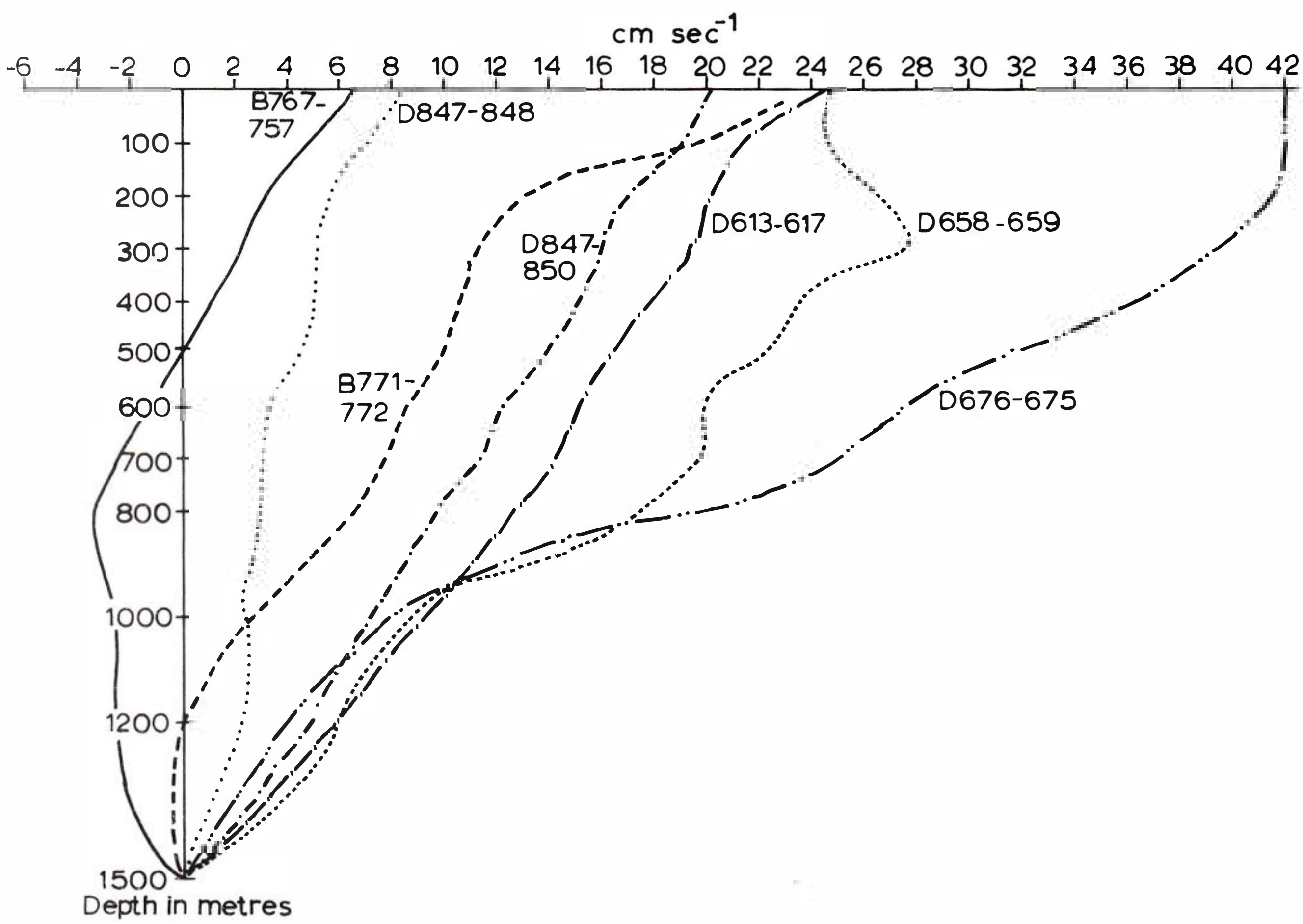

Fig. 20. Plots of relative geostrophic current speeds (cm sec^{-1}) with depth (m) in the large anticyclonic eddy located at approximately 41°30'S, 178°00'E, for several sets of data. Stns B757, B767, B771, B772, were occupied in February/March 1963 by Garner (1967a); D613, D617 in April 1967 by Heath (1968); D658, D675, D676, D695 in October 1967 by Heath (1972a) and D847, D848, D859 in March 1967 (Appendix II).

The full solution is

$$\psi = - Jy + C_3 \sin \frac{2\pi x}{\ell} + C_4 \cos \frac{2\pi x}{\ell} + C_1 e^{-Ex} + C_2 \qquad (17)$$

Boundary Conditions : The two boundary conditions of interest in the present study are V = 0 at x = 0 (i.e. no meridional velocity at the top of the ridge) and V = 0 at x = ℓ/4 (i.e. no meridional velocity midway between the top of the ridge and the bottom of the trench with the flow crossing the ridge at an angle). Using these conditions we have for $v = 0$ at $x = 0$

$$\frac{2\pi}{\ell} C_3 = C_1 E$$

and for $v = 0$ at $x = \frac{\ell}{4}$

$$C_1 = - \frac{C_4}{\ell} \frac{2\pi}{E} e^{\frac{E\ell}{4}}$$

Defining ψ such that $C_2 = 0$ and after substituting the values of the coefficients determined from the

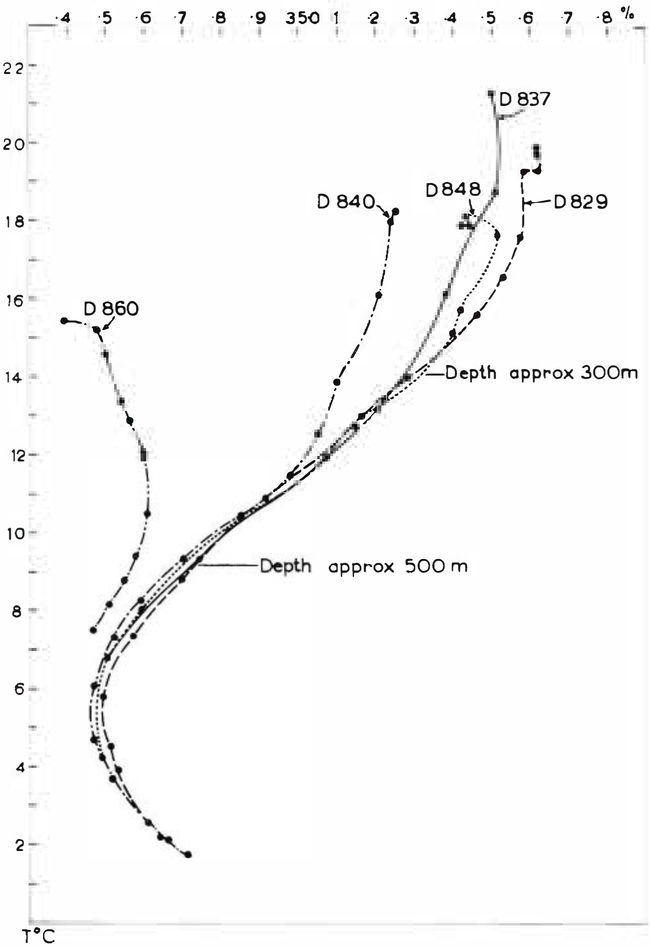

Fig. 21. Temperature (°C) / Salinity (‰) curves for Stns D829, D837, D840, D848, D860. These station positions are shown in Fig. 4.

TABLE 3

Regression analysis of the dynamic height anomalies (dyn. cm) at the sea surface (D) relative to various depths (H) on the temperature at a depth of 200 m (D_H = mT + c); σt, σD the standard deviations, r the regression coefficient, N the number of sets of data.

I. Data collected between 21 February and 14 March 1969 (*see* Appendix II).

H(m)	m dyn.cm/ °C	C dyn.cm	σt °C	σD dyn.cm	r	N
400	3.19	28.59	1.68	5.97	0.897	50
500	3.57	37.82	1.69	6.46	0.919	49
800	4.37	64.11	1.63	7.67	0.9308	38
1000	4.78	81.05	1.64	8.38	0.9377	36
1100	5.08	86.76	1.55	8.33	0.9448	31
1200	4.98	97.56	1.49	7.87	0.9452	29
1300	5.54	99.56	1.41	8.25	0.9453	28
1400	5.74	105.61	1.37	8.47	0.925	26
1500	5.61	116.26	1.48	9.24	0.895	26
1600	6.32	113.93	1.39	9.60	0.914	23
1700	6.36	120.51	1.39	9.87	0.896	23

II. Data collected between 25 September and 11 October 1967 (*see* Heath 1972a).

H(m)	m dyn.cm/ °C	C dyn.cm	σt °C	σD dyn.cm	r	N
500	2.21	44.50	1.22	3.01	0.897	33
800	2.37	79.65	1.20	3.71	0.763	18
1000	3.42	89.72	1.19	5.53	0.737	15

boundary conditions V = 0 at x = 0 equation 17 becomes

$$\psi = - Jy + M \left(\frac{2\pi}{E\ell}\right)^2 e^{-Ex} + \frac{2\pi}{E\ell} M \sin \frac{2\pi x}{\ell} + M \cos \frac{2\pi x}{\ell} \qquad (18)$$

and for V = 0 at x = ℓ/4

$$\psi = - Jy - M \left(\frac{2\pi}{E\ell}\right) e^{\frac{E\ell}{4} - Ex} + \frac{2\pi}{E\ell} M \sin \frac{2\pi x}{\ell} + M \cos \frac{2\pi x}{\ell} \qquad (19)$$

The physical significance of the terms in equations 18, 19 can be examined by comparing the equations obtained from equation 10 by applying different approximations.

Case I - Constant Depth Ocean : For the case of a constant depth ocean with constant zonal flow, equation 10 reduces to

$$\frac{\partial\psi}{\partial x} \beta + r \frac{\partial^2\psi}{\partial x^2} = 0$$

which has the solution

$$\psi = C_1 e^{-\frac{\beta x}{r}} + C_2 - Jy \tag{20}$$

i.e.

$$V = \frac{-C_1\beta}{r} e^{-\frac{\beta x}{r}} = V_0 e^{-\frac{\beta x}{r}} \quad U = J \tag{21}$$

where $V = V_0$ at $x = 0$, i.e. any transport in the y direction decreases exponentially towards the east (positive x direction). The meridional transport V increases as β increases, and decreases as r increases. The rate of decay of V increases as β increases or r decreases. For $r \to 0$, $V \to 0$ i.e. there can be no meridional transport in a frictionless, rotating, constant depth ocean (*see* e.g. Neumann 1960).

Case II - Variable Depth Ocean $\beta = 0$: For the case of a variable depth ocean with $\beta = 0$, equation 12 reduces to

$$r \frac{\partial^2 \psi}{\partial x^2} = g\rho \frac{\partial \xi}{\partial y} \frac{\partial D}{\partial x} = - r\beta \frac{2\pi a}{\ell} \sin \frac{2\pi x}{\ell}$$

which has a solution

$$\psi = \frac{Ba\ell}{2\pi} \sin \frac{2\pi x}{\ell} + C_1 x + C_0 - Jy$$

$$\frac{\partial \psi}{\partial x} = V = Ba \cos \frac{2\pi x}{\ell} + C_1$$

i.e. for

$$C_1 = 0,$$

$$V = 0 \text{ at } x = \frac{\ell}{4}$$

This is the Ekman type deflection. The streamlines have the same form in the horizontal plane as the bathymetry has in the vertical but are 90° out of phase.

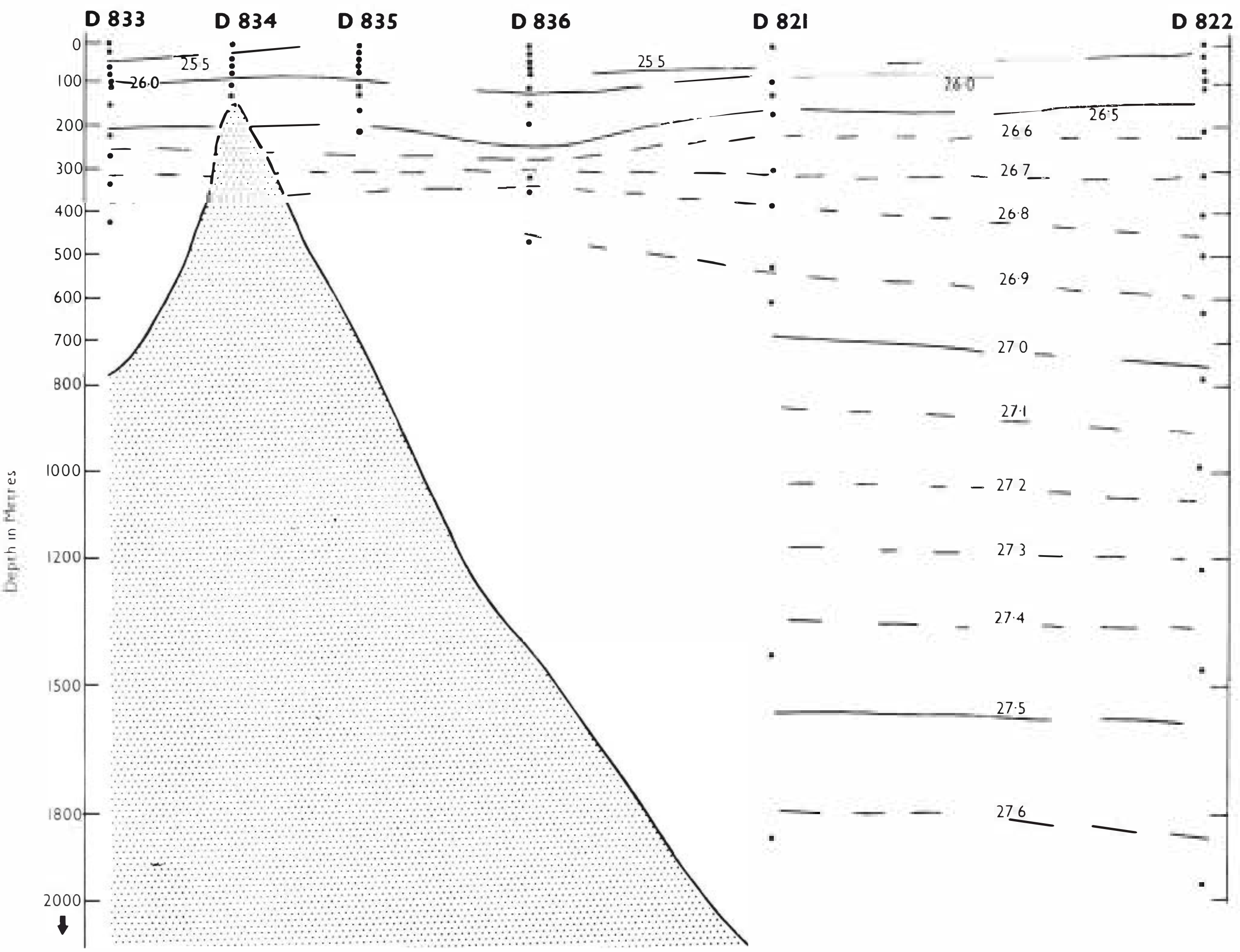

Fig. 22. Cross-sectional plot of sigma-T between Stns D822, D833. These station positions are shown in Fig. 4.

Case III - Variable Depth Ocean r = 0 : In this case equation 10 reduces to

$$\frac{\partial\psi}{\partial x}\beta = -g\rho\,\frac{\partial\xi}{\partial y}\,a\,\frac{2\pi}{\ell}\,\sin\frac{2\pi x}{\ell}$$

which has a solution

$$\psi = \frac{\xi\rho\,\frac{\partial\xi}{\partial y}a\,\cos\frac{2\pi x}{\ell}}{\beta} + C_1 = Jy$$

The meridional transport is given by

$$\frac{\partial\psi}{\partial x} = V = -\,\frac{Ba}{\xi}\,\frac{2\pi}{\ell}\,\sin\,\frac{2\pi x}{\ell}$$

which is zero at x = 0. The stream function is in phase with the bottom topography and is $\pi/2$ out of phase with the previous case. This is the Sverdrup type deflection.

From the above brief analysis we see that in equation 17 the exponential term arises from the interaction between the change of planetary vorticity (β) and frictional (r) terms, the sine term from the interaction between the frictional and topographic terms (the Ekman type deflection), and the cosine from the interaction between the planetary vorticity and the topographic terms (Sverdrup type deflection).

The Influence of the Bottom Topography Near East Cape

In the region to the north of Cape Runaway (Fig. 15) the flow is mainly zonal (Figs 5-7). Therefore for the boundary condition V = 0 at x = 0, using equation 18, we have Jy is linearly related to

$$M\,(\frac{2\pi}{E\ell})^2\,e^{-Ex} + \frac{2\pi}{E\ell}\,M\,\sin\,\frac{2\pi x}{\ell} + M\,\cos\,\frac{2\pi x}{\ell}$$

$$= S = MQ \qquad (22)$$

on a mass transport streamline. From equation 19 we have a similar relationship for the other boundary condition.

The quantity S has been computed for both boundary conditions by taking successive increments of 1 kilometre in x along five separate lines across the bottom topography found near East Cape. (Positions of the lines are shown in Fig. 15. Parameters for lines A and A^1 are the same.) Along these lines the portion of interest, the western side of the Kermadec Trench, has been approximated by the function

$$D = D_0 + a\,\cos\,\frac{2\pi x}{\ell}$$

where D is the depth, D_0 and a are constants on any one line, x = 0 represents the top of the East Cape Ridge or Ranfurly Bank (Fig. 15) and x = ℓ/2 represents the bottom of the Kermadec Trench.

Latitudinal and Longitudinal Variations on a Streamline : Equation 18 may be written in the form

$$\psi = -\,Jy + MQ \qquad (23)$$

where

$$Q = (\frac{2\pi}{E\ell})^2\,e^{-Ex} + \frac{2\pi}{E\ell}\,\sin\,\frac{2\pi x}{\ell} + \cos\,\frac{2\pi x}{\ell}$$

In the sinusoidal terms ℓ corresponds to the wave length, and the amplitude of the sine and exponential terms decrease as ℓ increases. Along a transport streamline (say ψ = 0) with a constant ℓ we have

$$Jy = QM \quad \text{or} \quad (y_2 - y_1) = \frac{M}{J}\,(Q_2 - Q_1) \qquad (24)$$

where y_2, y_1 are latitudinal co-ordinates of the streamline at the top of the ridge and the bottom of the trench respectively. Expanding equation 24, assuming the zonal transport at the top of the ridge is given by

$$U = J = \frac{D_T g}{f}\,\frac{\partial\xi}{\partial y}\,\rho$$

where D_T is the depth of the water above the top of

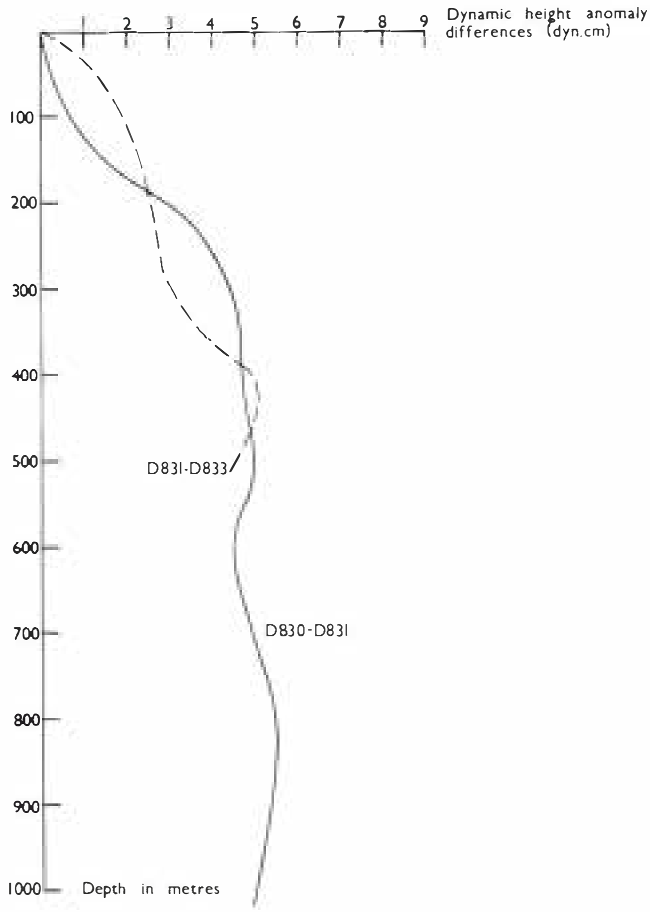

Fig. 23. Changes in the dynamic height anomaly difference (dyn. cm.) with depth (m) between Stn pairs D831-D833 and D830-D831.

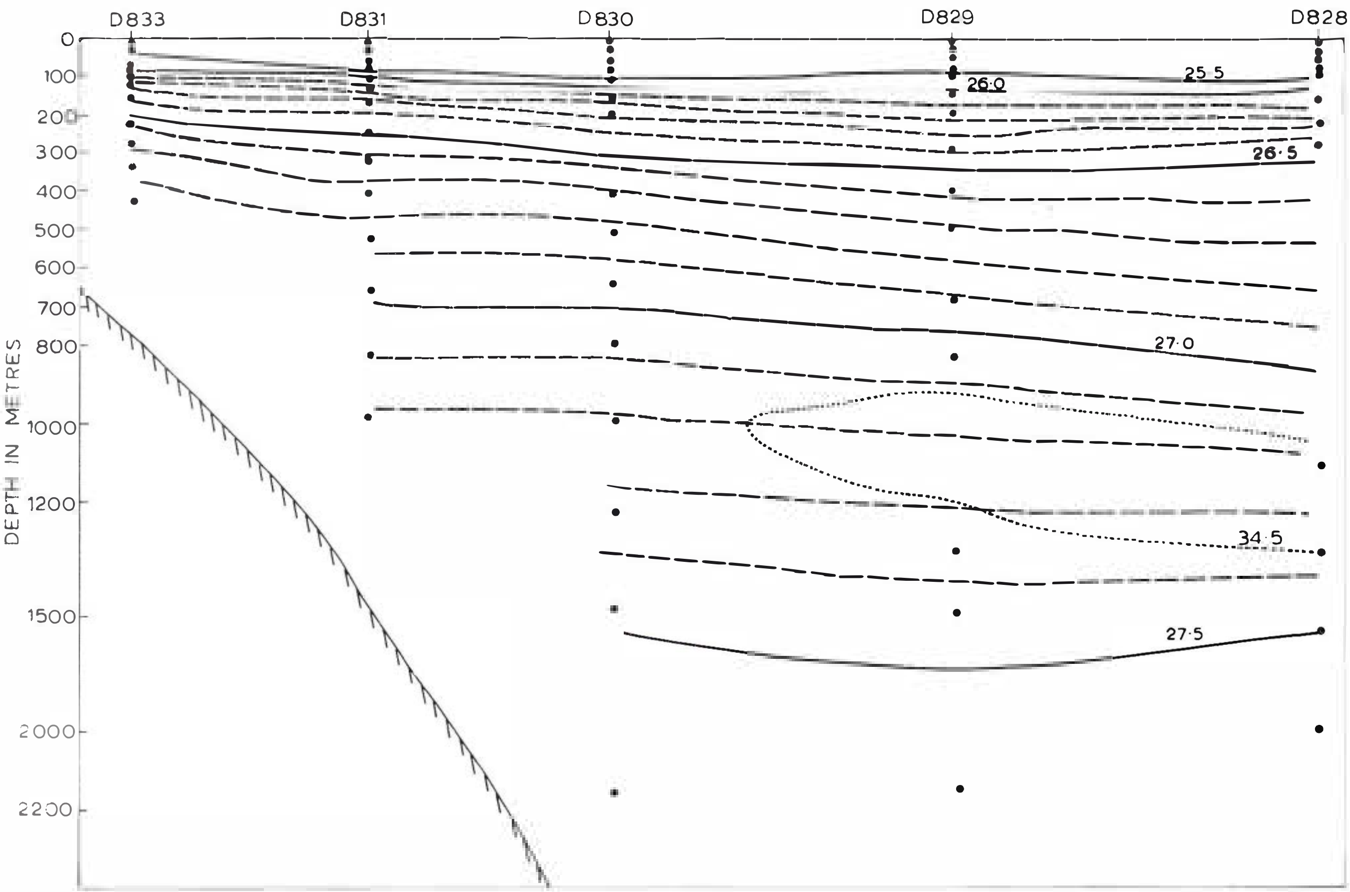

Fig. 24. Cross-sectional plot of sigma-T for a line of stations occupied north from East Cape in March 1969. The 34.5‰ isohaline which marks the core of the Intermediate Water is also shown. The station positions are shown in Fig. 4.

the ridge, we have

$$y_2 - y_1 \simeq \frac{g\rho}{r}\frac{\partial\xi}{\partial y} \frac{af\ (Q_2 - Q_1)}{[E + \frac{1}{E}\ (\frac{2\pi}{\ell})^2]\ D_T\ \frac{\partial\xi}{\partial y}\ \rho} \qquad (25)$$

$$\simeq \frac{af\ (Q_2 - Q_1)}{D_T\ [E + \frac{1}{E}\ (\frac{2\pi}{\ell})^2\ ]}$$

On a streamline, as a, the amplitude of the bathymetry oscillation increases, so does the latitudinal variation, and, as D_T the depth at the top of the ridge, increases the latitudinal variation decreases. For the case of V = 0 at x = 0 with typical values of ℓ for this region and E (E = 0.5 x 10 ^{5}) it is seen that because $2\pi/E\ell > 1$ the exponential term dominates; the flow is directed south by the bottom topography and the initial vorticity balance appears to be between the planetary vorticity (βv) and vorticity generated through friction (r $\partial v/\partial x$). The streamlines are deflected southward, with the latitudinal distance towards the south before the streamlines are markedly affected by the sinusoidal terms being given by

$$(\frac{2\pi}{E\ell})\ e^{-Ex} = 1 \quad \text{i.e. } 76 = 4 \times 10^5\text{m},\ Dy = 6 \times 10^6\text{m}.$$

(Note that with ℓ large the exponential term will not dominate if $2\pi/E\ell < 1$).

For the case of V = 0 at x = $\ell/4$ the exponential term is not dominant. The latitude and longitude variations on streamlines for five different bottom temperatures for this case are given in Table 1 and a streamline for line C (Fig. 15) is shown in Fig. 16.

Comparisons of the Theoretical Influence of the Bottom Topography Near East Cape with the Geostrophic Currents

Flow South of 37°S : The zonal geostrophic flow between Cape Runaway and East Cape south of 37°S (approx.) (Figs 5, 6) satisfies the boundary condition V = 0 at the top of the Ranfurly Bank (x = 0). The deflection caused by the bottom topography from the top of the Ranfurly Bank into the Kermadec Trench is in the same sense as the observed deflection. In the theoretical case, the flow south of East Cape is approximately meridional between East Cape and Cape Kidnappers (Fig. 5) but any further comparison of the theoretical and observed streamlines is limited by the following two facts :-

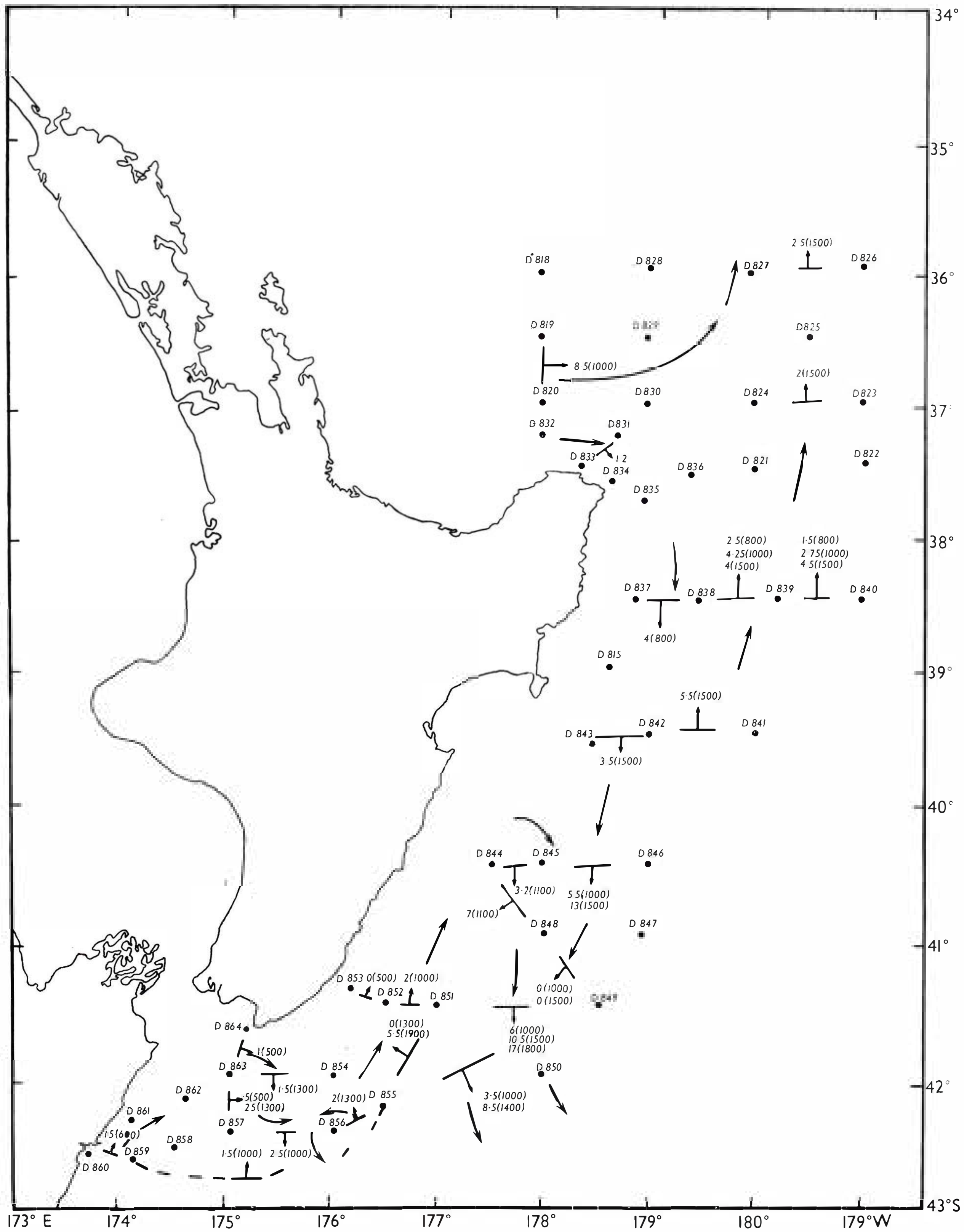

Fig. 25. Geostrophic volume transports between station pairs occupied in February/March 1969. The value outside the brackets gives the volume transport in Sverdrups ($\approx 10^6\,m^3\,sec^{-1}$) in the direction of the arrow above the reference surface (dbars) shown within the brackets (i.e. assuming the speed of the current component perpendicular to the station pair is zero at the reference surface).

1. In the theoretical results the meridional bottom gradient was assumed to be zero, whereas the axis of the Kermadec Trench lies at a slight angle to the meridians (Fig. 15) and is limited in the south by the Chatham Rise. The Chatham Rise is situated at approximately 44°S and extends in a near-zonal direction with a minimum depth of approximately 200 m.

2. South of Cape Turnagain, the Southland Current flows northwards between the east coast of New Zealand and the East Cape Current (the model does not hold in this region, the boundary condition U = 0 not being satisfied) and is eventually totally absorbed in the East Cape Current. The northwards flow of the Southland Current tends to push the East Cape Current further offshore south of Cape Turnagain.

Flow North of 37°S : To the north of 37°S near East Cape the observed flow is in an anticlockwise direction (Figs 5-7) and some of the water which is diverted clockwise around East Cape south of 37°S re-enters the general meridional flow east of longitude 179°E.

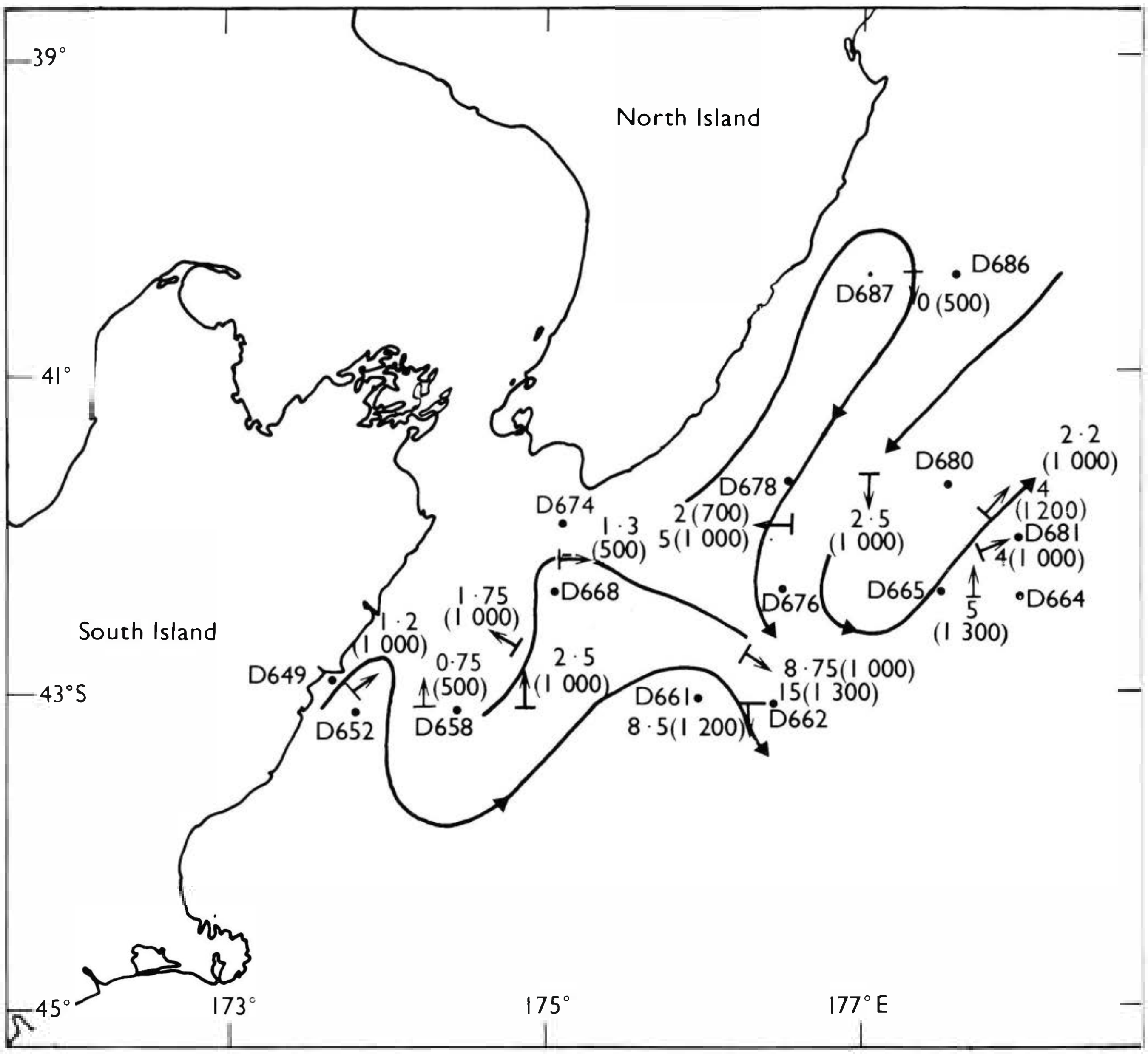

Fig. 26. Geostrophic volume transports between station pairs occupied in September/October 1967. The value outside the brackets gives the volume transport in Sverdrups ($\approx 10^6$ m ^{3}sec^{-1}) in the direction of the arrow above the reference surface (dbars) shown within the brackets (i.e. assuming the speed of the current component perpendicular to the station pair is zero at the reference surface).

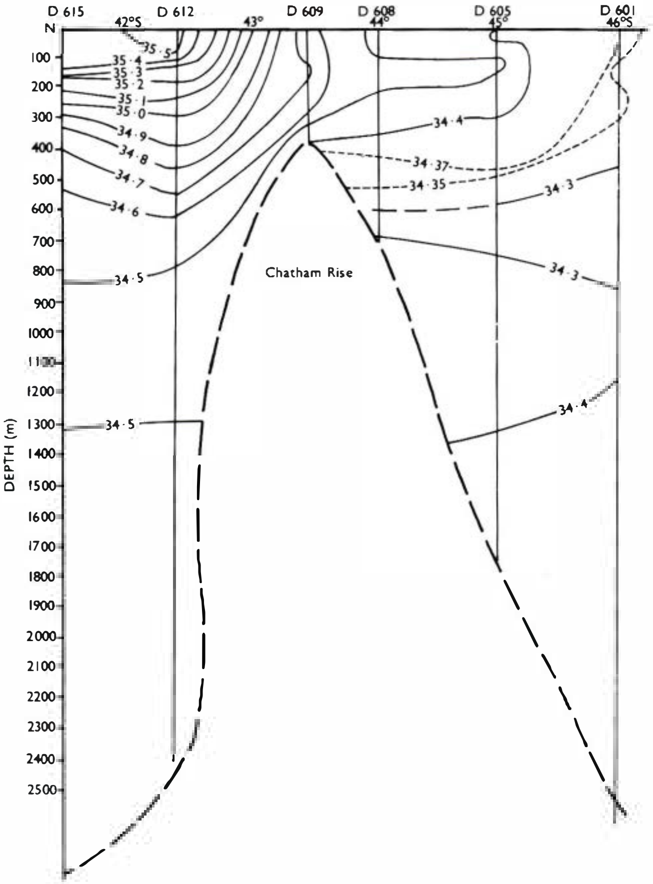

Fig. 27. Meridional salinity (‰) cross-section across the Chatham Rise at longitude 178°50'E from data collected in April 1967. The depth scale is in metres. (Fig. 4 of Heath 1968).

The flow of the East Cape Current in the Hikurangi Trench results from the bottom topography near East Cape producing a perturbation on the general flow past East Cape. The tongue in the distribution of the hydrological parameters is created by the adjustment of the mass field to the current.

The observed flow north of 37°S near East Cape cannot be explained solely by the effect of the bottom

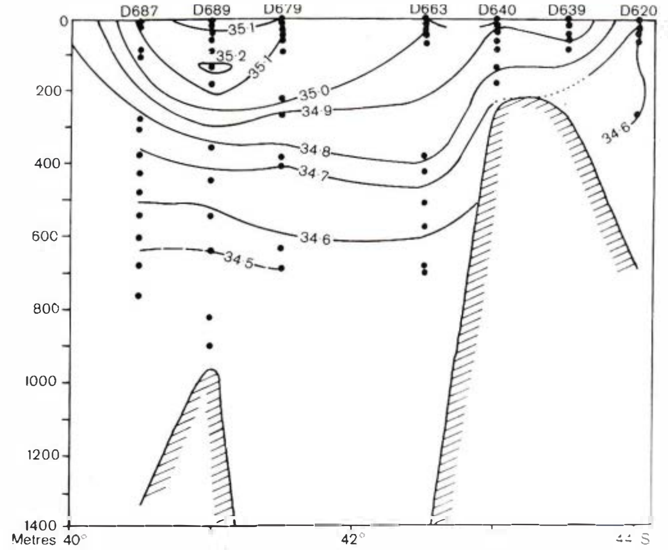

Fig. 28. Meridional salinity (‰) cross-section across the Chatham Rise at longitude 177°00'E from data collected in September/October 1967.

topography used in the theoretical investigation (i.e. the western side of the Kermadec Trench). North of 37°S the depth decreases as the water flows eastward towards the East Cape Ridge and from the theoretical investigation a deflection of the streamline towards the north would be expected. This deflection is observed in the geostrophic currents. At the top of the East Cape Ridge north of 37°S the flow is nearly meridional and the flow satisfies approximately the boundary condition $V = 0$ at $x = \ell/4$. For this boundary condition ($V = 0$ at $x = \ell/4$) the theoretical streamlines turn southwards at $x = \ell/4$. The observed geostrophic circulation is, however, not as simple as this although there is a southwards deflection over the Kermadec Trench (*see* Fig. 13). North of latitude 37°S the theoretical streamlines differ from the observed geostrophic circulation. Possibly closer agreement could be obtained by considering a complex bathymetry but at present this is not warranted as the data from which the circulation (Figs 12-14) was deduced were collected in different years and thus only the broad circulation is represented.

EAST CAPE CURRENT SOUTH OF EAST CAPE

The East Cape Current flows southwards along the western side of the Hikurangi Trench and mixes on its coastal side south of approximately latitude 40°S with the Southland Current flowing in from the west (Figs 5-7). This combined current continues south and is deflected eastwards at approximately latitude 42°S. Where this deflection occurs an anticyclonic eddy is formed. Part of the water that does not recirculate in the eddy flows northward along the eastern side of the Hikurangi Trench forming the outer arm of the East Cape Current System (Figs 5-7), while the rest meanders towards the northeast (Figs 12-14). The current speeds in this meandering flow are slower than in the tongue of the East Cape Current System.

THE ANTICYCLONIC EDDY IN THE EAST CAPE CURRENT

The anticyclonic eddy formed in the tip of the tongue of the East Cape Current System has been

Sig. 5

TABLE 4. Source of data, period of collection, and longitudinal positions of lines of hydrological stations occupied across the Subtropical Convergence east of New Zealand. The surface salinity and temperature ranges across the Convergence are also given.

Source of Data	Period Collected	Longitude	Surface Salinity Range North limit	Surface Salinity Range South limit	Surface Temperature Range North limit	Surface Temperature Range South limit
Garner 1967b	18 February to 1 March 1963	178°20' E	35.4‰ 42°00' S	34.6‰ 43°00' S		
Heath 1968	11 to 16 April 1967	177°20' E	35.5‰ 42°25' S	34.5‰ 43°50' S	18 °C 42°30' S	14 °C 43°30' S
Heath 1968	11 to 16 April 1967	178°30' E	35.5‰ 42°20' S	34.6‰ 44°00'S	18 °C 42°40' S	14.5°C 43°10' S
Heath 1972a	25 September to 11 October 1967	177°00' E	35.0‰ 43°00' S		11.5°C 43°00' S	
Ridgway (pers. comm.)	20 January to 2 February 1969	179°00' W	35.5‰ 42°00' S	34.4‰ 45°00' S	18 °C 42°00' S	15° C 45°30' S
	22 to 26 January 1969	174°00' W	35.0‰ 45°00' S	34.5‰ 45°30' S	17 °C 45°00' S	15° C 45°50' S

noted by previous authors (Sdubbundhit and Gilmour 1964; Garner 1967a; Heath 1968, 1972a). The approximate position of the centre of this eddy found during the cruises conducted in this area are listed in Table 2. The centre of the eddy is generally found slightly to the east of the axis of the Hikurangi Trench (Fig. 5) (Table 2); this position most likely results from the Southland Current forcing the East Cape Current to the east. A longitudinal sectional salinity plot through this anticyclonic eddy is shown in Fig. 17 and a zonal cross-sectional plot in Fig. 18. The anticyclonic eddy was developed from the sea surface to bottom with isolines of salinity, temperature and density sloping downwards towards the centre of the eddy. The cool, low salinity water of the Southland Current meets the warm, saline Subtropical Water of the eddy on its western and southern sides and on these sides the slopes of the isolines are largest. At the surface the presence of the eddy is masked to some extent by mixing between the different water types and consequently it is best defined from subsurface measurements (*compare* Figs 8, 10). The salinity of the Intermediate Water decreases from the centre of the anticyclonic eddy outwards (Fig. 19). Garner (1967a) attributed the higher salinity in the centre of the eddy to the relatively long residence time of the water in the eddy which allows a greater amount of vertical mixing to occur. The Intermediate Water appears to mix predominantly with overlying Subtropical Water rather than with the underlying Deep Water (Garner 1967a).

Plots of the relative geostrophic current speeds with depth in the anticyclonic eddy from several sets of data collected in this area are shown in Fig. 20 [Stns B757, B767, B771, B772 February/March 1963 (Garner 1967a); Stns D613, D617 April 1967 (Heath 1968); Stns D675, D676 October 1967 (Heath 1972a); Stns D847, D848, D850 March 1969 (Appendix II]. Because a reference surface of 1500 dbars was used in drawing these plots and, because the station pairs

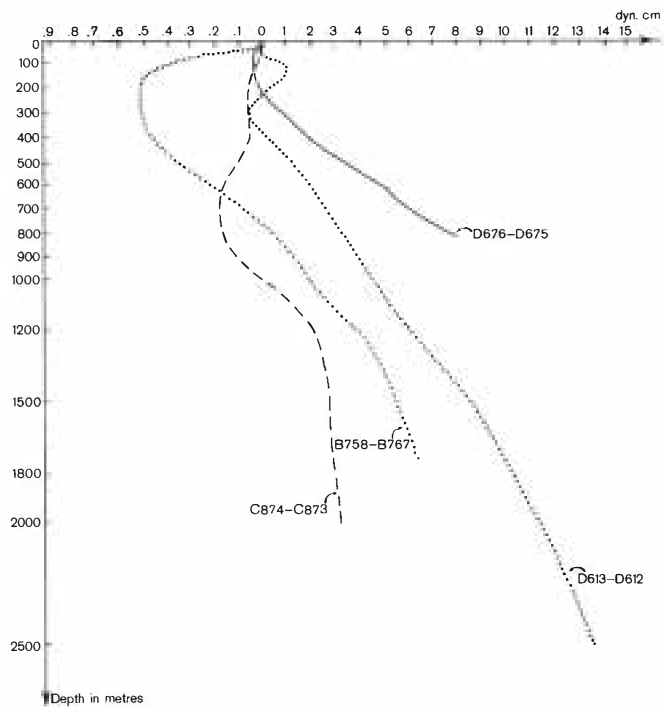

Fig. 29. Changes in the dynamic height anomaly differences (dyn. cm) with depth (m) for four station pairs occupied off the east coast of New Zealand at different times.

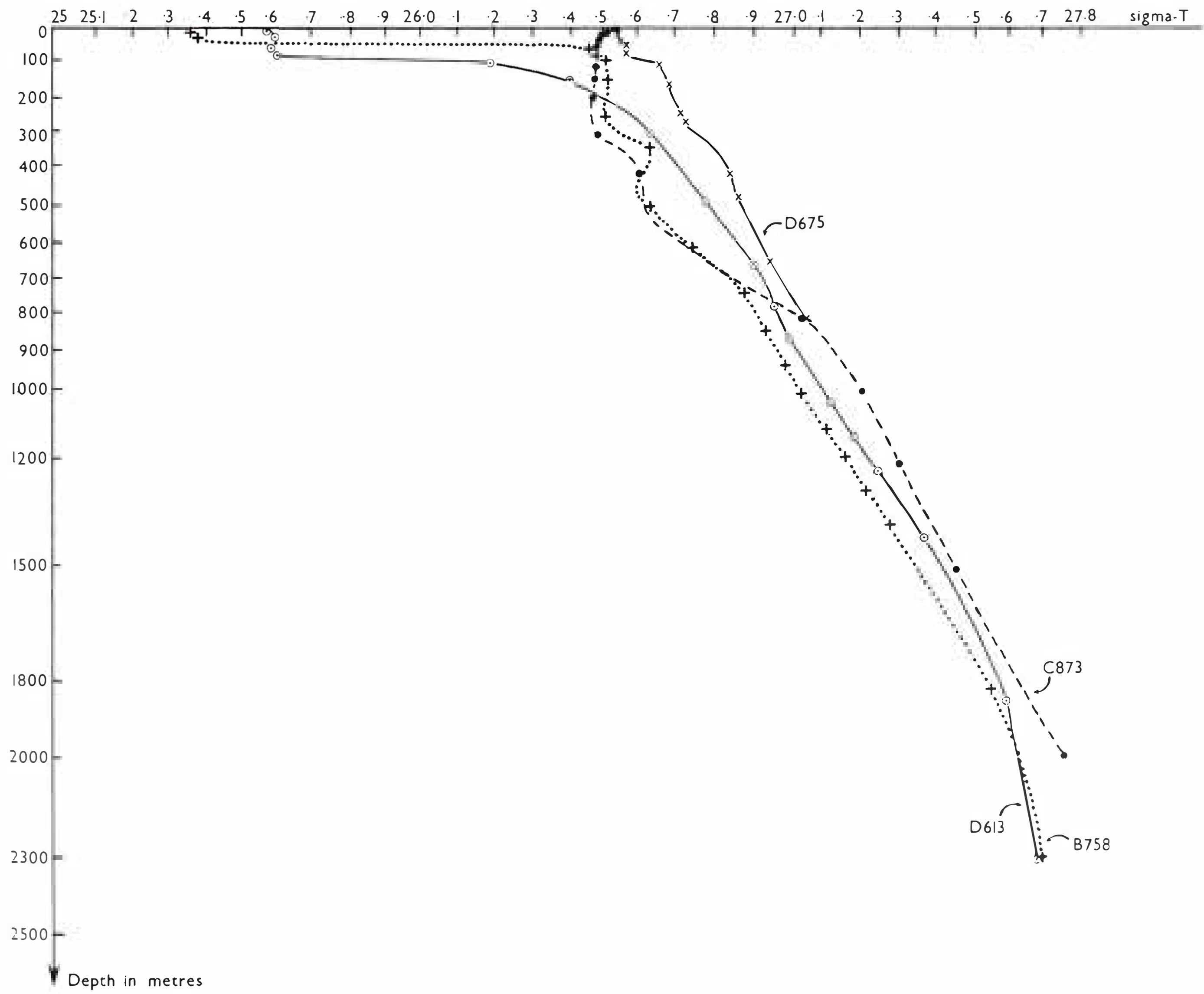

Fig. 30. Variations of sigma-T with depth at four stations occupied off the east coast of New Zealand.

were most likely not in the most intense regions of the eddy, too much emphasis should not be placed on the absolute speeds in Fig. 20.

The currents in the upper 200 m in winter (Stn pair D676, D675) are nearly constant whereas in summer the current gradient is nearly uniform in the upper 1500 m; the change in structure will be elaborated on in a later section (p. 41). Better definition of the currents was achieved by closer station spacing during the September/October 1967 cruise, and this is reflected in the larger current speeds between Stns D676, D675 compared to the other station pairs.

Approximating the currents (Fig. 20) by a linear speed/depth relationship $C = kZ + d$, where C is the speed, Z the depth (positive upwards), k the slope of the speed/depth curve and d the surface speed, we can calculate the average potential and kinetic energies per unit area between station pairs in the eddy. The kinetic energy per unit area of a column of water of depth Z is given by

$$\text{kinetic energy} = -\frac{1}{2}\int_0^{-z_B} \rho\,(k\,z + d)^2\,dz$$

$$= -\frac{1}{2}\,\rho\,z_B\left[\frac{k^2 z_B^2}{3} + d^2 - d\,k\,z_B\right]$$

where ρ is the density. The potential energy in the flow relative to the homogeneous undisturbed ocean, taking the zero of potential energy at $Z = -Z\beta$, is given by

$$\text{potential energy} = \frac{\int_0^L \int_{-z_B}^0 \rho\,\Delta D\,dz\,dx}{\int_0^L dx} = L\rho f\,z_B\,\frac{C}{4}$$

where ΔD is the horizontal difference in dynamic height anomaly at length x from the centre of the eddy, i.e. $\Delta D = D_0 - ax$ where D_0 is the dynamic height anomaly at the centre of the eddy and a is a constant given by $a = D_0/L$. In these formulae the density given explicitly has been assumed to be constant.

The kinetic, potential and total energies, together with the values of k, d and L used in the calculation for Stn pairs D675-D676 and D847-D850 are given below. Between Stns D675-D676 the current was uniform in the upper 200 m and therefore the slope below 200 m has been used to give a current of 0.44 m s^{-1} at the surface.

Station Pair	k s^{-1}	d $m\,s^{-1}$	ℓ km	PE $J.m^{-2}$	KE $J.m^{-2}$	Total Energy $J.m^{-2}$
D675-D676	$+2.9 \times 10^{-4}$	0.44	38	0.65×10^{6}	3.4×10^{5}	1×10^{6}
D847-D850	$+1.33 \times 10^{-4}$	0.20	84	0.65×10^{6}	7×10^{4}	0.7×10^{6}

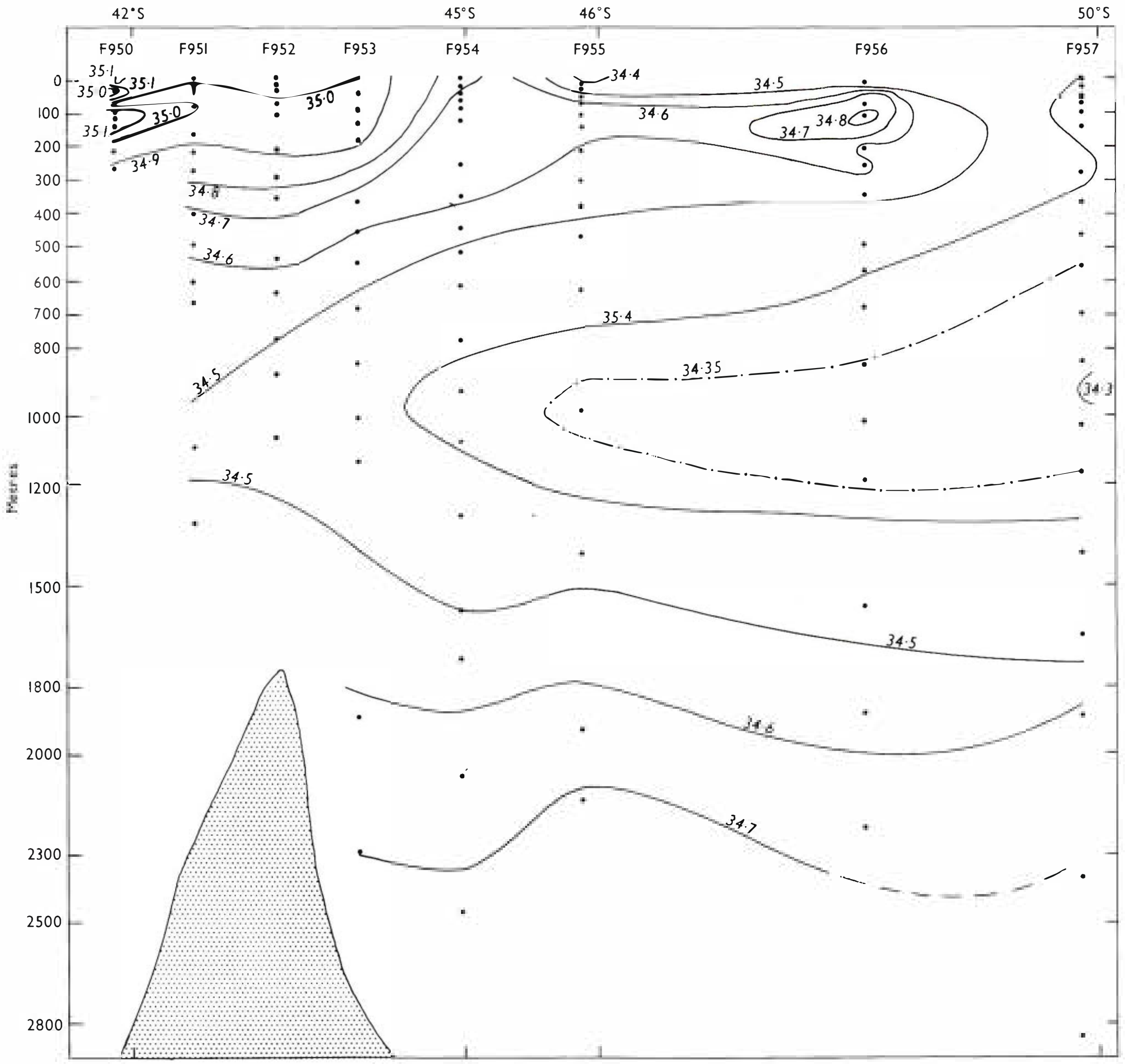

Fig. 31. Meridional salinity (‰) cross-section immediately east of the Chatham Islands at longitude 174°00'W from data collected in January/February 1969 by Ridgway (pers. comm.). The depth scale is in metres.

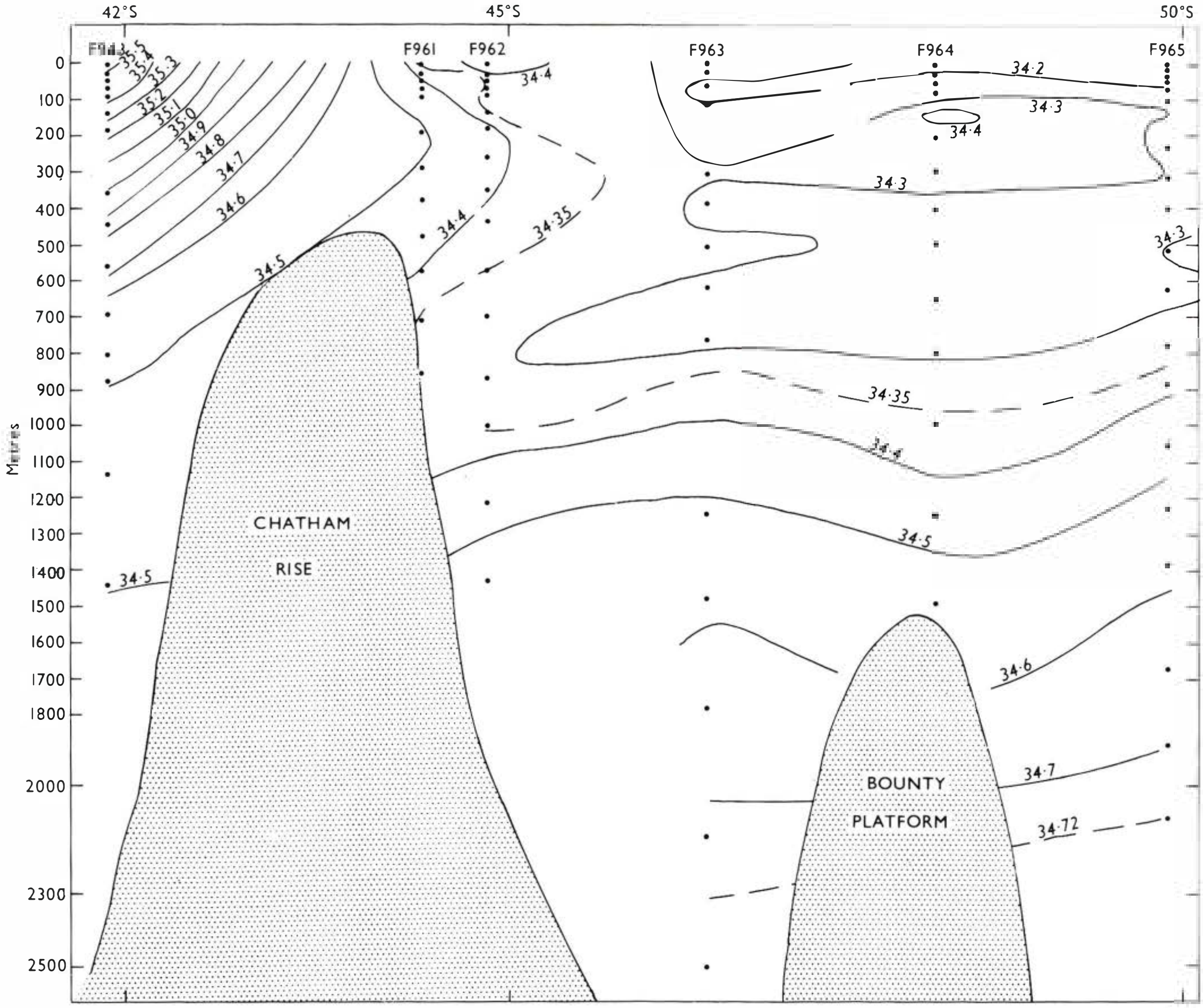

Fig. 32. Meridional salinity (‰) cross-section across the Chatham Rise at longitude 179°00'W from data collected in January/February 1969 by Ridgway (pers. comm.). The depth scale is in metres.

The range within which the energy in this eddy off the east coast falls (using the station spacings given above as radii, and the energies per unit area given above as representative of the whole eddy) and the range of energy calculated by Patzert (1969) for some eddies found near Hawaii are given below.

	Hawaiian Eddies (J)	Eddies off East Coast New Zealand (J)
Kinetic energy	$0.07 - 0.6 \times 10^{15}$	$1.5 - 1.6 \times 10^{15}$
Potential energy	$0.42 - 5.67 \times 10^{15}$	$0.3 - 2.4 \times 10^{16}$
Ratio PE/KE	5 - 40	2 - 10
Total energy	$0.49 - 6.27 \times 10^{15}$	$0.4 - 2.6 \times 10^{16}$

The total kinetic and potential energies off the east coast of New Zealand were nearly a factor of ten larger than in the Hawaiian eddies (this was also the case for the average energies) but the ratios of potential to kinetic energies were much the same.

Using the value of the total energy we can now calculate the time for which a certain velocity wind would have to blow to supply this energy and hence find if the eddy could be generated by the winds in this area. The amount of energy added per unit area to the circulation from a wind blowing parallel to the ocean current is given by

$$d\ (\text{Energy}) = \int_0^t \underline{V_0} \cdot \underline{\tau_0}\ dt$$

(Sverdrup *et al* 1942) where V_0 is the surface speed

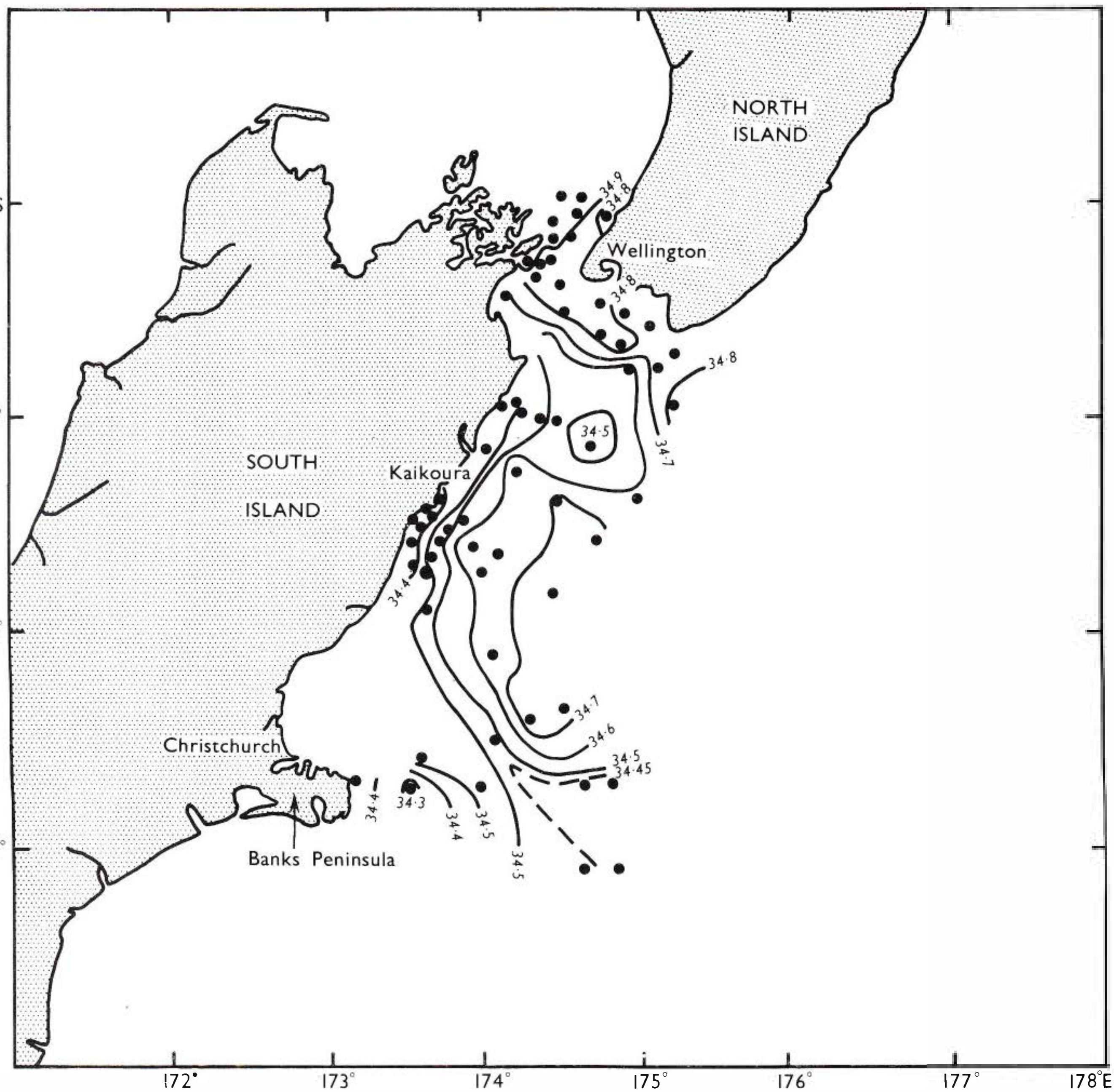

Fig. 33. Isohalines (‰) at the sea surface for data collected in November/December 1968. (Fig. 8 of Heath 1971).

of the ocean, τ_0 is the wind stress at the sea surface and t is the time for which the stress acts. Taking V_0 as half the geostrophic velocity and with a surface stress of 0.6 newton m^{-2} (i.e. a wind speed w of approximately 15 m s^{-1} using $\tau_0 = 2.6 \times 10^{-3} \rho' |w| \underline{w}$, ρ' the air density *see* Neumann and Pierson 1966), the time required to supply the energy would be 85 days for the eddy surveyed in October 1967 and 135 days for the eddy surveyed in March 1969, i.e. for the wind to supply the energy in this eddy it would need to blow at a speed of approximately 15 m s^{-1} parallel to the ocean current for a period in excess of 100 days. Alternatively, as the wind stress/wind speed relationship used has the stress proportional to the square of the wind speed if the wind speed is doubled, the time to supply the energy would be 21 days for the eddy surveyed in March 1969. As the residence time of an atmospheric anticyclone in this area is at least a factor of ten less than the time calculated above (the anticyclone takes only six days to pass over New Zealand (Garnier 1958)) it appears that the local wind plays only a minor role in supplying energy to this anticyclonic eddy.

There is evidence (Figs 5-7) that smaller anticyclonic eddies containing Subtropical Water are shed off from the East Cape Current System and move southwestwards south of the major eddy. The influence that these smaller eddies have on the hydrology of this region will be examined later in this paper.

Spatial Modification of Temperature and Salinity Characteristics of the East Cape and Southland Currents

In the southern end of the Hikurangi Trench the southwards flowing East Cape Current meets the northwards flowing Southland Current (Fig. 1). Typical T/S curves for the water in both the East Cape Current north of Hawke Bay (Stn D837) and in the Southland Current north of Banks Peninsula (Stn D860) are shown in Fig. 21. The water of the East Cape Current is modified from its original subtropical nature (e.g. at Stn D829, Fig. 21) during its passage down the east coast of the North Island. This modification results mainly from mixing with the water of the Southland Current. This process is illustrated by the sequence of Stns D829, D848 and D840 (Fig. 21). The water flowing north in the eastern branch of the East Cape Current System is of mixed East Cape Current, Southland Current origin (Stn D840, Fig. 21).

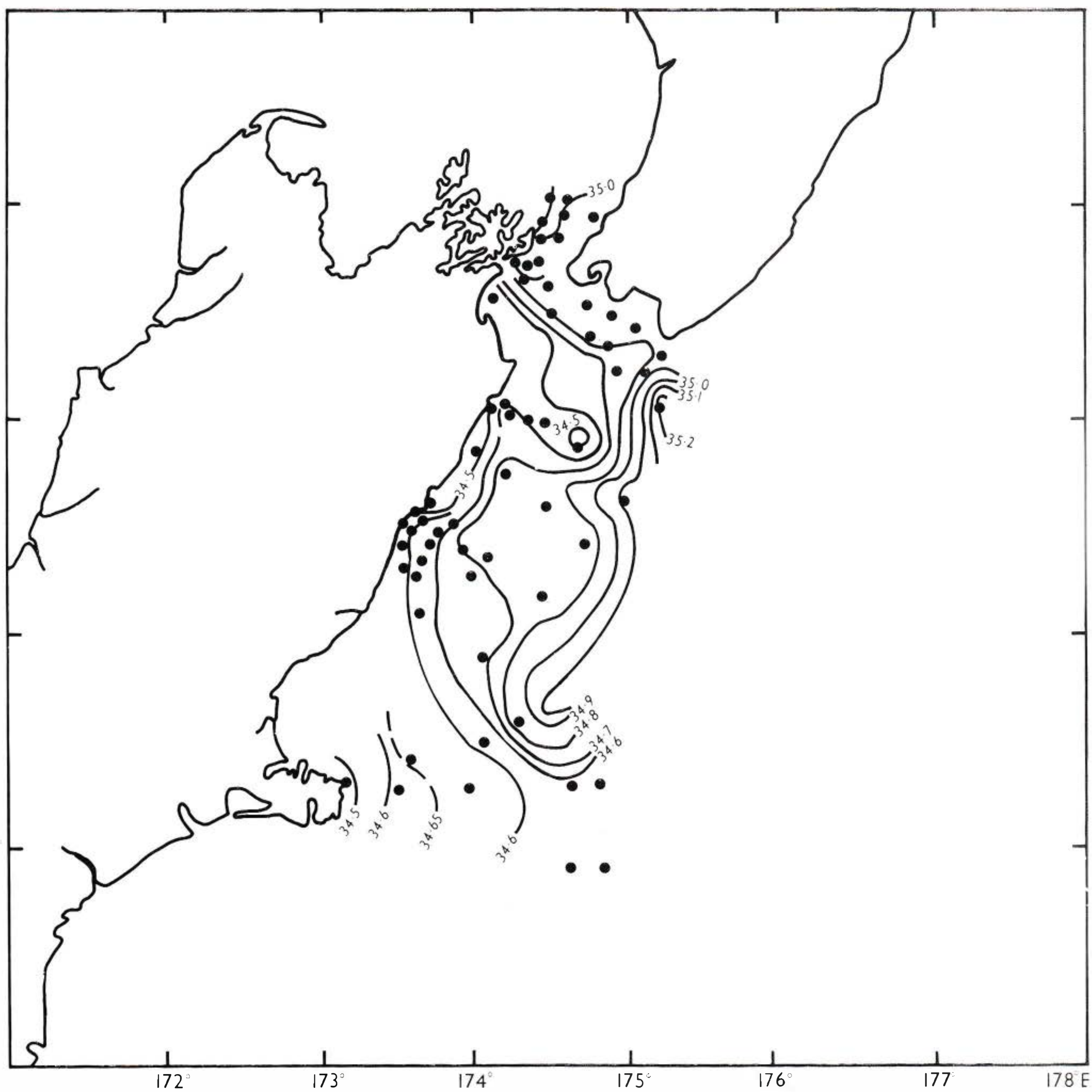

Fig. 34. Isohalines (‰) of maximum near-surface salinity (i.e. above approximately 200 m) for the data collected in November/December 1968.

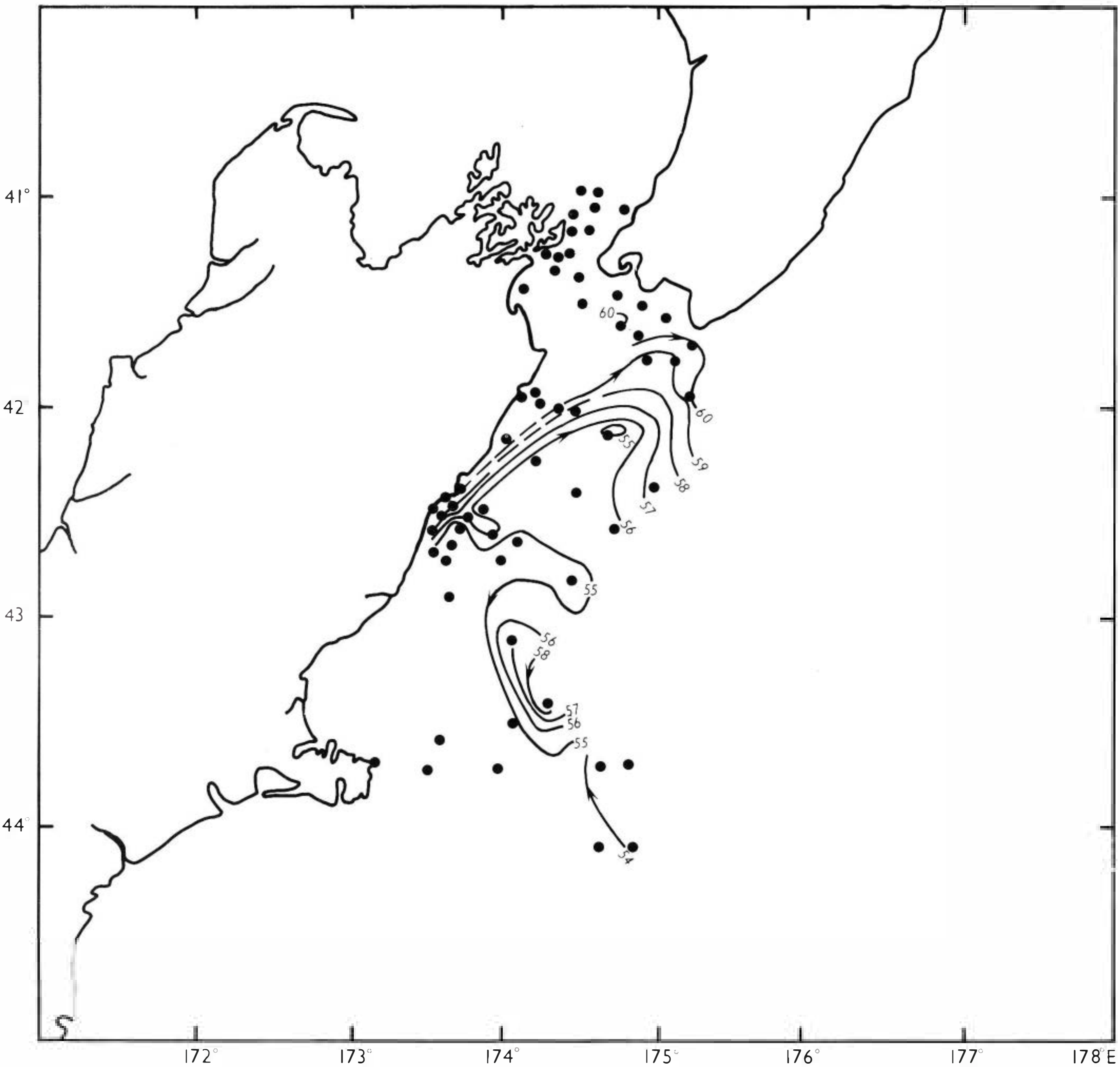

Fig. 35. Dynamic height anomaly contours (dyn. cm) at the surface relative to 400 dbars for data collected in November/December 1968. Arrows show flow direction.

The Vertical Structure of the Currents off the East Coast of New Zealand

Off the east coast of New Zealand sub-surface isolines at fixed depths are oriented similarly to the dynamic height anomaly contours (*compare* Figs 5, 8 9; *see also* Sdubbundhit and Gilmour 1964; Garner 1967a; Heath 1968, 1972a). This similarity shows that the currents adjust the mass field such that this circulation can be defined by either the horizontal salinity and temperature distribution or by the depth of the upper mixed layer. Reflection of the circulation in the 200 m temperature distribution and in the depth of the upper mixed layer raises the possibility of tracking the currents in this region by measuring the sub-surface properties at a constant depth in a similar way to that undertaken in the Gulf Stream by Fuglister and Veronis (1965).

The Seasonal Variation : During the winter cruise conducted between 19 September and 11 October 1967 (Heath 1972a) the main vertical velocity gradient of the offshore currents (i.e. East Cape and mixed East Cape - Southland Currents) existed between 200 m and

500 m rather than nearer the surface. However during the 1969 summer cruise the main vertical velocity gradient of the offshore currents existed in the upper 300 m rather than at deeper depths (*compare* Figs 5, 7, 20). Comparing the dynamic height anomaly plots between various levels in the upper 1500 m for the other hydrological surveys conducted in this region (Sdubbundhit and Gilmour 1964; Garner 1967a; Heath 1968) shows a similar situation; in winter the main vertical gradient of the offshore current occurs in the sub-surface layers (depth greater than 300 m) while in summer the vertical gradient of the current is more uniform with depth, the maximum gradient being in the upper 300 m. This seasonal change in the vertical gradient of the currents can also be seen from the seasonal change in the gradient of the linear correlation equation between the 200 m temperature (T) and the surface dynamic height anomalies DH (DH = mT + C), the change in dynamic height anomaly with the 200 m temperatures (i.e. m) being greater in summer than in winter (Table 3). Most likely the decrease in the gradient of the correlation equation results from meteorological conditions having a larger

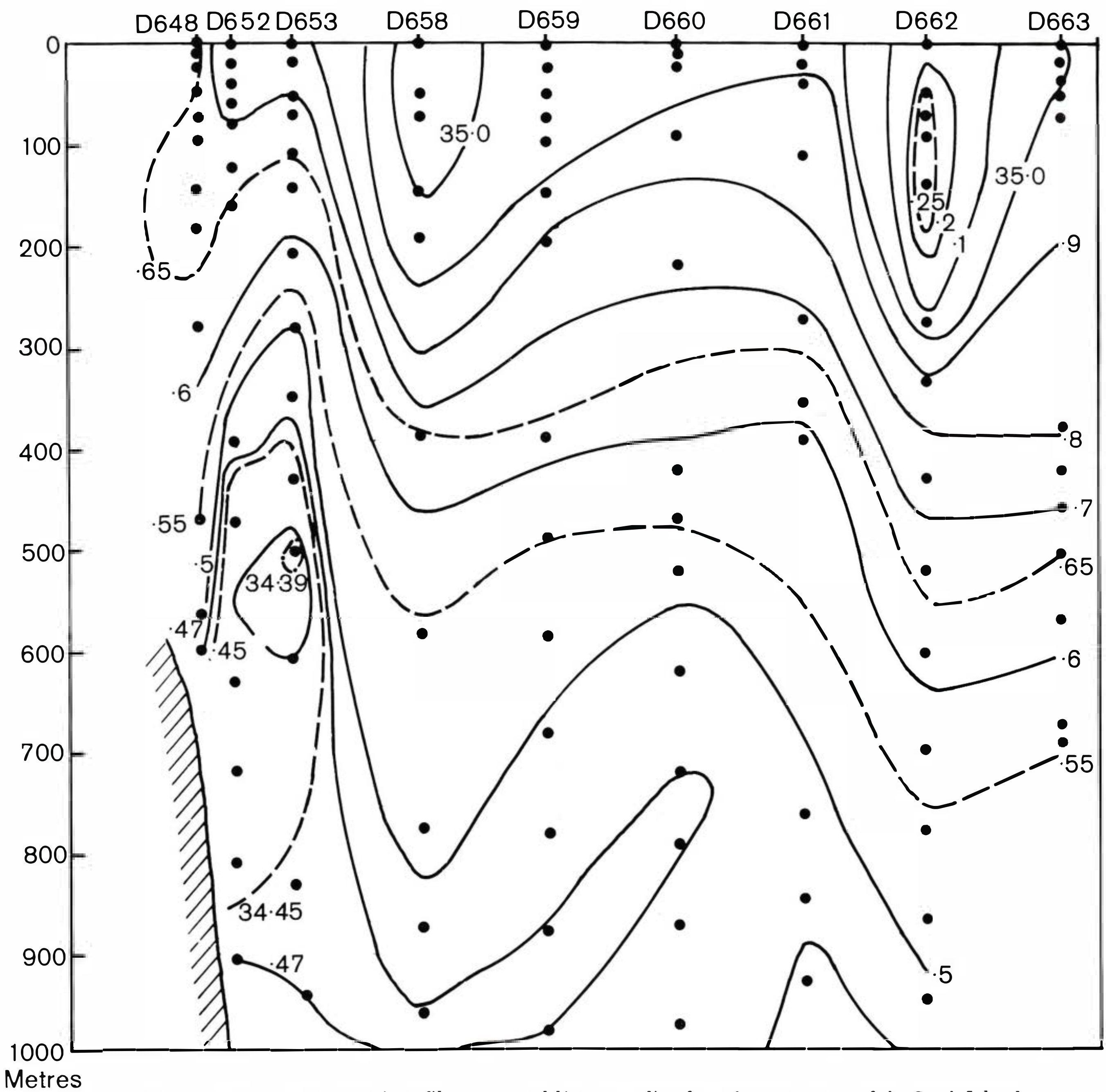

Fig. 36. Cross-sectional salinity (‰) profile on a zonal line extending from the east coast of the South Island, New Zealand, at latitude 42°30'S for data collected in September/October 1967. (Fig. 6 of Heath 1972c).

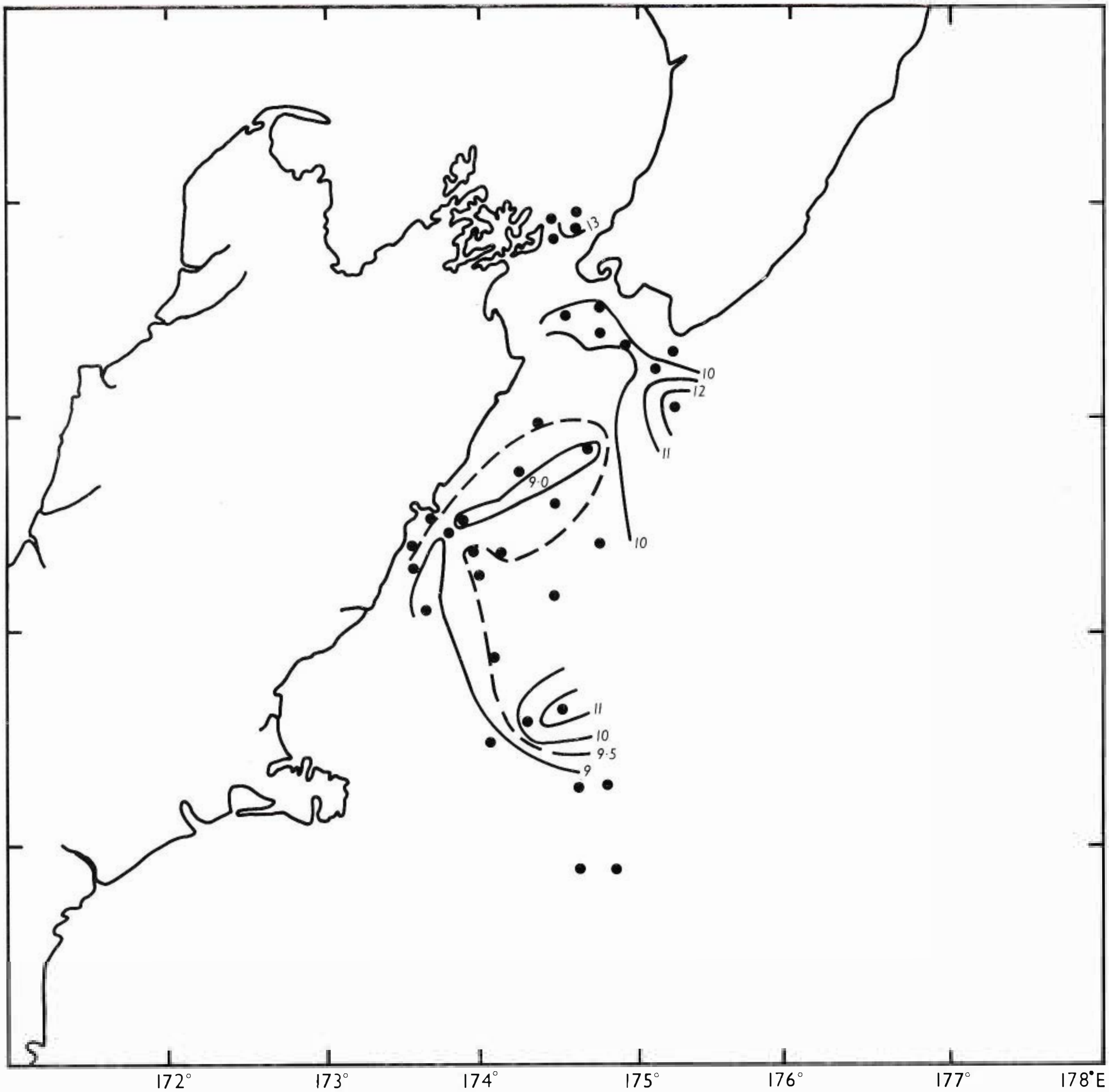

Fig. 37. Isotherms (°C) at a depth of 200 m for data collected in November/December 1968.

effect on the near surface temperature distribution in winter than in summer.

The vertical gradient of the geostrophic currents is due solely to variations in the baroclinic currents and therefore the seasonal variation in the current structure must be interpreted in terms of the seasonal changes in the mass field. During the summer surveys a well-developed thermocline was formed but this thermocline was absent in winter. The large vertical variation in the density that exists at the thermocline provides a mechanism for generating strong baroclinic currents with large horizontal pressure gradients resulting where there are large variations in depth of the thermocline. These horizontal pressure gradients produce a vertical current structure in the upper layers which is not present in winter when the thermocline is absent and the surface waters are well mixed.

The largest variation in depth of the thermocline found during the summer survey of 1969 was present where the currents were strongest (*compare* Figs 5-7, 9). A similar comparison of Garner's 1963 results shows the same effect and suggests the development of a summer thermocline may be the mechanism for continuing the vertical gradient of the currents into shallower depths in summer.

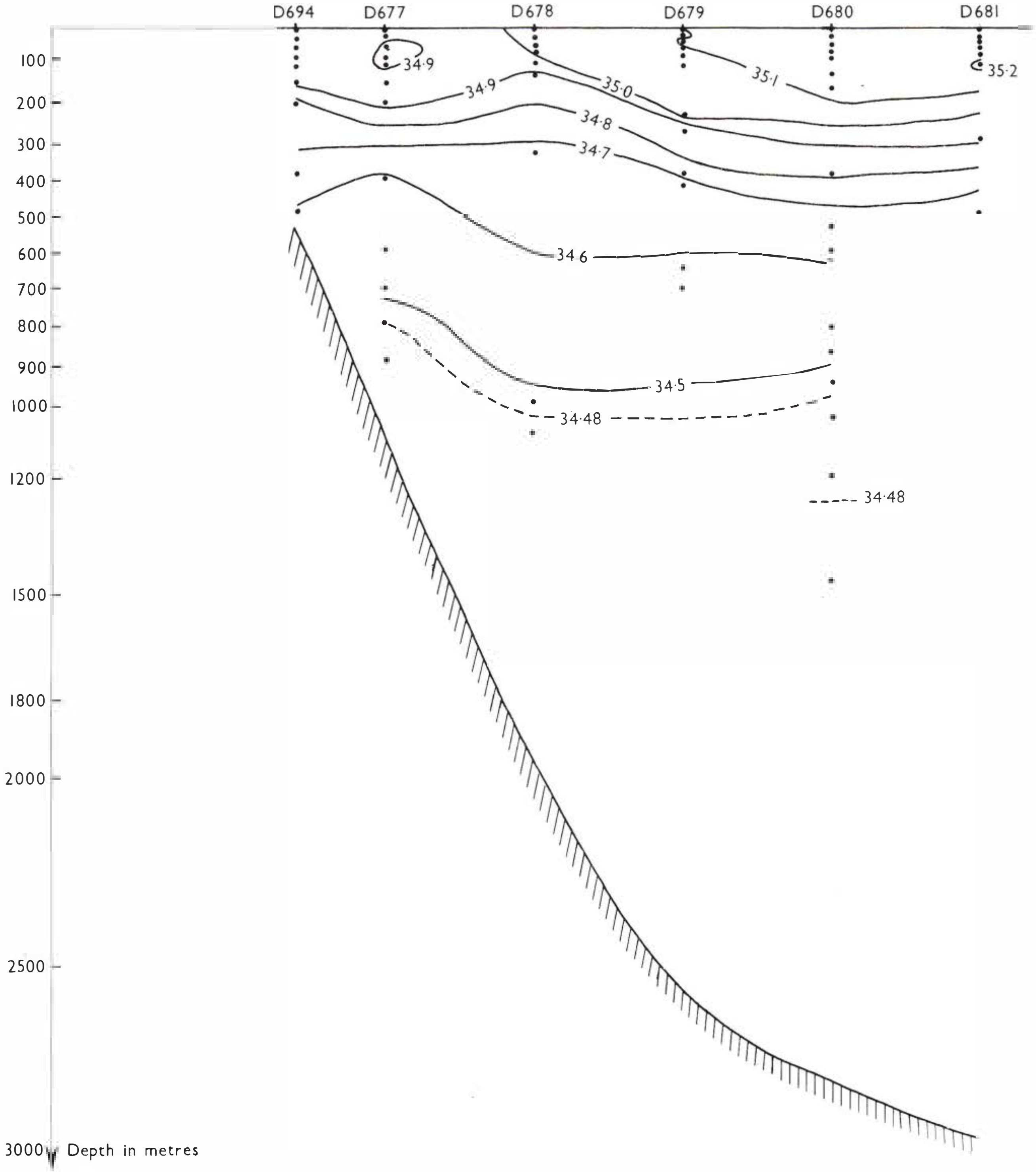

Fig. 38. Cross-sectional salinity (‰) plot at latitude 41°30'S for data collected in September/October 1967.

The Volume Transport Around East Cape

It is evident from the geostrophic circulation patterns that the transport towards the south around East Cape is not large enough to solely support the circulation in the Hikurangi Trench. There must therefore be some recirculation in the eddy centred at Stn D847 (Fig. 4). In the cross-sectional sigma-T plot in a line east from East Cape between Stns D822 and D833 (Fig. 4) there is a change in sign of the gradient of the surfaces at Stn D836 (Fig. 22). The gradient is upwards towards the coast west of D836 indicating that the East Cape Current flowed southwards there, but the stations on this line are not deep

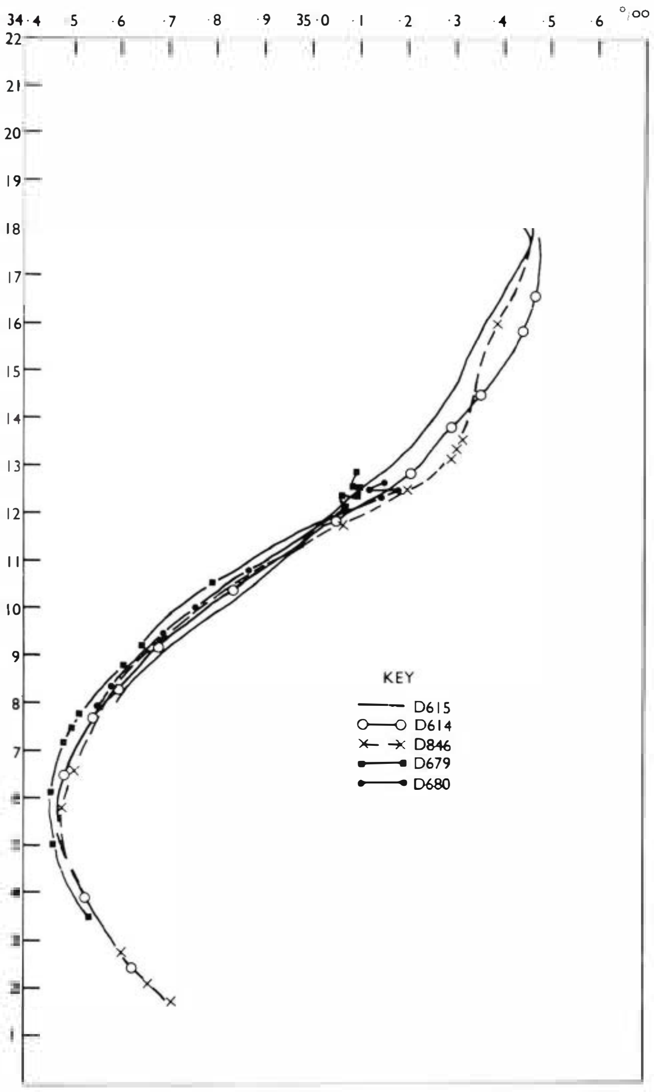

Fig. 39. Temperature (°C) / Salinity (‰) curves for Stns D614, D615 (Heath 1968), D680, D679 (Heath 1972a) and D846 (Appendix II).

enough to enable a meaningful volume transport to be computed. The geostrophic streamline (Fig. 5) and 200 m isotherm (Fig. 8) passing closest to Stn D836 also pass closest to Stn D831 and, therefore, assuming that the water passing between Stn D831 and the coast flows into the East Cape Current we can get an estimate of its transport around East Cape.

Because the current structure between Stn pairs D831, D833 and D830, D831 is similar (Figs 23, 24), by taking the volume transport between Stns D830, D831 it is possible to use a deeper reference depth (i.e. 1000 dbars) than between the other station pair to give an estimate of the transport between Stn D831 and the coast. The use of 1000 dbars was determined by the maximum depth of the data but appears to be valid, for 1000 m is approximately the average depth between Stns D831, D833 and also the Ranfurly Bank will limit the flow below that depth (Fig. 15).

The volume transport around East Cape (V_{EC}) is given by

$$V_{EC} = V_{1000\,D830-D831}\left(\frac{v_1A_1}{v_2A_2}\right)(1+K)$$

where $V_{1000\ D830-D831}$ is the geostrophic transport relative to 1000 dbars between Stns D830, D831; v_1, v_2 are the surface geostrophic current speeds relative to 500 dbars (this reference depth was also determined by the data) between Stns D831, D833; D830, D831 respectively, A_1, A_2 are the distances between the corresponding station pairs; K is the ratio of the area between Stn D833 and the coast and between Stns D831, D833. The surface geostrophic current relative to 500 dbars (v_1) is 13.2 cm s^{-1} and v_2 is 14.2 cm s^{-1} with both currents directed towards the southeast. An approximate linear bathymetry between D830 and the coast gives a value of 0.09 for K. The values for A_1, A_2 are 38×10^3m and 40.5×10^3m respectively. $V_{1000\ D830-D831}$ is 1.2 Sverdrups (1 Sverdrup = $10^6 m^3 s^{-1}$) and the approximate volume transport in the East Cape Current around East Cape is 1.16 Sverdrups.

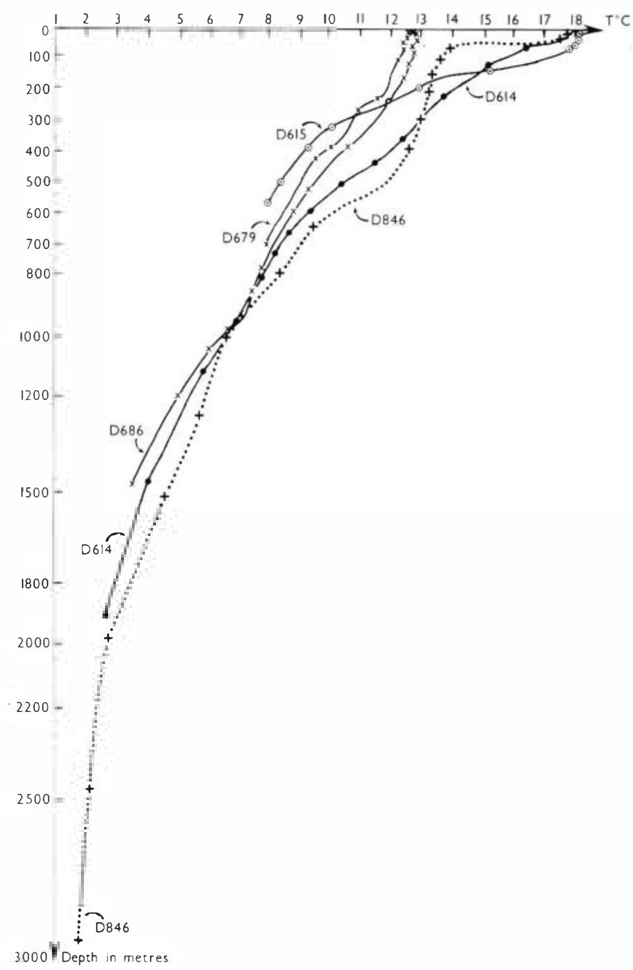

Fig. 40. Variation of temperature (°C) with depth (m) at stations occupied in the East Cape Current.

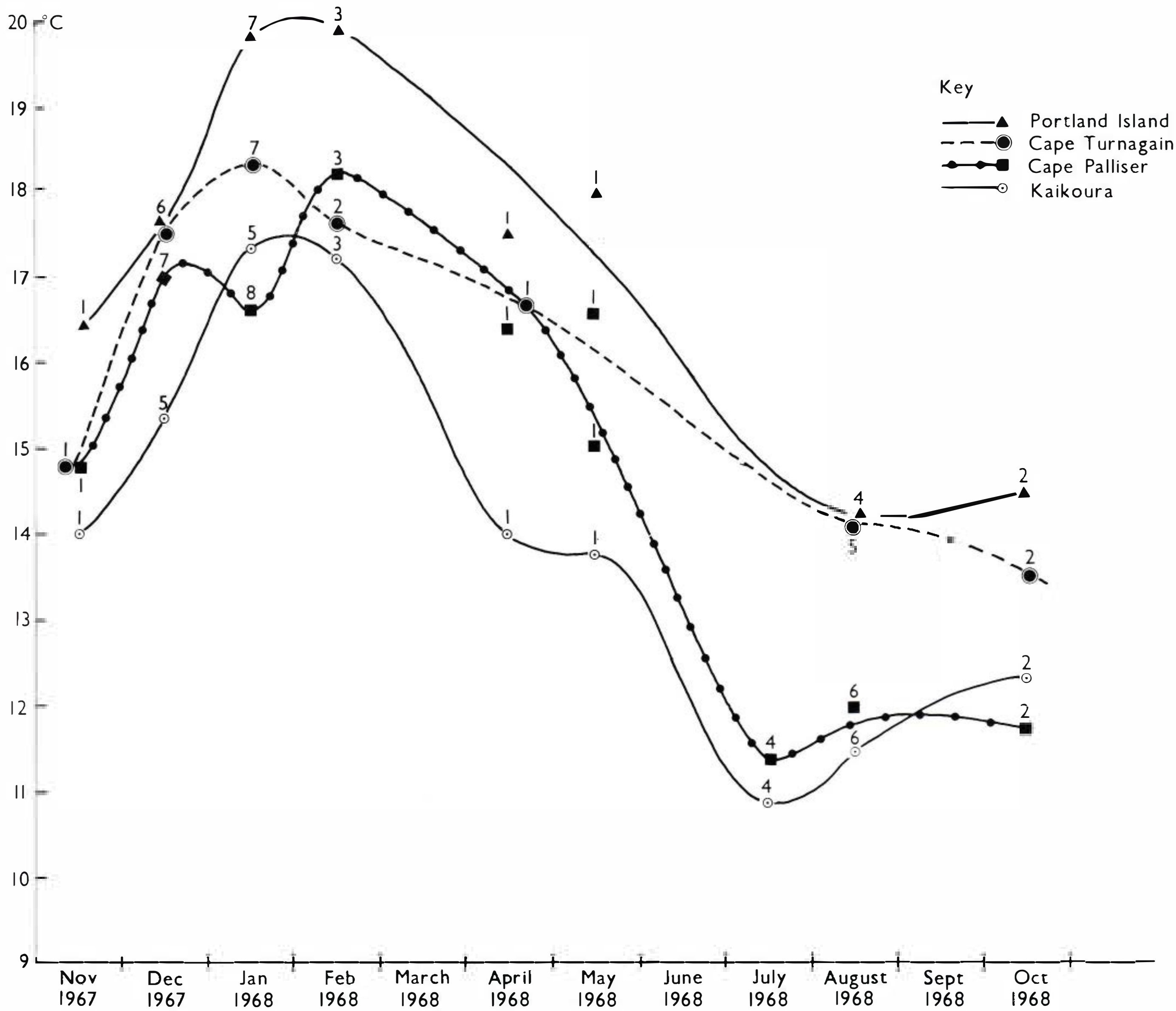

Fig. 41. Monthly average surface temperature recorded from a thermograph on M.V. *Hawea* offshore from Portland Island, Cape Turnagain, Cape Palliser and Kaikoura in the period November 1967 to October 1968. The numbers give the numbers of readings per month. The approximate track of M.V. *Hawea* is shown in Fig. 43.

In this estimate the East Cape Current was assumed to pass between Stn D831 and the coast. There is evidence however that at least some of the water passing between Stns D831, D830 may have contributed to the East Cape Current. In Fig. 9 the 55 m isobath passing between Stns D831, D830 passed through Stn D836 [the original assumption of the flow into the East Cape Current being that between Stn D831 and the coast was influenced by the fact that this is a region of upwelling, (*see* Figs 51, 55) the 200 m isotherm and the isobaths of the mixed layers are deflected further north by sub-surface water being brought closer to the surface and therefore the closest isoline to the coast that passed through D834 was chosen; the transport between Stns D837, D838 just south of East Cape was 4 Sverdrups relative to 800 dbars]. These facts suggest that 1.2 Sverdrups is an underestimate of the flow around East Cape which is most likely between 2 and 4 Sverdrups.

The volume transport and surface speed in that portion of the East Auckland Current deflected northward between Stns D819, D832 were 8 Sverdrups and 23 cm s^{-1} towards the east respectively for a 1000 dbar reference surface.

The Volume Transport in the Currents off the East Coast of New Zealand between East Cape and Banks Peninsula

The volume transports relative to various reference depths between station pairs off the east coast of New Zealand have been calculated from data collected in February/March 1969 (Appendix II, Fig. 25) and in September/October 1967 (Heath 1972a, Fig. 26). In this region the currents flow in approximately the same direction down to at least 1500 m (Heath 1972c) and thus a deep reference surface of at least this depth should be used. This is not always possible as the choice of reference surface is determined by the maximum depth of the observations. Also the horizontal spacing of the stations limits the scale of the motions that can be examined and the lateral extent of the different currents cannot be determined exactly. However, within these limitations a general summary of the volume transport of the circulation off the east coast of New Zealand can be given. The values are those from the February/March 1969 data (Fig. 25).

The East Cape Current was fed by a clockwise flow of 2-4 Sverdrups around East Cape. This water flowed southwards down the western side of the Hikurangi Trench and was joined from the west, south of latitude 42°S, by a flow of water from the Southland Current. The water of this combined current entered an anticyclonic eddy in which the volume transport was from 10-20 Sverdrups. Some of the water in this eddy recirculated while the rest flowed northwards along the eastern side of the Kermadec Trench forming the eastern side of the tongue of the East Cape Current System. A smaller anticyclonic eddy shed off from the main anticyclonic eddy had a volume transport of 2 Sverdrups (i.e. between Stns D856 and D855). The volume transport of the Southland Current in this region was approximately 6 Sverdrups (i.e. volume transport for a zero level at 1500 m between Stns D859 and D855 plus that for a zero level at 600 m between Stns D859 and D860) and by neglecting any volume transport through Cook Strait an estimate of approximately 7-10 Sverdrups is obtained for the water leaving the Hikurangi Trench in the eastern arm of the East Cape Current System.

SUBTROPICAL CONVERGENCE

East of Banks Peninsula, Subantarctic Water meets the Subtropical Water of the East Cape Current in the Subtropical Convergence (Fig. 1). Deacon (1937, 1945) and Garner (1953, 1959) both defined the position of this feature from surface distributions of temperature and salinity and showed the Subtropical Convergence extending along the Chatham Rise and northwards along the east coast of New Zealand, meeting the coast near Castlepoint (*see* Garner 1959, fig. 1).

Subtropical Convergence Near the Chatham Rise

All the hydrological studies made east of New Zealand across the Chatham Rise have located the Subtropical Convergence near the Rise at a mean position of 43°S (approx.) (Garner 1967a; Heath 1968, 1972a) whereas on the west coast of New Zealand the Convergence is usually found further south at about 46°S (approx.) (Garner 1967b, 1959). This difference in the latitudinal position of the Convergence can be explained by the effect of the Chatham Rise on the circulation east of New Zealand. In the Hikurangi Trench, no reference surface exists at any depth less than the maximum depth of the Chatham Rise (*see* Heath 1972c). The Chatham Rise is therefore a southern barrier to the southwards water movement at greater depths than the Rise. This water is frictionally coupled to the water above which is therefore also limited in its southward movement by both this coupling and by the Subantarctic Water south of the

TABLE 5. Source of data, period of collection, surface temperature and salinity, and temperature at a depth of 200 m at the bottom of the tongue on the East Cape Current System.

Source of Data	Garner 1967b	Heath 1968	Heath 1972a	See Appendix II
Period of Observation	18 February to 3 March 1963	10 to 18 April 1967	19 September to 11 October 1967	1 to 14 March 1969
Surface temperature at bottom of tongue of East Cape Current System	20°C	18°C	13°C	18.5°C
Surface salinity at bottom of tongue	35.4‰	35.1‰	35.0‰	35.3‰
Temperature at 200 m at the bottom of tongue	13°C	13°C	12°C	13°C

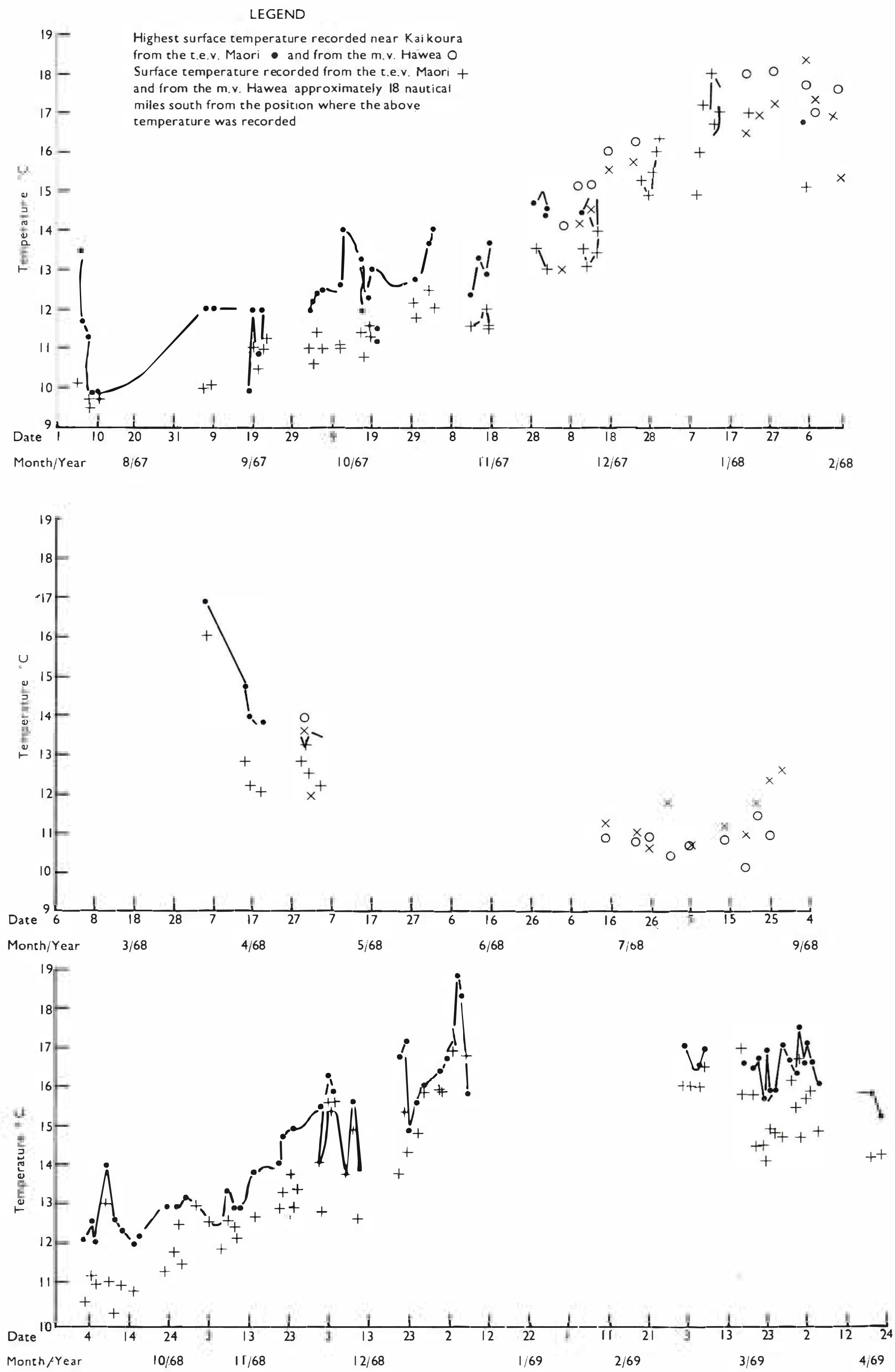

Fig. 42. Highest surface temperature (°C) recorded from T.E.V. *Maori* and M.V. *Hawea* near Kaikoura and approximately 18 miles south from where the above temperature was recorded in each case for the period August 1967 to April 1969. The approximate track of M.V. *Hawea* is shown in Fig. 43.

Rise which must also be guided by the Rise. Thus the Chatham Rise limits the southward flow of the Subtropical Water and effectively determines the position of the Subtropical Convergence in this region.

Structure of the Subtropical Convergence Across the Chatham Rise

To date there have been seven sets of hydrological data collected by the N.Z. Oceanographic Institute which can be used to define, in some detail, the vertical structure of the Subtropical Convergence east of New Zealand [Garner 1967a; Heath 1968 (2 sets), 1972a (2 sets); Ridgway (in press) (2 sets)]. The periods during which the observations were made, the longitude of the sections, the surface temperatures and salinity ranges across the highest surface gradient in the region of the Convergence for these sections are listed in Table 4.

The structure of the Subtropical Convergence can conveniently be illustrated by considering the typical meridional salinity profile across the Convergence shown in Fig. 27. A salinity, rather than temperature, profile was chosen because the change in the vertical gradient of salinity across the Convergence is greater than the change in temperature gradient.

At the Convergence the cool, less saline Subantarctic Water meets the warmer, more saline Subtropical Water and the isohalines and isotherms generally

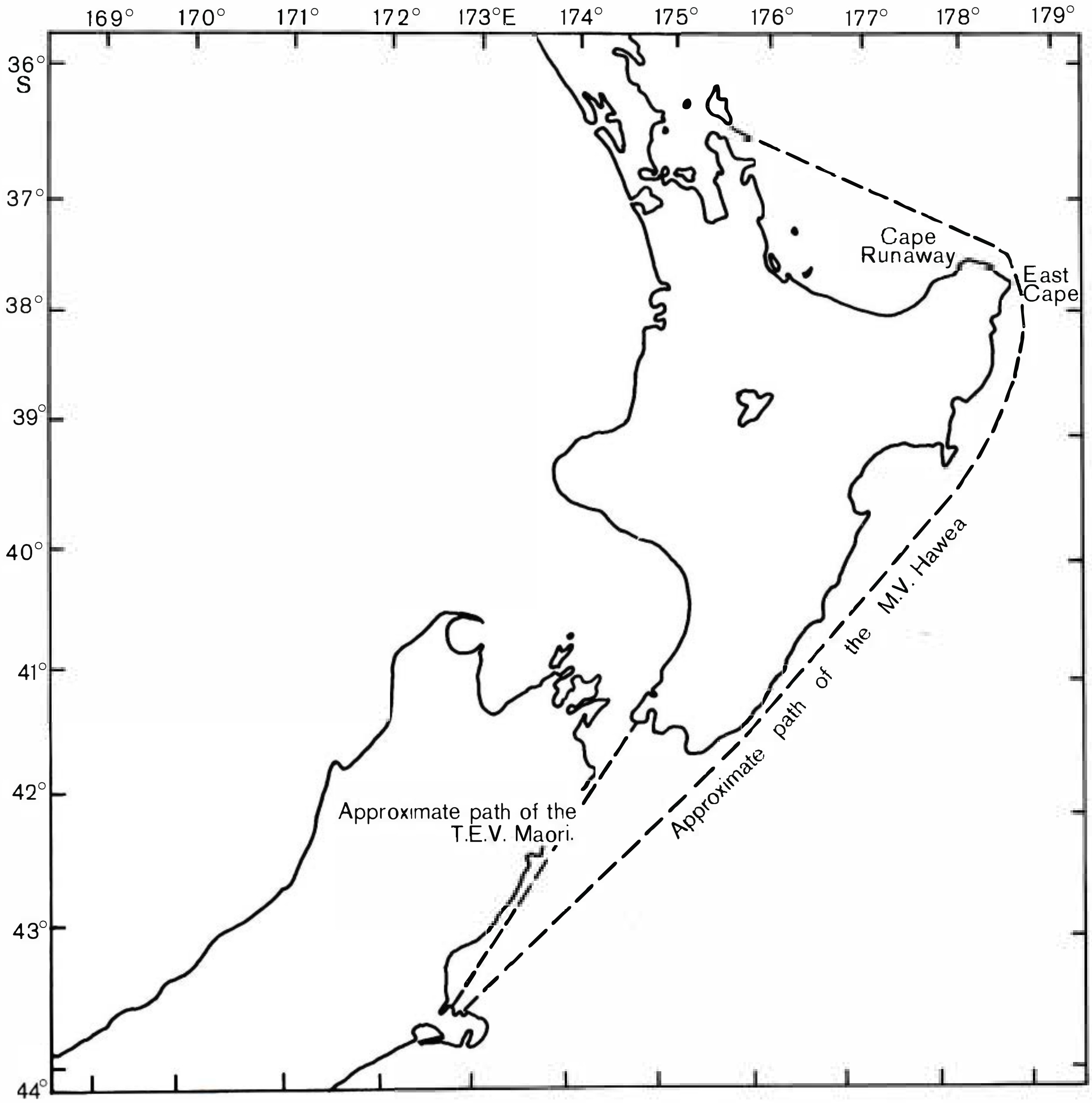

Fig. 43. Approximate tracks of M.V. *Hawea* and T.E.V. *Maori*. (Fig. 14 of Heath 1971).

slope downwards towards the north (Fig. 27 and figs 12-13 in Garner 1967a). In several sections across the Convergence there is evidence of a tongue of higher salinity sub-surface water extending southwards into the lower salinity Subantarctic Water. This higher salinity tongue was found between 80 m and 200 m by Deacon (1937) and between 100 m and 300 m by Garner (1967a) and Heath (1968). Deacon (1937, p.50) explained the presence of a southwards movement of water in this tongue as follows...'whilst the wind drives the surface [Subantarctic] water towards the north, another factor - the difference of climate between the southern and northern parts of the [Subantarctic] zone, sets up a density gradient which tends to cause a current in the opposite direction'. Deacon found that the high salinity sub-surface tongue extended nearly as far south as the Antarctic Convergence, but his measurements were made away from any bottom topographic feature such as the Chatham Rise which could influence the flow. At the longitudes of the Chatham Rise the higher salinity sub-surface tongue does not extend as far south as in the open ocean; the furthest south it has been found in this region is 45°S (Fig. 27) for even though it is found above the depth of the Chatham Rise, the Rise still hinders its southwards movement. The largest horizontal gradients of the three parameters, salinity, temperature and density, across the Subtropical Convergence over the Chatham Rise occur in the upper 600 m (Fig. 27).

Seasonal Variation in the Position of the Subtropical Convergence Over the Chatham Rise

In the open ocean the latitudinal position of the Subtropical Convergence is determined by the relative strengths of the southwards flowing Subtropical Water and the north-easterly flowing Subantarctic Water. This is in contrast to the case of the Antarctic Convergence where the latitudinal position is determined by the position where the Deep Water is forced upwards over the more dense Bottom Water (Deacon 1937, p.21). In most parts of the ocean the Subtropical Convergence is subject to much greater variation than the Antarctic Convergence (it advances towards the south in summer, recedes to the north in winter, and, in the central part of the Atlantic Ocean, it has other irregular movements with a range of as much as 6° of latitude (Deacon 1937)) but a zonal morphological barrier, such as the Chatham Rise, limits its latitudinal variation.

Comparing two salinity cross-sections from data collected across the Chatham Rise along longitude 177°E (Fig. 27, from data collected April 1967 [Heath 1968]; Fig. 28, from data collected September 1967 [Heath 1972a]) it can be seen that the Subtropical Water extended further south in the winter than in the summer in that year. This can also be seen by comparing the surface salinity distributions for these cruises (i.e. *compare* Fig. 27 with Heath 1972a, fig. 12). All the data collected across the Chatham Rise, except that for September/October 1967, have been collected in summer and in no case was Subtropical Water found as far south as in September/October 1967. Comparison of the surface and 200 m temperature distributions for the two 1967 cruises shows that the tongue of the East Cape Current System is best developed in summer, as would be expected (*see* section on Seasonal Changes), but finding the Subtropical Water further south in winter appears contrary to the general seasonal movement of the Subtropical Convergence. One possible explanation for this can be offered in terms of the seasonal variation of the vertical structure of the currents in this region. It has been shown that here during the summer the vertical shear of the currents is nearly uniform to a depth of at least 1000 m, whereas in winter the vertical shear is larger in the sub-surface layers (depth greater than 300m, *see* p. 41). The difference in the dynamic height anomalies between station pairs (these curves represent the vertical structure of the current) occupied during different periods are shown in Fig. 29 (Stns C874, C873, September 1962, Sdubbundhit and Gilmour 1964; Stns B758, B767, February 1963, Garner 1967; Stns D612, D613, April 1967, Heath 1968; Stns D676, D675, October 1967, Heath 1972a). In those curves for the summer data (B758-B767, D612-D613) there are sharp changes in the gradients in the upper 300 m. These changes are due to the horizontal density gradient. Plots of sigma-T (σt) with depth for stations occupied during different seasons in this area are shown in Fig. 30. In summer there was a large change in the density across the thermocline (found in the upper 100 m at Stns B758, D613). Below the thermocline the gradient of σt decreased until it reached a nearly constant value below a depth of approximately 500 m. Therefore, in the upper 500 m, the vertical changes in the density can act as a mechanism for producing large vertical gradients in the currents by creating horizontal density gradients. During winter, however, no strong thermocline is formed off the east coast of New Zealand (Stns C873, D675, Fig. 30), the water in the upper 300 m has a nearly constant density, and therefore the density field does not provide a mechanism for creating a large change in the vertical gradient of the currents (i.e. the turbulent momentum exchange will be small). An explanation of the southward extension of Subtropical Water in the winter can now be offered by considering the gradient of the vertical stress component

$$(\propto \frac{\partial^2 V}{\partial Z^2}$$

assuming that the eddy viscosity coefficient is constant). During summer, when sharp changes occur in the vertical gradient of the currents, the vertical stress term will be large, the water above the depth of the Chatham Rise will be strongly coupled to that below and will be partially restrained in its southward

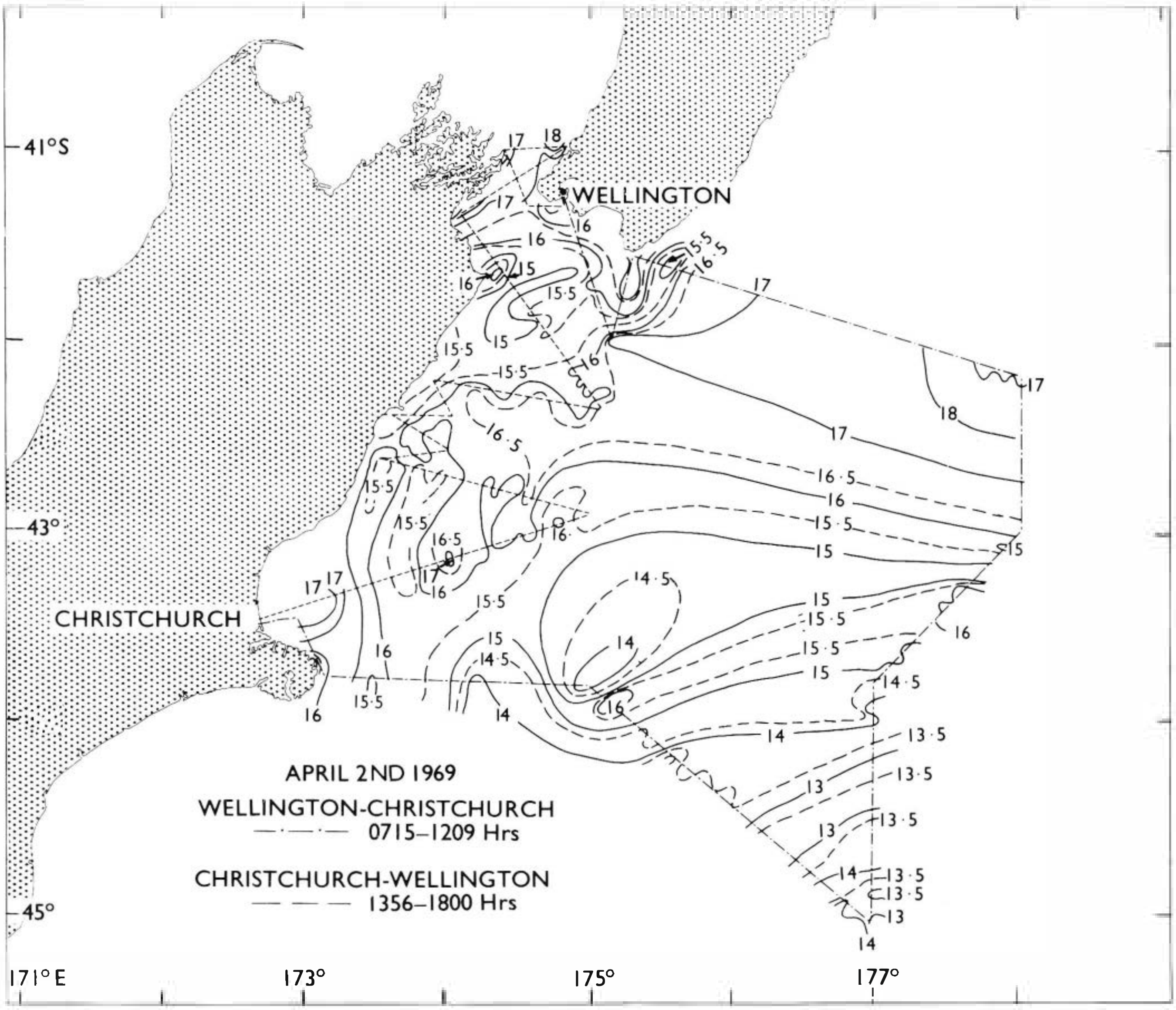

Fig. 44. Sea surface temperature (°C) distribution measured with an infrared radiation thermometer on 2 April 1969. The dashed line shows the flight path.

movement. In winter, no sharp changes generally occur in the vertical gradient of the currents and the coupling between the water in the mixed layer and the water below will not be as strong as in summer. This decrease in the coupling may be sufficient to allow the Subtropical Water to push further south in winter; however this seasonal change is probably also linked to some seasonal wind variability.

The Subtropical Convergence East of the Chatham Islands

Further evidence of the influence that the Chatham Rise has on the structure and position of the Subtropical Convergence is given by a meridional salinity plot constructed from data collected in January 1969 to the east of the Chatham Islands along longitude 174°00'W (Fig. 31) by Ridgway (in press). A subsurface tongue of high salinity water was developed to a depth of 400 m south of the latitude of the Chatham Rise (Fig. 31). A similar, but not so well developed salinity tongue was also present in the upper 400 m over the Chatham Rise in February 1969 (Fig. 32). The detached high salinity patch, centred at a depth of approximately 125 m in the tip of both of these tongues, suggests that the southwards movement of this Subtropical Water occurs as a series of pulses rather than a constant southwards drift. In the upper 600 m the Subtropical Water extended further south to the east of the Chatham Islands (longitude 174°W, Fig. 31) than to the west (longitude 179°, Fig. 32). This agrees with the Chatham Rise

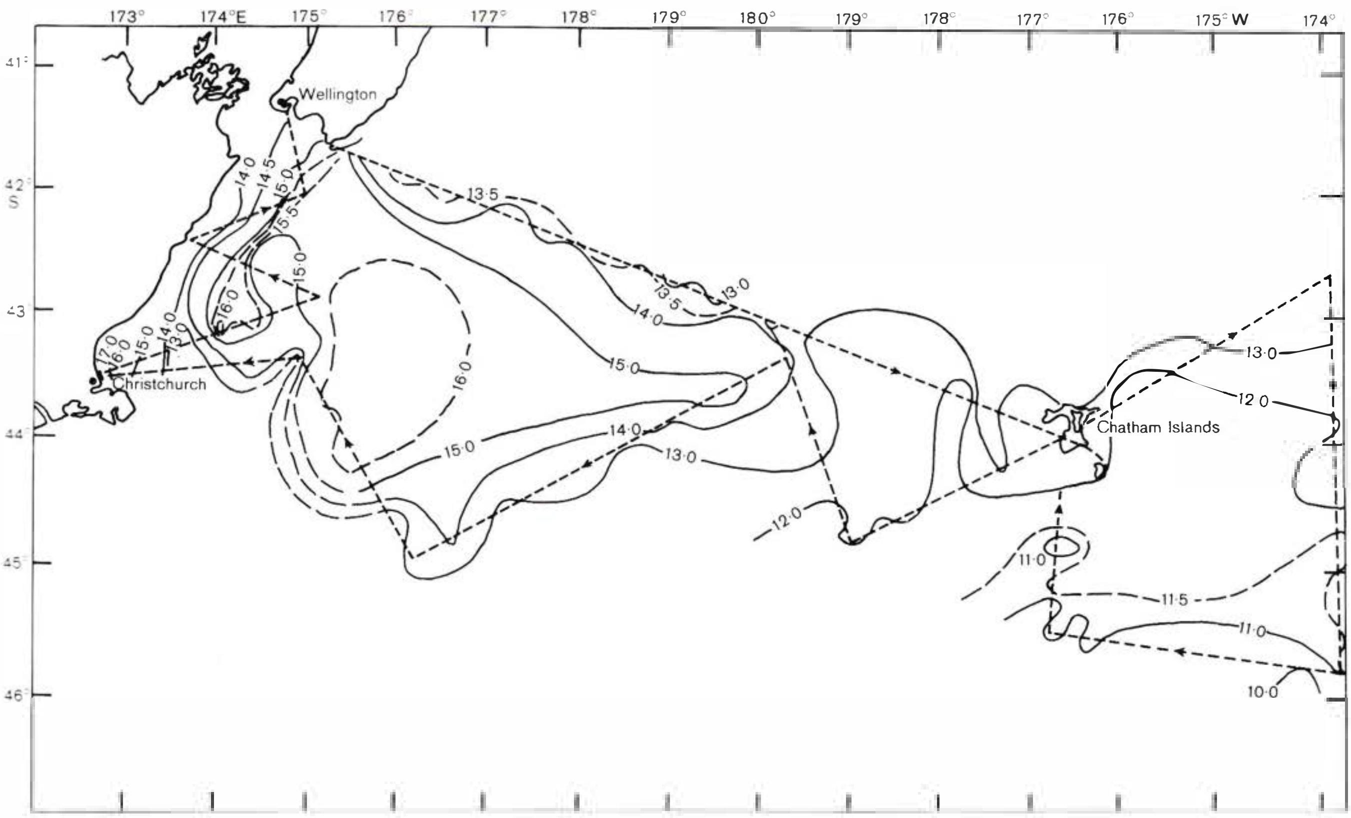

Fig. 45. Sea surface temperature (°C) distribution measured with an infrared radiation thermometer on 17/18 November 1969. The dashed line shows the flight path.

limiting the southwards flow of Subtropical Water as discussed above.

The influence that the extension of the Chatham Rise, to the east of the Chatham Islands, has on the movement of Deep Water is also illustrated in Fig. 31. The Deep Water was forced upwards on its passage northwards and at Stn F954 (Fig. 31) it is in direct contact with the Subtropical Water above, cutting off the direct supply of Antarctic Intermediate Water from the south. This is illustrated by the 34.5% isohaline which rises from a depth of 1630 m at 50°S (Stn F957) to a depth of 1250 m at the latitude of the Chatham Rise (Stn F952, latitude 43°30'S) (Fig. 31).

The Subtropical Convergence North of Banks Peninsula

West of longitude 175°E on the eastern side of the Mernoo Gap, the Subtropical Convergence extends northward as the boundary between the cool, low salinity water of the Southland Current flowing northward (Heath 1972a) and the warmer, more saline water of the East Cape Current flowing southwards. Garner (1959) found the Convergence followed approximately the surface isotherm of 15°C in February and 10°C in August and the surface isohalines of 34.7% to 34.8% with little seasonal change. In the period 26 November to 4 December 1968 a hydrological cruise was conducted off the east coast of the South Island north of Banks Peninsula and in Cook Strait. Station circumstances for this cruise, other than those stations reported elsewhere by Heath (1971, 1972b), are given in Appendix I, and the station data are given in Appendix II. The temperatures and salinities that

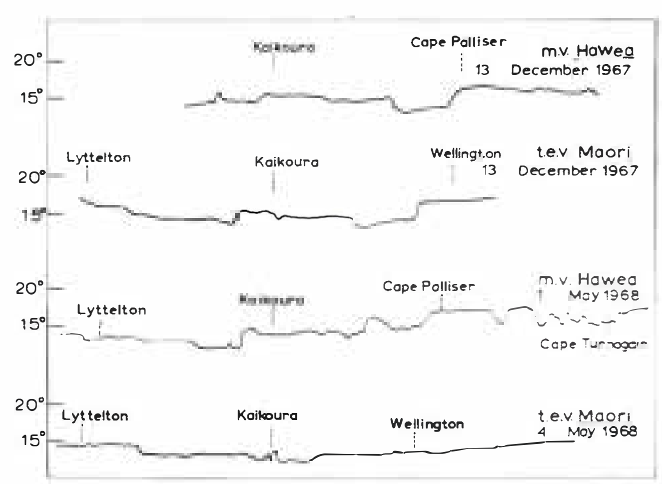

Fig. 46. Surface temperature records off the east coast of New Zealand from thermographs installed on M.V. *Hawea* and T.E.V. *Maori*. The approximate tracks of M.V. *Hawea* and T.E.V. *Maori* are shown in Fig. 43.

TABLE 6. Linear regression analysis (S = mT + c) of the sea surface salinity (S) on the sea surface temperature (T) for the different sets of data collected off the east coast of New Zealand. N gives the number of sets of observations used, r the regression coefficient and σ the standard deviation.

Period of Observation	Source of Data	m ‰°C	C ‰	σt	σs	r	N
18 February to 3 March 1963	Garner 1967	0.19	31.57	1.48	0.29	0.962	26
24 February to 13 March 1965	Ridgway 1970	0.10	33.43	0.69	0.11	0.646	32
	Combined Garner (1967) and Ridgway (1970a)	0.19	31.71	1.25	0.25	0.922	58
25 September to 11 October 1967	Heath 1972a	0.11	33.59	1.05	0.15	0.790	60
1 to 14 March 1969	Appendix II	0.21	31.37	1.63	0.38	0.928	56
26 November to 4 December 1968	Appendix II	0.16	32.61	0.88	0.17	0.864	47

approximately parallel the Convergence for the September/October 1967 and November/December 1968 cruises are shown below.

Cruise	Temperature at S.T.C. Surface	Temperature at 200 m	Salinity at S.T.C. Surface	Maximum in upper 200 m
Sept. / Oct. 1967	11°C	9°C	34.8‰	34.8‰
Nov. / Dec. 1968	11.5°C	9°C	34.6‰	34.8‰

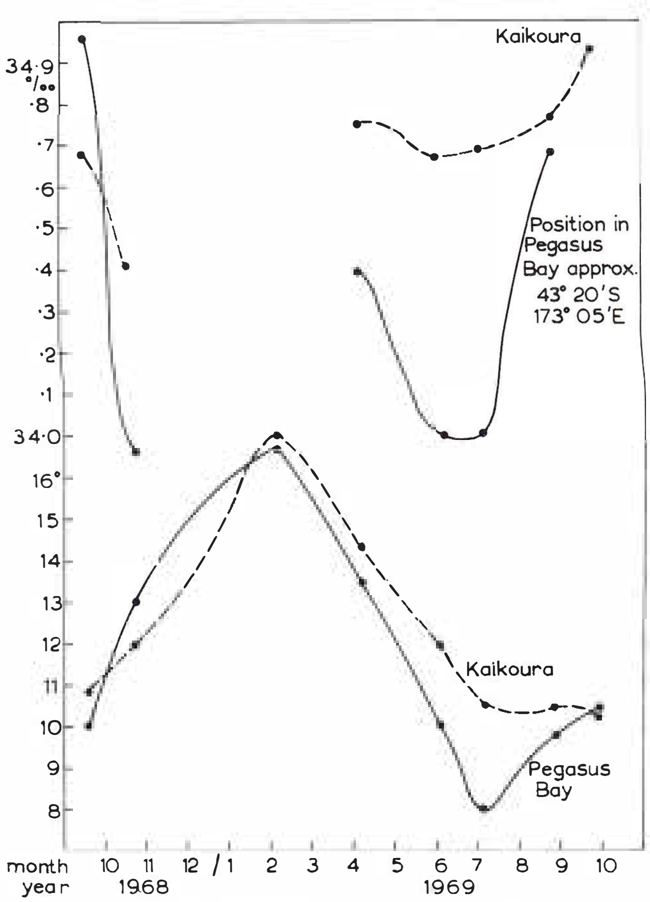

Fig. 47. Seasonal variation of surface salinity (‰) and temperature (°C) abeam of Kaikoura and at latitude 43°20'S, longitude 173°05'E in Pegasus Bay, from observations made on board T.E.V. *Maori* between October 1968 and October 1969. The approximate track of T.E.V. *Maori* is shown in Fig. 43.

The surface temperature defining the Convergence for both cruises and the salinities in September/October 1967 agree with the characteristic values given by Garner (1959). The decrease in the seasonal range of the 200 m temperatures compared to the surface values is expected, for the largest seasonal changes occur near the surface.

The surface salinities were lower in November/December 1968 than in September/October 1967. At most of the stations in November/December 1968 the salinities initially increased with depth (*compare* Figs 33, 34) but in September/October 1967 the maximum salinity generally occurred at the surface. The maximum near surface isohaline defining the position of the Convergence in November/December 1968 also agrees with Garner's surface value. The surface geostrophic currents relative to 400 dbars in November/December 1968 (Fig. 35) show that the surface water of the Southland Current extended over the relatively more saline water of the East Cape Current during this period, and this would create the inversions in the salinity/depth plots. The occurrence of low surface salinities in November/December 1968 emphasises the need for caution in using only surface hydrological data in coastal areas since the surface data can have large non-seasonal variations.

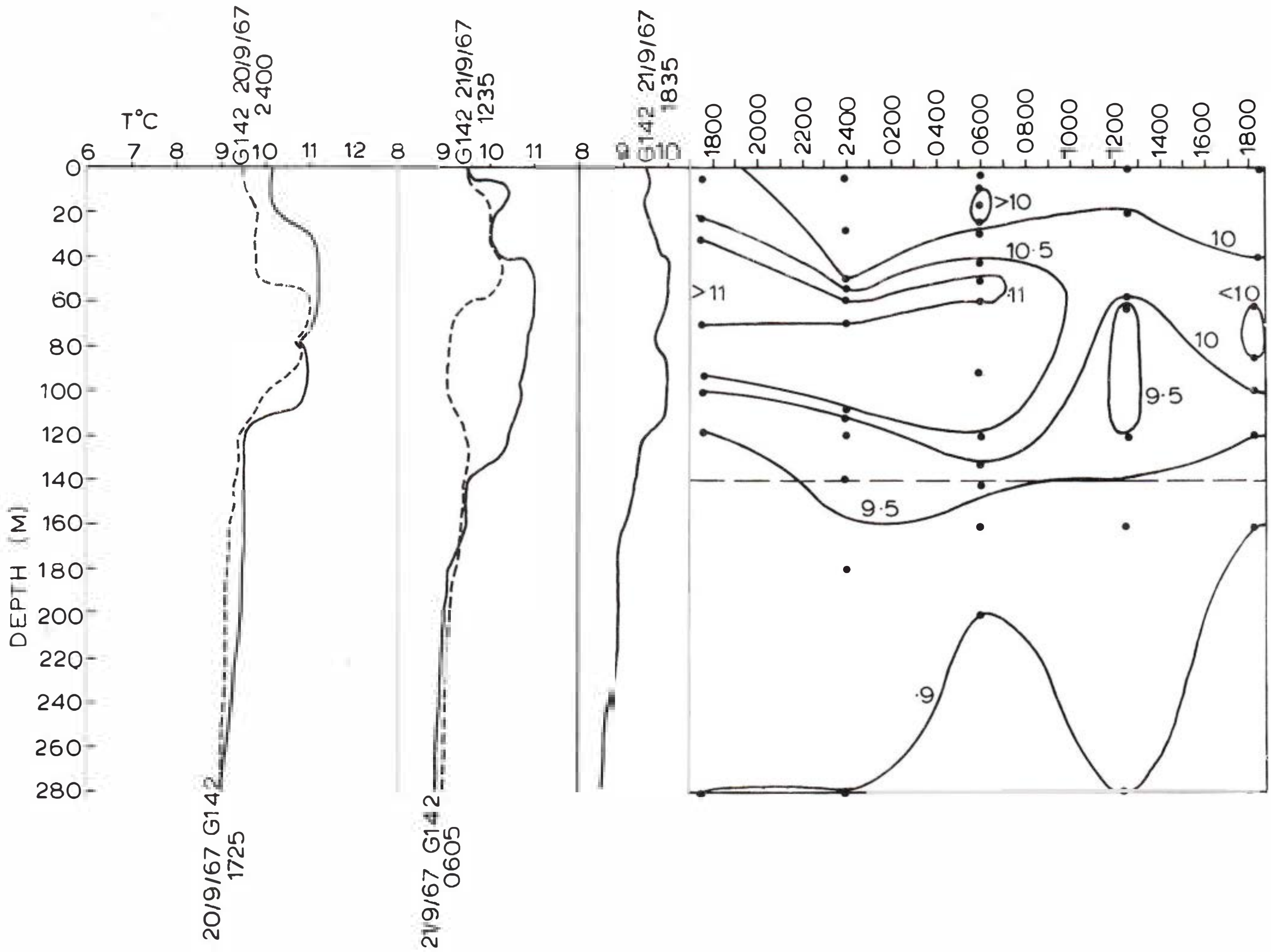

Fig. 48. Five bathythermograph records collected over a 24-hour period at Stn G142 (latitude 42°25'S, longitude 173°57'E) and the resultant plot of temperature with depth over the period.

The Northern Limit of the Subtropical Convergence East of New Zealand

The northwards extension of the Subtropical Convergence forms the outer arm of the cool, low salinity tongue of the Southland Current; the inner arm of this tongue is the Southland Front (Heath 1972a). Both the Subtropical Convergence and the Southland Front are developed to a depth of at least 900 m (where depth permits) north of Banks Peninsula (Fig. 36). During September/October 1967 both the Subtropical Convergence and the Southland Front were present as far north as Kaikoura (Fig. 36) but in November/December 1968 they could also be traced north of Kaikoura (Fig. 37). The development of the northward extension of the Subtropical Convergence is closely connected with the anticyclonic, subtropical eddies that are sometimes shed off from the main flow of the East Cape Current System; the periodicity of these eddies will be discussed later in this paper. These eddies extend to a depth of at least 900 m (Figs 17, 38) and will therefore be guided southwestwards by the bottom topography (Fig. 3). When one of these eddies is present near Kaikoura the northern passage of the Southland Current is hindered; the pressure force developed between the Subtropical Water in the anticyclonic eddy and the cooler, less saline water of the Southland Current creates a component of the Southland Current directed offshore. During September/October 1967 a well developed anticyclonic eddy was present near Kaikoura and a strong component of the Southland Current was directed offshore near Kaikoura (*see* Figs 25-27, Heath 1972a). In November/December 1968 a relatively weak anticyclonic eddy was present offshore south of Kaikoura centred at Stn D767 (Figs 3, 35) and the main flow of the Southland Current extended further north past Kaikoura. The water of the main northwards flow of the Southland Current which did not enter southern Cook Strait (*see* Heath 1971) was limited in its northern passage by an anticyclonic eddy situated just south of Cape Palliser, centred at Stn D783 (Figs 3, 37).

When only a small anticyclonic eddy is present near Kaikoura, the Subtropical Convergence may be

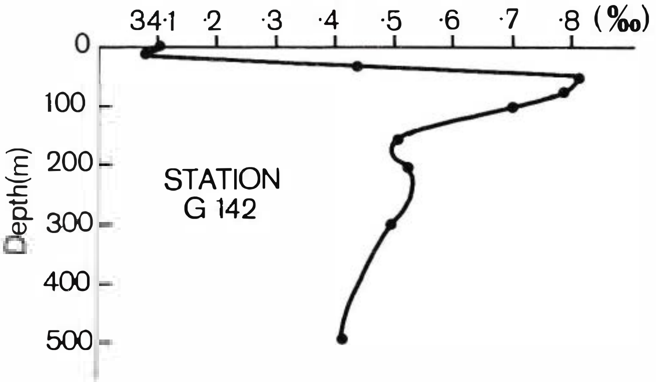

Fig. 49. Salinity (‰) / Depth (m) curve of Stn G142.

defined as a continuous feature as far north as the east coast of the North Island (as in November/December 1968). However, when a large anticyclonic eddy is present near Kaikoura, the Subtropical Convergence may be defined as a continuous feature only as far north as Kaikoura; the Convergence may still be formed north of Kaikoura, between the component of the Southland Current which flows north and the main flow of the East Cape Current (Fig. 38), but will be cut off from the main Convergence south of Kaikoura by the component of the Southland Current that turns east near Kaikoura (as in September/October 1967) (*see* Heath 1972a). Should a strong anticyclonic eddy exist just north of the Mernoo Gap, the Southland Current could be diverted towards the east along the Chatham Rise. Then the northwards extension of the Subtropical Convergence would not be formed and the Convergence would only be defined along the Chatham Rise.

TEMPERATURE AND SALINITY VARIATIONS

From the available data it is possible to give only a very general account of the seasonal and non-seasonal changes of salinity and temperature off the east coast of New Zealand.

Seasonal Changes

Fig. 39 shows T/S diagrams for stations occupied in different periods at approximately the same positions relative to the circulation, (Stns D614, D615, April 1967, Heath 1968; Stns D679, D680, September 1967 Fig. 2, Heath 1972a; Stn D846, March 1969, Fig. 4). Temperature/depth diagrams for these stations are shown in Fig. 40. Temperature and salinities in the southern extremity of the tongue of the East Cape Current System for the different cruises in this area are listed in Table 5. The seasonal surface temperature change of the water in the southern extremity of East Cape Current between early October and early March was approximately 5°C and the corresponding surface salinity change was approximately 0.35% (Table 5). Both the seasonal salinity and temperature variations were greatest at the surface and were relatively uniform immediately above the depth of the summer thermocline (at a depth of 50-70 m) i.e. *see* Stn D615, Fig. 40. The variations decrease in size with increasing depth and are practically non-existent below a depth of approximately 900 m (Fig. 40). The horizontal surface temperature and salinity gradients

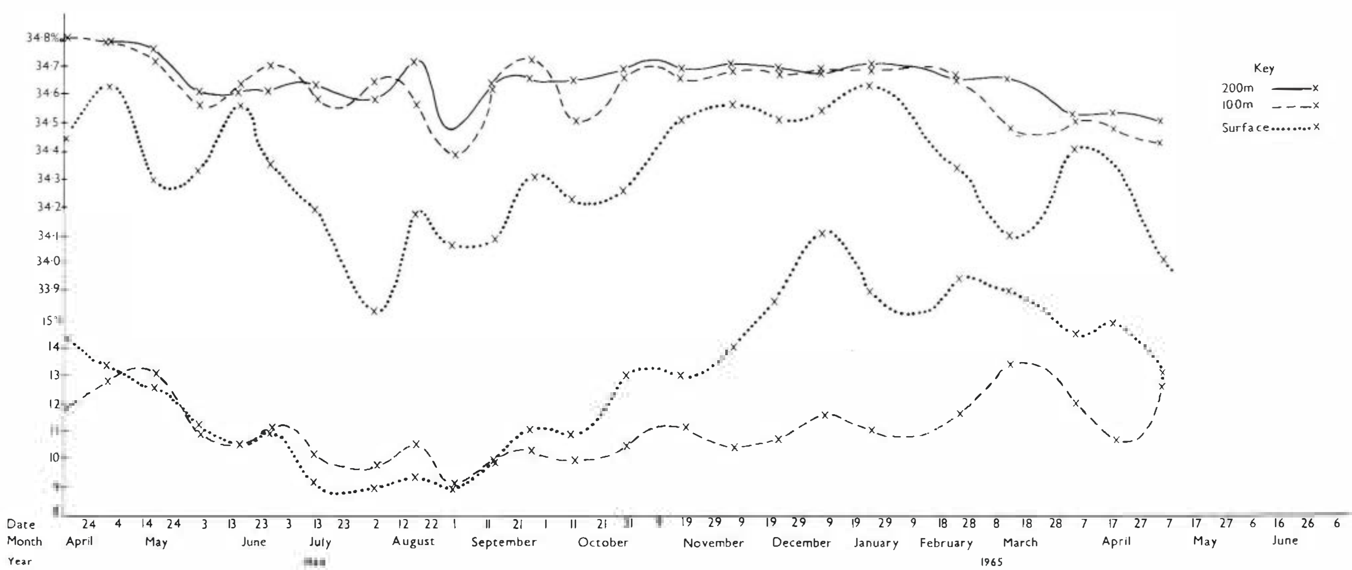

Fig. 50. Variations with time of the temperature (°C) at the surface and at a depth of 100 m and the salinity (%) at the surface, 100 m and 200 m, near Kaikoura in the period April 1964 to June 1965.

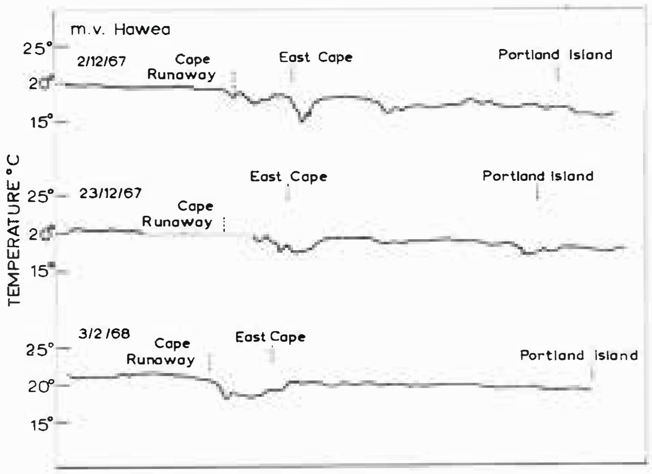

Fig. 51. Three surface temperature records collected near East Cape from a thermograph installed on M.V. *Hawea*, the track of which is shown in Fig. 43.

in the tongue of the East Cape Current System were more strongly developed in summer than winter (*compare* Figs 10, 11 with Figs 11, 12, Heath 1972a).

Monthly average temperatures for four locations along the east coast of New Zealand (Portland Island, Cape Turnagain, Cape Palliser, Kaikoura) taken from thermograms collected from M.V. *Hawea* and covering the period November 1967 / October 1968 have been plotted in Fig. 41. Surface temperatures at positions abeam from Kaikoura in the period October 1968 /April 1969 recorded on thermographs installed in both M.V. *Hawea* and T.E.V. *Maori* are shown in Fig. 42. The normal tracks of both vessels are shown in Fig. 43. The seasonal temperature range at Kaikoura and Cape Palliser was approximately 7°C, while at Portland Island and Cape Turnagain it was approximately 6°C. The temperatures were highest during the period January/February and lowest in the period July/August.

Spatial Variations of Surface Temperature and Salinity

Coefficients of linear regression equations between the surface temperature and surface salinity for the data collected off the east coast of New Zealand are given in Table 6. There is little correlation between the surface temperature and salinity and only small changes of salinity with a change in temperature (i.e. small m) for data collected in the vicinity of an individual water mass (e.g. Ridgway 1970a, in the Subtropical Water), but the correlation is much higher for data collected near the boundary of two water masses (e.g. Garner 1967a, near the boundary between the Subtropical Water of the East Cape Current and the cooler, less saline water of the Southland Current - this cruise was conducted in the same months but two years earlier than that by Ridgway 1970a). The decrease in the value of the correlation coefficient can be explained by the small variation of the surface temperature or salinity in these individual water masses; *compare* the standard deviations of the surface temperature and salinities for the two cruises - Garner 1967a, Ridgway 1970a in Table 6 - the fact that the standard deviation is smaller for the combined set of surface data for these two cruises than for the Garner (1967a) cruise alone shows that the size of the standard deviation is evidently not a function of the number of sets of data.

The ratios of the horizontal surface salinity gradient in winter to that found in summer near the boundary between the Southland and East Cape Currents was smaller than the corresponding ratio of the horizontal surface temperature gradients [*compare* the gradients (m) for the data collected by Garner (1967a) and that collected during September/October 1967 by Heath (1972a) and November/December 1968 (Appendix II).

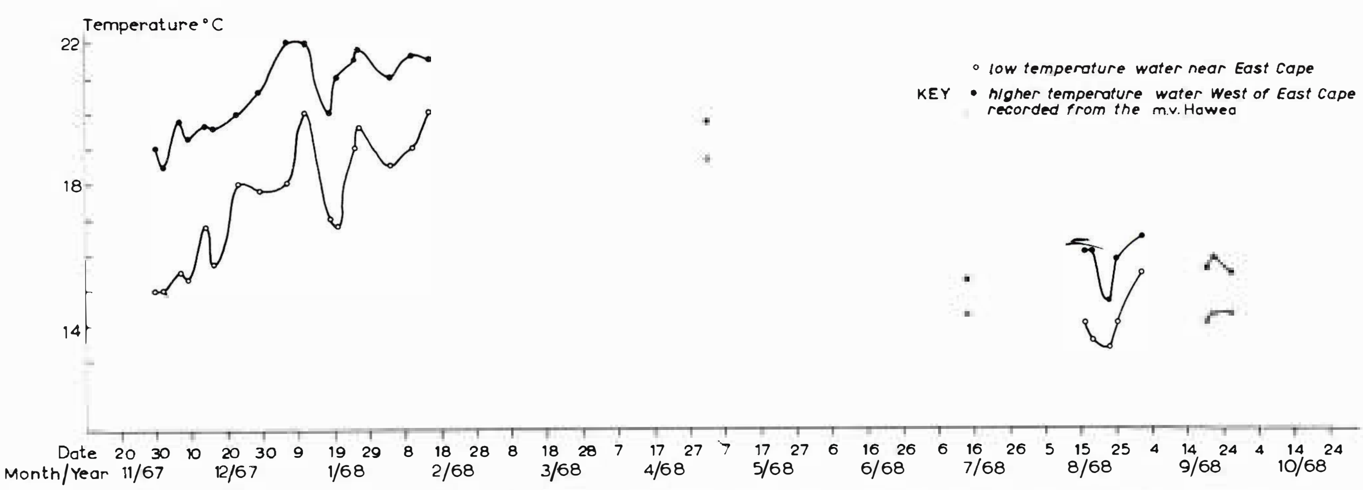

Fig. 52. Seasonal surface temperature (°C) variations of cool water near East Cape (lower curve) and the warmer water found adjacent to the cool water over the period November 1967 to October 1968. The surface temperatures were recorded on a thermograph installed on M.V. *Hawea*. The approximate track of M.V. *Hawea* is shown in Fig. 43.

HYDROLOGY OF THE WATER BETWEEN BANKS PENINSULA AND CAPE PALLISER

Garner (1953) found tongues of Subtropical Water in both southern Cook Strait and close inshore near Kaikoura, and explained their presence by the guiding effect of the bottom topography. The complicated day-to-day variations in the surface temperatures and salinities along this entire coast were attributed by Garner (1953) to the effect of both wind-derived upwelling and upwelling caused by water impinging on to the continental shelf. A reported occurrence of wind-derived coastal upwelling along this coast has been made by Heath (1972b). A more detailed analysis of the hydrology on this coast using the circulation as discussed above and by Heath (1972a) can now be given.

Observations : To supplement the data from hydrological cruises the following hydrological data have also been collected.

1. Thermograph records taken from a thermograph installed in the engine room of the T.E.V. *Maori* over the period from August 1967 to April 1969. The sensing element of this instrument was located in a sea-water intake supplying cooling water to the engines. Sea surface salinity data measured from hourly water samples collected from the T.E.V. *Maori* during seven trips between October 1968 and October 1969. The salinities were measured onshore with an inductive salinometer (Brown and Hamon 1961).

2. Sea surface temperatures taken from a thermograph installed in the engine room of the M.V. *Hawea* over the period August 1967 to April 1969.

3. Two near-synoptic, sea surface temperature distributions measured with an airborne infrared radiation thermometer on 2 April and 17/18 November 1969.

WATER TYPES ON THE NORTH CANTERBURY COAST

The North Canterbury Coast is bathed by the cool, low salinity water of the Southland Current (Heath 1972a) with regular intrusions of Subtropical Water derived from the East Cape Current. The presence of the Southland Current on this coast was marked by the 15.5°C and 16°C isotherms in the surface temperature distribution measured with the infrared radiation thermometer (I.R.T.) on 2 April 1969 (Fig. 44), and by the 13.5°C and 14°C isotherms for an I.R.T. survey made on 17/18 November 1969 (Fig. 45). The patch of water represented by the 16.5°C and 17°C isotherms in Fig. 44 and by the 16°C isotherm in Fig. 45 most likely represents the intrusion of water derived from the East Cape Current. An intrusion of water with a temperature of 16°C near Kaikoura in April appears to have limited the supply of water of the Southland Current north of Kaikoura during the period, whilst in November the low temperature water of the Southland Current extended eastwards from Cape Palliser cutting off the supply of Subtropical Water from the north. The cold tongue of the Southland Current is also evident in the thermograph records collected from both T.E.V. *Maori* and M.V. *Hawea*. One thermogram from each ship collected in December 1967 and May 1968 is shown in Fig. 46.

HYDROLOGY OF PEGASUS BAY

The seasonal temperature range in Pegasus Bay (i.e. 8.5°C approx.) is, as expected, greater than at Kaikoura (i.e. 7°C approx.) (Fig. 47). Solar heating effects are greater in the relatively sheltered, shallow water of Pegasus Bay than in the open ocean. Coastal run-off also has a marked effect on the waters of Pegasus Bay and accounts for the very low salinities (34.0‰) measured by T.E.V. *Maori* during November 1968 and July/August 1969 (Fig. 47).

HYDROLOGY OFF KAIKOURA

The Southland Current flows northwards along the North Canterbury coast with a component being deflected offshore near Kaikoura (Heath 1972a), the strength of this latter component being greatest when an anticyclonic eddy of Subtropical Water derived from the East Cape Current System is present near Kaikoura (p. 53). The non-seasonal and spatial variations of temperature and salinity are quite large near Kaikoura with day-to-day changes of surface temperature of 2°C and spatial changes of 1.5°C over the 18 miles (33 km) not being uncommon (Fig. 42). Comparison of the thermograph records shown in Fig. 46 shows that the warm water often found near Kaikoura is also present offshore (*see* the approximate track of the two ships shown in Fig. 43).

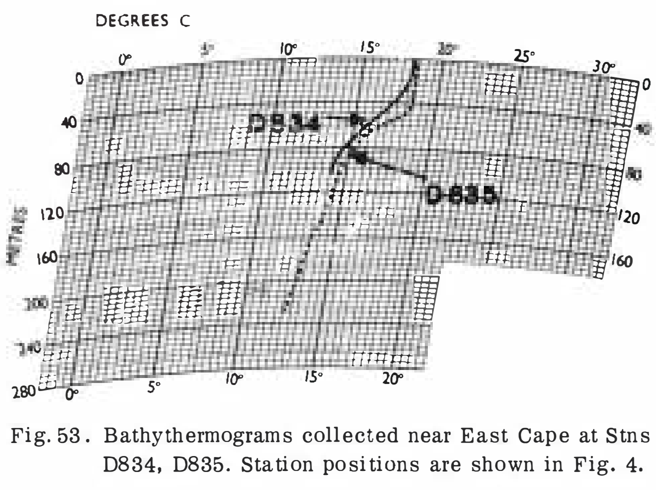

Fig. 53. Bathythermograms collected near East Cape at Stns D834, D835. Station positions are shown in Fig. 4.

The variability with time of the sub-surface temperatures near Kaikoura is illustrated by the five bathythermograph traces shown in Fig. 48. These records were obtained at Stn G142 (42°25'S, 173°57'E) at equally spaced time intervals over a 24-hour period, on 20/21 September 1967. The water temperatures were highly variable above a depth of 140 m with a well-defined inversion centred at a depth of approximately 70 m caused by cool coastal water overlying the water of the Southland Current (Fig. 49). The advective transport of the Southland Current was most likely large enough to limit the effects of the river outflow to the upper 200 m (Fig. 49).

Mechanisms Generating the Non-seasonal Effects on the North Canterbury Coast

There are three mechanisms that would account for the warm water patches found near Kaikoura. The present study supports the opinion of Garner (1953) that warm water is guided towards Kaikoura by the bottom topography but the roles, if any, that the two other mechanisms play still need investigating. These are the result of Subtropical Water upwelling as proposed by Houtman (1965) or the result of the warm water of the East Cape Current being driven further south by local winds.

Houtman's postulate is based on warm Subtropical Water at a depth of 200 m upwelling through the cool water produced by the river run-off at Kaikoura. The tongue which defines the Southland Current in this region is still present at 200 m (Fig. 37) (*see also* Fig. 13, Heath 1972a) and thus the water will be colder at 200 m than at the surface unless there are large temperature inversions above 200 m. No temperature inversions of this depth were observed in the data collected for the present study (Appendix II). In Houtman's observations a thermocline was present at a depth of 70 m seawards of the Conway Ridge (this ridge lies approximately 8 miles (15 km) offshore south of Kaikoura and runs parallel to the coast), and any water that rose from below the thermocline would not be warmer than the surface water further to the north or south. It has been found that the occurrence of Subtropical Water near Kaikoura has a period of about 55 days (*Refer to* "Periodicity of the influx of warm water towards Kaikoura") and it therefore appears that the role that the amount of coastal run-off plays in determining the presence of Subtropical Water near Kaikoura is only minor for it is unlikely that this run-off also has a 55-day period.

The second possibility, warm water being driven south by local winds, has been examined by Heath (1972d) who found that the southwesterly wind-derived water movement, required to transport the warm water, occurred very seldom in the period September 1967/July 1968 although warm patches were present at Kaikoura in this period.

It appears that the main process is the guiding of this warm water towards Kaikoura by the bottom topography. Evidence for this warm water being transported in the form of small anticyclonic eddies is given by the presence of this type of eddy near Kaikoura in several of the distributions of the relative geopotential anomaly topography of the sea surface near Kaikoura (Figs 7, 8, 35; *see also* Heath 1972a). These eddies are probably derived from the larger anticyclonic eddy in the East Cape Current System.

Periodicity of the Influx of Warm Water Towards Kaikoura

Garner (1961, p.51) states that "subtropical water appeared off the Kaikoura coast in a series of incursions at intervals of approximately two months". This statement was based on thermograph records taken from the inter-island ferry T.E.V. *Hinemoa.* At 2-weekly intervals in the 15-month period from April 1964/June 1965, Bradford (1972) collected surface and sub-surface temperature and salinity data at a 'permanent station' located five miles east of Kaikoura Peninsula in 200 m (approx.) of water. Salinities were measured by the Knudsen Method (Oxner 1920) and the temperatures were digitised from bathythermograph records. From the surface temperatures and salinities alone, Bradford (1972) found that the intervals between the incursions of Subtropical Water near the Kaikoura coast were not as regularly spaced as those recorded by Garner (1961). Plots of the variations with time of the temperatures and salinities at the surface and 100 m, and also the salinity at a depth of 200 m, from Bradford's observations, are shown in Fig. 50. There is a noticeable non-seasonal fluctuation with a period of approximately 50-55 days superimposed on the seasonal fluctuation; this non-seasonal fluctuation is best defined from the sub-surface measurements where the influence of coastal run-off is less marked (*see* p. 56). The amplitude of the fluctuation of the sub-surface salinity is greatest in winter (May/October) and correlation between the salinity and temperature fluctuations is closest at this time (Fig. 50). In summer the sub-surface water found at this 'permanent station' was mainly of subantarctic origin derived from the Southland Current (in February at 100 m the temperature was 11°C and the salinity 34.7‰, while the respective typical values in Subtropical Water [e.g. Stn D849, Appendix II] are 15.5°C and 35.4‰ and in the Southland Current [e.g. Stn D860, Appendix II] the values are 12.5°C and 34.6‰). An explanation for this stronger fluctuation in winter than summer and the presence of water of mainly subantarctic origin in summer cannot be given in terms of the seasonal variation of the winds on the North Canterbury coast; the wind-derived transport of the Southland Current, being greater in winter (Heath 1972d), increases the amount of low salinity, low temperature water found near Kaikoura as well as hindering the passage of an anticyclonic eddy of Subtropical Water moving towards Kaikoura.

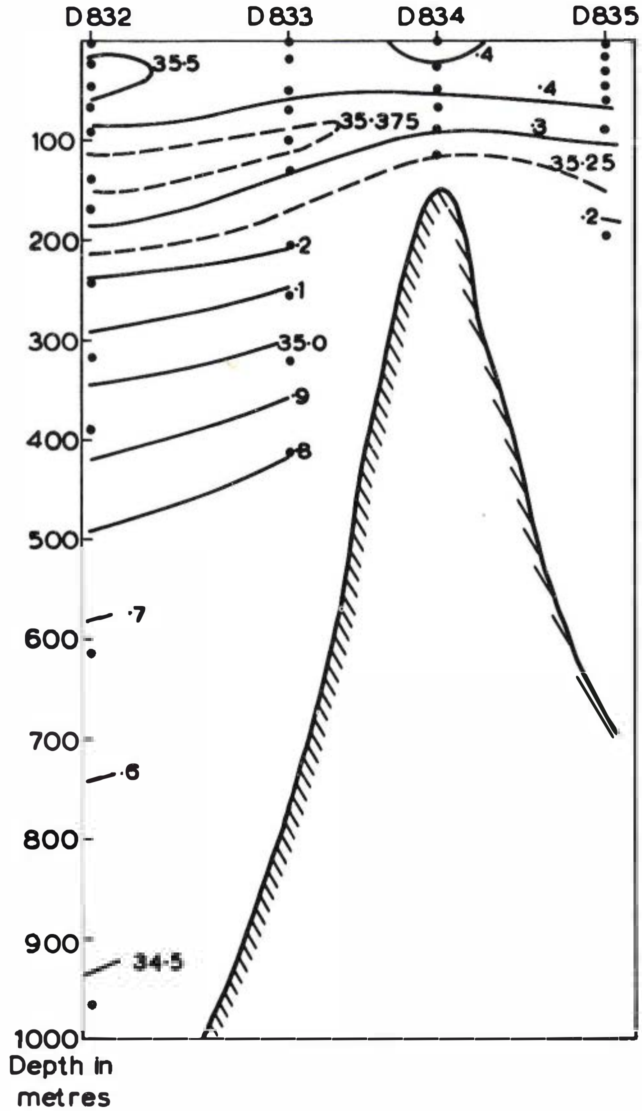

Fig. 54. Cross-sectional salinity (‰) profile across the Ranfurly Bank near East Cape. Station positions are shown in Fig. 4.

A tentative explanation for this phenomenon can be given in terms of the flow in the East Cape Current System. During February/March 1969 the tongue of the East Cape Current System was found further to the east (Fig. 6) than in September/October 1967 (Fig. 16, Heath 1972a). Assuming that this is the usual situation, with the tongue being further to the east in summer than in winter (the positions of the anticyclonic eddy in the East Cape Current [Table 2] supports this), we see that a small anticyclonic eddy shed off from this tongue will be more likely to be guided towards Kaikoura in winter than in summer. In summer the small eddy is likely to be guided further south. The data collected off this coast supports this, for in November/December 1968 an anticyclonic eddy was found just north of the Mernoo Gap and the deflection of the Southland Current near Kaikoura was very weak (Fig. 35); in February/March 1969 the deflection of the Southland Current near Kaikoura was also very weak (Figs 5, 8); in September/October 1967 an anticyclonic eddy was present near Kaikoura and there was a strong deflection of the Southland Current towards the east (Heath 1972a). Thus we see that in summer the tongue of the East Cape Current System is found further to the east, no anticyclonic eddies move towards Kaikoura and the main flow of the Southland Current is northwards past Kaikoura. This flow turns east near Cook Strait and moves along the east coast of the North Island and, in doing so, pushes the East Cape Current further offshore. In winter the tongue of the East Cape Current is found closer to the coast and the anticyclonic eddies shed off from this tongue move towards Kaikoura where they tend to deflect the Southland Current towards the east. The northwards flow of the Southland Current past Kaikoura is therefore reduced and the East Cape Current comes closer

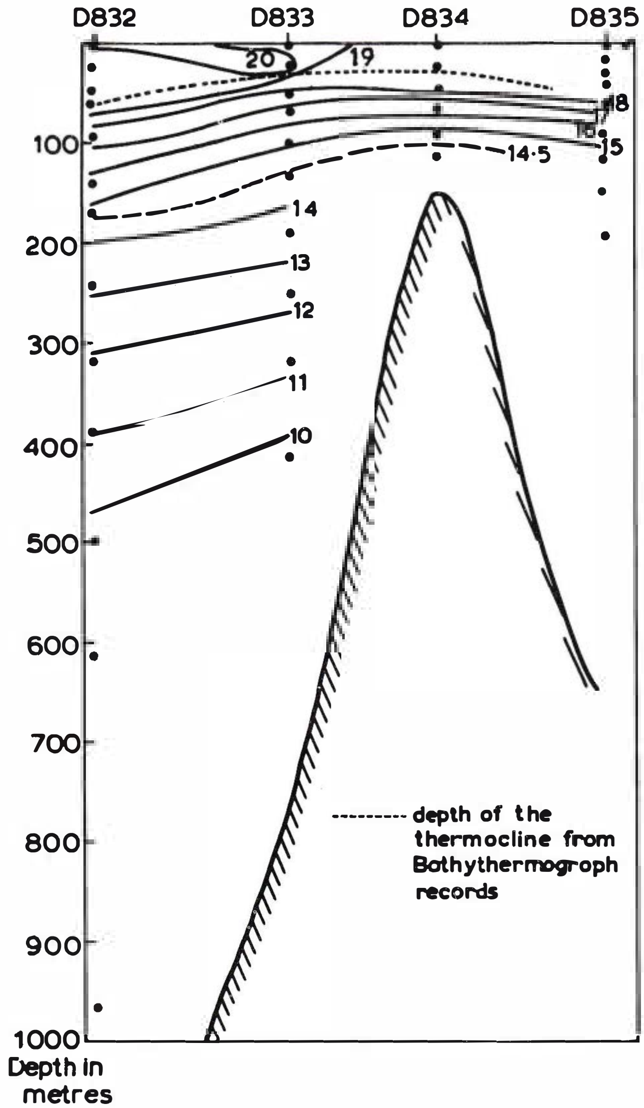

Fig. 55. Cross-sectional temperature (°C) profile across the Ranfurly Bank near East Cape. Station positions are shown in Fig. 4.

to the coast. These circumstances explain why patches of Subtropical Water are found near Kaikoura mainly in winter and why water of subantarctic origin is found near Kaikoura in summer, the type of water found depending on the position of the tongue of the East Cape Current System.

The Mechanism Generating the Eddies which Travel Towards Kaikoura

It has been found that the warm water near Kaikoura is transported there in the form of anticyclonic eddies which have probably broken off from the East Cape Current System (*see* p. 57). For these small eddies to develop, some mechanism must act to disturb the flow in the East Cape Current. The first disturbing mechanism that suggests itself is the influence of the passage of the atmospheric anticyclones over New Zealand. The direct effect that the winds associated with those atmospheric anticyclones have in generating these eddies can be examined by calculating the energy in an eddy, and relating this to the time needed for the winds to provide this energy. The variations of the geostrophic current with depth between a pair of stations (D658, D659) occupied in an eddy located near Kaikoura in October 1967 are shown in Fig. 20. A reference surface of 1500 dbars has been assumed between these stations but, as the current was most likely not zero at this depth, the calculated energies will be under-estimates. The current profile has been approximated (*see* p. 35) by the linear equation -

$$C = -2 \times 10^{-4} Z + 0.30$$

where C is the current speed (m s^{-1}) and Z is the depth (m) (Fig. 20). Little is known about the spatial variability in the eddy and therefore because of lack of knowledge to the contrary the speed has been assumed at a fixed depth. If, say, the horizontal variation were taken to be a linear function of the distance from the centre, both the kinetic and potential energies would be halved but the decrease would not affect the later argument based on the length of time to transfer the energy from the wind. The kinetic energy per unit area of a column of water from the surface to a depth of 1500 m in the eddy is 1.58×10^5 joules and the potential energy relative to a homogeneous ocean of the same column relative to 1500 m is 4.6×10^5 joules. For the wind to add a total energy per unit area to the column of 6.2×10^5 joules, taking the average current speed during the transfer as half the final surface speed (i.e. 0.15 m s^{-1}), the wind would have to blow parallel to the current at a speed of 15 m s^{-1} for 79 days or, alternatively at a speed of 30 m s^{-1} for a period of 20 days (*see* p. 36). As the typical period of the passage of atmospheric anticyclones over New Zealand is six days (approx.) (Garnier 1958), it is unlikely that the passage of a single anticyclone is the generating mechanism behind the formation of these small eddies for -

1. the period is less than the periodicity of the influx of the eddies at Kaikoura;
2. the wind speed/time factor in the atmospheric anticyclones is considerably less than that required to provide the energy in the eddies.

Assuming that the disturbance in the flow of the East Cape Current would have the same period as that found for the occurrence of warm water near Kaikoura, we can look for a disturbance of this period in the source of the East Cape Current. The East Cape Current has its source initially in the East Australian Current, the water having moved westwards across the Tasman Sea to pass around North Cape and along the northeastern coast of New Zealand as the East Auckland Current (Garner 1969). Hamon (1968) analysed the spectrum of the sea level at Lord Howe Island in relation to the circulation of the East Australian Current and found that there are periods in the spectrum between two months and a year which are due to the movement of the circulation pattern relative to the island. Also, Hamon and Kerr (1968) examined the time and space scales of variations in the East Australian Current by correlating different surface current velocities estimated by merchant ships operating along the east coast of Australia. They concluded that the East Australian Current System has a period of the order of 70 days (i.e. approximately two months). This period is reasonably close to that of the influx at Kaikoura and it therefore seems likely that a periodic increase in the amount of water entering the East Cape Current System around East Cape, linked to the periodic nature of the East Australian Current System, increases the flow of the East Cape Current such that a small anticyclonic eddy is formed. This eddy is then guided by the bottom topography towards Kaikoura, where the temperature and salinity contrast between this warm, saline water and the cool, low salinity water of the Southland Current is observed. One possible method for the formation of these eddies would be for the increased flow of water around East Cape to generate meanders in the East Cape Current which might, on meeting the sloping bottom at the southern end of the Hikurangi Trench, become unstable and grow to form eddies. A tentative theory of such a mechanism is given in Appendix III.

Influence of Local Winds on the Hydrology of the Water Along the North Canterbury Coast

Alongshore winds from both directions influence the temperature and salinity distribution on the North Canterbury coast. Southerly winds decrease the temperature and salinity by the increased advection of this water in the Southland Current, a reported instance being given by Heath (1970) when the surface temperature at Kaikoura decreased 5°C in 24 hours. Northerly winds also produce a decrease in the near-surface temperature and salinity through the effects of coastal upwelling (Heath 1972b). Thus on the coast because nearly all winds will have an alongshore component, local winds will play a large role in determining the changes in the day-to-day temperature and salinity distributions.

HYDROLOGY OF THE WATER ALONG THE EAST COAST OF THE NORTH ISLAND

The east coast of the North Island is bathed in the south by the relatively cool, low salinity water of the northward flowing Southland Current and in the north by the warm, saline Subtropical Water of the southward flowing East Cape Current. The type of water found at any particular time or place on this coast depends essentially on the position of the northern boundary between the Southland and East Cape Currents. Heath (1972a) has discussed the fluctuations in the temperature and salinity distributions that occur on this coast and he showed that though most of the water in the Southland Current turns east near Cape Turnagain, the near-surface water may travel further north than the deeper water, such that cool, low salinity water may be found on this coast north of Hawke Bay. The surface temperature boundary between the Southland and East Cape Currents has also been examined with an Infra-red Radiation Thermometer by Ridgway (1970b), who also found the boundary present near Cape Turnagain.

At East Cape the surface temperature and salinities are markedly influenced by upwelling of cool, low salinity water which adds to the complexity of the hydrology of this region.

Occurrence of Low Temperature Water Near East Cape

Relatively low surface water temperatures found near East Cape by Garner (1959) were associated by him with upwelling 'possibly by southward moving water impinging against the shelf edge which extends well offshore from East Cape to the Ranfurly Bank'. Several typical thermograph traces collected from M.V. *Hawea* which show this phenomenon are given in Fig. 51 and from these it can be seen that the low temperature water can exist over a considerable distance near East Cape. The lowest recorded surface temperature and the surface temperature of the adjacent warmer water near East Cape are shown for different times in the period between November 1967 to October 1968 (Fig. 52). The horizontal temperature changes are larger in summer than in winter and this most likely results from the presence of a strong summer thermocline (Fig. 53), which increases the vertical temperature gradient in the upper layers and thus the horizontal surface temperature gradient near the upwelling. Sub-surface hydrological observations collected in February/March 1969 confirm Garner's interpretation of the low temperatures being the result of upwelling in this region. The isohalines (Fig. 54), the isotherms and depth of the thermocline (Fig. 55) drawn from these observations slope upwards into the shallow water. The isobaths of the depth of the upper mixed layer (top of the thermocline) for January/February 1969 data (Fig. 9) show that near East Cape the thermocline sloped sharply downwards away from the coast. These isobaths (Fig. 9) were contoured from spot readings only and possibly in the centre of the upwelling the thermocline would be broken by the water upwelling from below.

CONCLUSION

The circulation off the East Coast of New Zealand forms an essential part of the circulation in the Southwest Pacific Ocean with New Zealand lying, as it does, athwart the general easterly water movement. It is therefore of value to examine how this circulation is integrated with the general circulation in the Southwest Pacific and in so doing assess the present knowledge of the circulation off the east coast.

Reid's (1961) analysis of the geostrophic circulation at the surface relative to 1000 dbars in the Pacific Ocean shows a general west to east flow past New Zealand, with the East Auckland and East Cape Currents represented by a southwards protrusion of the 1.4 dyn.m contour. Garner (1969) used all the then available NZOI data collected in a series of block surveys (Garner 1967a, b, 1970; Ridgway 1970a) to examine the offshore circulation around New Zealand. He showed that there are large spatial fluctuations in the general west-east flow north of New Zealand, with a strong flow southwards down the east coast of New Zealand north of Banks Peninsula. To aid further discussion of the circulation, a generalised figure of the mean surface currents is shown in Fig. 1.

An examination of the depth of the reference surface, to be used with the geostrophic method, using Defant's method in conjunction with the flow of Intermediate Water and supported by the depth of maximum correlation between the slope of the sea surface relative to different depths and the 200 m temperature. has been made by Heath (1972c). This showed that off the east coast of New Zealand the reference depth was deeper than the 1000 dbar surface used by Reid

(1961) and Garner (1969) in this area and thus the speeds calculated from their geostrophic circulation patterns would be under-estimates of the actual speed but in the correct direction.

Reid (1961) showed that the circulation off the east coast of New Zealand is closely linked to the circulation off the east coast of Australia, with part of the flow of warm Subtropical Water eastwards from the East Australian Current System passing around North Cape and giving rise to the East Auckland Current. Garner (1969) showed the East Auckland Current as flowing along the east coast of the North Island between North Cape and East Cape (*see* Fig. 1). The present study has shown that near East Cape the main flow of the East Auckland Current (i.e. that part north of approximately 37°S latitude) turns north, while the rest turns in a clockwise direction around East Cape, giving rise to the southward flowing East Cape Current, which adjusts the mass field such that a warm saline tongue protrudes southwards from East Cape.

The warm saline water of the Southland Current, which is also derived from the East Australian Current System, flows eastwards both through Foveaux Strait and south of Stewart Island before turning northward along the continental shelf and slope on the east coast of the South Island (Heath 1972a). The Subtropical Water over the continental shelf and upper part of the continental slope off the east coast meets the less saline Subantarctic Water further offshore on the slope in the Southland Front. The water in the zone of large horizontal gradients, together with the coastal water further inshore, moves northwards as the Southland Current. South of Banks Peninsula the Southland Current is recognised at the surface by mainly warm, saline, Subtropical Water, bounded inshore by coastal water and offshore by Subantarctic Water. In its passage northwards through the western side of the Mernoo Gap, cool, low salinity Subantarctic Water is brought closer to the surface, (some of the Southland Current water most likely also turns offshore near Banks Peninsula); and north of Banks Peninsula the Southland Current is recognised by cool, low salinity water bounded inshore by the warm saline water which flows northwards on the continental shelf, also in the Southland Current and offshore by warm saline water derived from the East Cape Current. The Southland Current branches into two components near Kaikoura, with one component meandering towards the east and the other component continuing northwards from Kaikoura as a shallow flow between the southern end of the Hikurangi Trench and the coast (Heath 1972a). This northward extending component diverges seawards north of Kaikoura, most of the water sweeping across the southern end of Cook Strait and continuing northwards along the east coast of the North Island, while the rest enters the southwestern side of Cook Strait around Cape Campbell. The relative strength of these two components, one sweeping across the southern end of Cook Strait and the other entering Cook Strait, is most likely dependent on the strength of the component of the East Cape Current found over the Cook Strait Canyon (Heath 1971). The cool, low salinity water entering Cook Strait near Cape Campbell is mainly confined to the continental shelf. This cool, low salinity water mixes with both the warmer, more saline, surface and sub-surface Subtropical Water of the D'Urville Current (which is also derived from the East Australian Current System), which flows into Cook Strait from the north, and with the water over the Cook Strait Canyon, which has its origin in the East Cape Current. Mixed water derived from all three currents travels eastward across Cook Strait and around Cape Palliser to meet the water of the Southland Current that diverges seawards between Kaikoura and Cook Strait on its seaward side. The Southland Current turns eastwards south of Hawke Bay (usually near Cape Turnagain), and the combined Southland and East Cape Current waters, after flowing south, turn east, then northeast, at about the latitude of Cape Palliser, to form the outer arm of the East Cape Current System. It has been shown here that this outer arm is not as well developed as the inshore arm of the East Cape Current and is defined as far north as East Cape where the water becomes indistinguishable from the water of the East Auckland Current that turns north near East Cape. Where the East Cape Current turns northeast a large permanent anticyclonic eddy is formed. The presence of small eddies (dashed eddy in Fig. 1), which are shed off periodically from this larger eddy, has been shown here. These eddies are guided by the bottom topography towards Kaikoura where they influence the northward passage of the Southland Current. It is suggested that 50-70 days periodicity of these eddies is linked to the periodicity of the East Australian Current System, with the flow clockwise around East Cape being in the form of a series of pulses.

The warm, saline Subtropical Water of the East Cape Current meets the cool, less saline water of the Subantarctic Water in the Subtropical Convergence, which in this region extends along the Chatham Rise and northwards towards Kaikoura. The eastern boundary of the tongue of low salinity, cool water, which defines the Southland Current north of Banks Peninsula, is the northward extension of the Subtropical Convergence. The western or inshore arm of this tongue has been shown to be the Southland Front, which is formed between the inshore Subtropical Water and the Subantarctic Water components of the Southland Current.

ACKNOWLEDGMENTS

The writer is most grateful to the many individuals and establishments who have helped in this study. In particular I would like to thank: the extremely helpful masters (Captains R.D. and D.K. Matheson), officers and crew of M.V. *Taranui* from which observations were obtained; the N.Z. Oceanographic Institute cruise personnel who aided in collecting the data; the pilots of the Wellington Aero Club for their skilful flying and navigation during the aerial radiometer measurements; the Union Steam Shipping Company from whose vessels thermograph records and water samples were collected; the Applied Mathematics Division of the Department of Scientific and Industrial Research for computer facilities; Mr N.M. Ridgway, Mr J.W. Brodie, Dr A.E. Gilmour and Mr B.R. Stanton, all of N.Z. Oceanographic Institute for much helpful discussion; Miss P. Lawrence of N.Z. Oceanographic Institute and the Chief Cartographer, Information Service, Department of Scientific and Industrial Research, for preparing the many figures; Mrs R.M. Thompson of the N.Z. Oceanographic Institute for her care taken in typing the manuscript.

REFERENCES

BARKER, P.H.; KIBBLEWHITE, A.C. 1965: Physical oceanographic data from the *Tui* Cruise 1962. *N.Z. Jl Sci. 8(4)* : 604-34.

BRADFORD, J.M. 1972: Systematics and ecology of New Zealand central east coast plankton sampled at Kaikoura. *Mem. N.Z. oceanogr. Inst. 54. (Bull. N.Z. Dep. scient. ind. Res. 207).*

BRODIE, J.W. 1960: Coastal surface currents around New Zealand. *N.Z. Jl Geol. Geophys. 3(2)* : 235-52.

BROWN, N.L.; HAMON, B.V. 1961: An inductive salinometer. *Deep Sea Res. 8* : 65-75.

BURLING, R.W. 1961: Hydrology of circumpolar waters south of New Zealand. *Mem. N.Z. oceanogr. Inst. 10. (Bull. N.Z. Dep. scient. ind. Res. 143).*

DEACON, G.E.R. 1937: Hydrology of the Southern Ocean. *'Discovery' Rep. 15* : 1-124.

DEACON, G.E.R. 1945: Water circulation and surface boundaries in the ocean. *Q. Jl R. met. Soc. 71* : 11-25.

EKMAN, V.W. 1923: Über Horizontalgerlculation bei windergeugten Meeresstroungen. *Ark. Mat. Astr. Fys. 17(26)* : 1-74.

FLEMING, C.A. 1952: Some South Pacific sea-bird logs. *Emu 49* : 169-88.

FUGLISTER, F.C.; VERONIS, A.C. 1965: A new method of tracking the Gulf Stream. *Limnol. Oceanogr. Suppl. 10* : 115-24.

GARNER, D.M. 1953: Physical characteristics of inshore surface waters between Cook Strait and Banks Peninsula, New Zealand. *N.Z. Jl Sci. Technol. Sect. B. 35(3)* : 239-46.

GARNER, D.M. 1959: The Subtropical Convergence in New Zealand surface waters. *N.Z. Jl Geol. Geophys. 2(2)* : 315-37.

GARNER, D.M. 1961: Hydrology of New Zealand coastal waters, 1955. *Mem. N.Z. oceanogr. Inst. 8. (Bull. N.Z. Dep. scient. ind. Res. 138).*

GARNER, D.M. 1967a: Hydrology of the southern Hikurangi Trench region. *Mem. N.Z. oceanogr. Inst. 39. (Bull. N.Z. Dep. scient. ind. Res. 177).*

GARNER, D.M. 1967b: Hydrology of the Southeast Tasman Sea. *Mem. N.Z. oceanogr. Inst. 48. (Bull. N.Z. Dep. scient. ind. Res. 181).*

GARNER, D.M. 1969: The geopotential topography of the ocean surface around New Zealand. *N.Z. Jl mar. Freshwat. Res. 3(2)* : 209-19.

GARNER, D.M. 1970: Oceanic hydrology northwest of New Zealand. Hydrology of the northeast Tasman Sea. *Mem. N.Z. oceanogr. Inst. 58. (Bull. N.Z. Dep. scient. ind. Res. 202).*

GARNIER, B.J. 1958: 'The Climate of New Zealand'. Edward Arnold Ltd, London. 191 pp.

GULDBERG, C.M.; MOHN, H. 1876: Etudes sur les mouvements de l'atmosphere. *Smithson. misc. Collns 3* : 122-248.

HAMON, B.V. 1968: Spectrum of sea level at Lord Howe Island in relation to circulation. *J. geophys. Res. 73(22)* : 6925-7.

HAMON, B.V.; KERR, J.D. 1968: Time and space scales of variations in the East Australian Current from merchant ship data. *Aust. J. mar. Freshwat. Res. 19* : 101-6.

HEATH, R.A. 1968: Geostrophic currents derived from oceanic density measurements north and south of the Subtropical Convergence east of New Zealand. *N.Z. Jl mar. Freshwat. Res. 2* : 659-77.

HEATH, R.A. 1969: Drift card observations of currents in the central New Zealand region. *N.Z. Jl mar. Freshwat. Res. 3* : 3-12.

HEATH, R.A. 1970: An occurrence of low water temperature on the North Canterbury coast (Note). *N.Z. Jl mar. Freshwat. Res. 4(2)* : 223-6.

HEATH, R.A. 1971: Hydrology and circulation in central and southern Cook Strait. *N.Z. Jl mar. Freshwat. Res. 5(1)* : 178-99.

HEATH, R.A. 1972a: The Southland Current. *N.Z. Jl mar. Freshwat. Res. 6(4)* : 497-533.

HEATH, R.A. 1972b: Oceanic upwelling produced by northerly winds on the north Canterbury coast, New Zealand. *N.Z. Jl mar. Freshwat. Res. 6(3)* : 343-51.

HEATH, R.A. 1972c: Choice of reference surface for geostrophic currents around New Zealand. *N.Z. Jl mar. Freshwat. Res. 6(1 & 2)* : 148-77.

HEATH, R.A. 1972d: Wind-derived water motion off the east coast of New Zealand between Kaikoura Peninsula and Cape Campbell. *N.Z. Jl mar. Freshwat. Res. 6(3)* : 352-64.

HEATH, R.A. 1973: Present knowledge of the oceanic circulation and hydrology around New Zealand, 1971. *Tuatara 20(3)* : 125-40.

HOUTMAN, Th.J. 1965: Winter hydrological conditions south of Kaikoura Peninsula. *N.Z. Jl Geol. Geophys. 8(5)* : 807-19.

HOUTMAN, Th.J. 1966: A note on the hydrological regime in Foveaux Strait. *N.Z. Jl Sci. 9(2)* : 472-83.

HYDROGRAPHIC DEPARTMENT, 1958: 'The New Zealand Pilot'. 12th Edition, London. 500 pp.

JILLETT, J.B. 1969: Seasonal hydrology of waters off the Otago Peninsula, southeastern New Zealand. *N.Z. Jl mar. Freshwat. Res. 3* : 349-75.

NEUMANN, G. 1955: Dynamics of wind driven ocean currents. *Met. Pap. N.Y. Univ. 2(4)* : 1-33.

NEUMANN, G. 1960: On the effect of bottom topography on ocean currents. *Dt. hydrogr. Z. 13(3)* : 132-41.

NEUMANN, G.; PIERSON, W.J. 1966: 'Principles of Physical Oceanography'. Prentice-Hall Inc., Englewood Cliffs, New Jersey. 545 pp.

OXNER, M. 1920: Chloruation par le methode Knudsen. *Bull. Commn int. Explor. scient. Mer Mediterr. 3.*

PATZERT, W.C. 1969: Eddies in Hawaiian waters. *Hawaii Inst. Geophys. Tech. Rep. HIG-69-8* : 1-51.

REID, J.L. 1961: On the geostrophic flow at the surface of the Pacific Ocean with respect to the 1000 decibar surface. *Tellus 13(4)* : 490-502.

RIDGWAY, N.M. 1970a: Hydrology of the Southern Kermadec Trench region. *Mem. N.Z. oceanogr. Inst. 56. (Bull. N.Z. Dep. scient. ind. Res. 205).*

RIDGWAY, N.M. 1970b: Aerial radiometry of sea surface temperatures on the east coast, North Island, New Zealand. *N.Z. Jl mar. Freshwat. Res. 4(4)* : 474-8.

RIDGWAY, N.M. (in press): Hydrology of the Bounty Islands region. *Mem. N.Z. oceanogr. Inst.*

SDUBBUNDHIT, Cha Erb; GILMOUR, A.E. 1964: Geostrophic currents derived from oceanic density over the Hikurangi Trench. *N.Z. Jl Geol. Geophys. 7(2)* : 271-8.

STOMMEL, H. 1965: 'The Gulf Stream'. University of California Press, Berkeley. 248 pp.

SVERDRUP, H.U. 1941: The influence of bottom topography on the ocean currents. *J. appl. Mech. (von Karman Anniversary Vol.)* : 66-75.

SVERDRUP, H.U.; JOHNSON, M.V.; FLEMING, R.M. 1942: 'The Oceans, Their Physics, Chemistry and General Biology'. Prentice-Hall Inc., Englewood Cliffs, New Jersey. 1087 pp.

APPENDIX I

Station Circumstances

Stn No.	Date Time N.Z. Start	Finish	Latitude (S) ° '	Longitude (E) ° '	Depth (m)
September 1967					
G139	19/1436	19/2102	41 45	175 02	1939
G140	19/2215	20/0241	41 50	175 15	1991
G141	20/0437	20/0736	41 12	175 28	2670
G142	20/1438	20/	42 24.8	173 56.5	1211
G143	21/1447	21/1606	42 26.1	173 47.6	95
G145	21/2014	21/2133	42 24.6	174 21.6	1566
G147	22/0337	22/0510	42 43	174 48	1514
G148	22/0716	22/0828	43 03	174 48	686
G149	22/1131	22/1227	43 27.5	173 58	697
G150	22/2006	22/2117	42 08	174 33	1463
G151	22/2315	22/2400	41 47	174 34	124
G152	23/0143	23/0314	41 41	174 37	284
November/December 1968					
D745	27/0438	27/0506	42 07.8	173 58.3	18
D746	27/0534	27/0610	42 10.2	174 32	88
D747	27/0726	27/1014	42 17	174 16	960
D748	27/1140	27/1330	42 25	174 39	2200
D749	27/1505	27/1730	42 35	174 48	1800
D750	27/1933		42 50	174 29	1270
D751	27/2325	27/0130	42 38	174 09	2200
D752	28/0310	28/0447	42 29.4	173 53	1240
D753	28/0547	28/0623	42 25	173 45	29
D754	28/0702	28/0730	42 27	173 40	55
D755	28/0756	28/0855	42 30	173 41	410
D756	28/0930	28/1125	42 32	173 48	1200
D757	28/1217	28/1525	42 37	173 57	1760
D758	28/1651	28/1857	42 35	173 44	1280
D759	28/1940	28/2059	42 35.3	173 36.7	710
D760	28/2134	28/2232	42 40	173 41.6	310
D761	28/2300	28/2345	42 43	173 38.6	120
D762	29/0008	29/0145	42 42.5	173 35	490
D763	29/0436	29/0505	42 46.7	173 24.2	18
D764	29/0636	29/0728	42 54.5	173 39	230
D765	29/1015	29/1118	43 98	174 05	680
D766	29/1405	29/1510	43 23	174 33	480
D767	29/1611	29/1703	43 26	174 21	540
D768	29/1827	29/1927	43 31	174 06.5	610
D769	29/2255	29/2400	43 37.5	173 36	85
D770	30/0254	30/0330	43 44.5	173 09	25
D771	30/0543	30/0627	43 45	173 33	80
D772	30/0925	30/1020	43 45	174 00	230
D773	30/1353	30/1500	43 45	174 38	520
D774	30/1820	30/1935	44 07	174 38	540
D775	30/2035	30/2135	44 07	174 50	500
D776	1/0005	1/0145	43 44	174 49	455
D777	1/0847	1/1040	42 43	174 00	1500
D783	2/0940	2/1220	41 57.5	175 16	2015
D784	2/1355	2/1520	41 47	175 23	1090
D785	2/1612	2/1728	41 41.5	175 16	400
D786	2/1800	2/1910	41 46	175 09.7	770
February 1969					
D808	21/1555	21/1700	41 40.5	175 28	550
D809	21/2005	21/2200	41 33	176 00	1160
D810	21/2315	21/2355	41 20.5	176 00	160
D811	22/0510	22/0635	40 54	176 49	1060
D812	22/0857	22/0939	40 30.5	176 49.5	162
D813	22/1535	22/1700	40 00	177 40	980
D814	22/1940	22/2030	39 35	177 54	360
D815	23/0157	23/0350	39 00	178 31	1350
D816	23/0950	23/1057	38 14	178 49	220
D817	23/1423	23/1550	37 44	178 58	550
March 1969					
D818	1/0626	1/0845	36 00	178 00	1800
D819	1/1137	1/1533	36 30	178 00	2500
D820	1/1810	1/2006	37 00	178 00	2000
D821	2/1005	2/1255	37 30	180 00	4400
D822	2/1753	2/1939	37 28	178 59 W	2340
D823	2/2255	3/0055	37 00	179 00 W	2880
D824	3/0648	3/0855	37 00	180 00 W	3500
D825	3/1304	3/1503	36 30	179 30 W	4480
D826	3/1900	3/2220	37 57	178 59 W	6000
D827	4/0445	4/0653	36 01	179 59	2690
D828	4/1200	4/1633	35 58	179 01	2500
D829	4/2050	4/2305	36 30	179 00	2500
D830	5/0223	5/0452	37 00	179 00	2500
D831	5/0737	5/0955	37 15	178 40	1300
D832	5/1430	5/1603	37 15	178 00	1480
D833	5/1807	5/1928	37 28.5	178 20	760
D834	5/2110	5/2150	37 36	178 38	145
D835	5/2325	6/0050	37 44	178 58	650
D836	6/0325	6/0721	37 34	179 22	1395
D837	6/1400	6/1535	38 30	178 53	1250
D838	6/1822	6/2310	38 30	179 30	3560
D839	7/0335	7/0735	38 30	179 45	3600
D840	7/1058	7/1426	38 30	179 99 W	3520
D841	8/0040	8/0315	39 30	180 00 W	2200
D842	8/0828	8/1105	39 30	179 00	3400
D843	8/1400	8/1525	39 34	178 27.5	1700
D844	9/0025	9/0205	40 30	177 30	1790
D845	9/0430	9/0624	40 30	178 00	2100
D846	9/1120	9/1335	40 30	179 00	3200
D847	9/1700	9/1920	41 00	179 00	3100
D848	10/0120	10/0623	41 00	178 00	3000
D849	10/0939	10/1152	41 30	178 00	2900
D850	10/1704	10/1902	42 00	178 00	2660
D851	11/0140	11/0623	41 30	177 00	2850
D852	11/1100	11/1235	41 22.5	176 32	1820
D853	11/1420	11/1535	41 23	176 12	1010
D854	11/2105	11/2300	42 00	176 00	2252
D855	12/0206	12/0422	42 15	176 30	2690
D856	12/0730	12/0858	42 26	176 00	1790
D857	12/1400	12/1530	42 26	175 00	2100
D858	12/1853	12/2020	42 30	174 30	1990
D859	12/2320	13/0100	42 35.5	174 05	2100
D860	13/0545	13/0644	42 30	173 40	1160
D861	13/0923	13/1017	42 17	174 10	1120
D862	13/1230	13/1355	42 08	174 38	1760
D863	13/1555	13/1725	42 00	175 00	2150
D864	14/0040	14/0135	41 41	175 12	600

APPENDIX II

Under station numbers below are listed measured depths, temperatures, and salinities. These are followed by derived values of density, dynamic height anomaly, sound velocity and potential energy anomaly. The meaning of the table headings is as follows.

D is the sampling depth in metres.

T is the sampling temperature in °C x 100.

S is the sample salinity in ‰ x 100.

σ_t is the density reduced to surface pressure isothermally.

σ_{stp} is the *in situ* density.
The 'σ' value is derived from the relative density, ρ, from the relation $\sigma = (\rho - 1) \times 10^5$.

$\Sigma\Delta h$ is the anomaly of the geopotential distance from the sea surface to the sample depth in dynamic metres x 100.

C is the *in situ* sound velocity in m s^{-1} x 10.

Cm is the integral mean sound velocity between the sea surface and the sample depth in m s^{-1} x 10.

K is the correction (m x 10) to be applied to an echo sounding reading of D on a machine calibrated for a velocity of 1 500 m s^{-1}.

$\Sigma\Delta X$ is the potential energy anomaly from the sea surface to the sample depth in kgm m s^{-4} x 10^3.

D	T	S	σ_t	σ_{stp}	$\Sigma\Delta D$	C	C_m	K	$\Sigma\Delta X$
G139									
0	1186	3500	2663	2663	0.0	14970	14970	0	0.0
6	1187	3502	2665	2668	0.9	14972	14971	-0	2.5
15	1188	3502	2665	2671	2.1	14974	14972	-0	15.8
30	1186	3502	2665	2679	4.2	14975	14973	-1	63.3
45	1149	3493	2665	2685	6.3	14964	14972	-1	142.5
60	1130	3493	2669	2696	8.4	14959	14969	-1	252.3
G140									
0	1164	3498	2666	2666	0.0	14962	14962	0	0.0
9	1171	3497	2664	2668	1.3	14966	14964	-0	5.7
22	1180	3497	2662	2672	3.1	14971	14966	-0	34.3
43	1178	3500	2665	2684	6.1	14973	14969	-1	131.2
G141									
0	1115	3486	2666	2666	0.0	14943	14943	0	0.0
10	1115	3486	2666	2670	1.4	14945	14944	-0	7.0
24	1117	3487	2666	2677	3.3	14947	14945	-1	40.1
49	1113	3487	2667	2689	6.8	14951	14947	-2	167.2
74	1117	3488	2667	2700	10.3	14957	14949	-2	381.6
98	1111	3487	2667	2712	13.7	14958	14951	-3	670.3
147	1105	3487	2668	2735	20.5	14964	14955	-4	1511.1
164	1067	3478	2668	2742	22.9	14952	14955	-5	1882.3
259	935	3490	2700	2818	34.9	14920	14948	-9	4420.1
G142									
0	1091	3420	2619	2619	0.0	14926	14926	0	0.0
10	987	3418	2635	2640	1.8	14890	14908	-1	8.9
25	1035	3454	2655	2667	4.1	14915	14905	-2	50.5
50	1142	3491	2665	2687	7.8	14961	14922	-3	187.0
75	1117	3489	2668	2702	11.3	14957	14934	-3	406.0
100	1073	3480	2669	2714	14.8	14944	14938	-4	709.7
150	953	3461	2675	2743	21.6	14906	14934	-7	1561.7
194	960	3463	2675	2763	27.5	14916	14928	-9	2578.0
292	919	3460	2679	2812	40.6	14917	14924	-15	5757.5
490	833	3452	2687	2909	66.5	14915	14921	-26	15886.3

D	T	S	σ_t	σ_{stp}	ΣΔD	C	C_m	K	ΣΔX
G143									
0	1001	3372	2597	2597	0.0	14888	14888	0	0.0
10	976	3398	2622	2626	1.9	14884	14886	-1	9.6
25	938	3432	2654	2666	4.4	14877	14882	-2	53.2
50	924	3446	2668	2690	8.0	14877	14880	-4	188.5
75	927	3448	2669	2703	11.5	14883	14880	-6	404.3
G145									
0	1182	3500	2664	2664	0.0	14968	14968	0	0.0
10	1181	3497	2662	2667	1.4	14969	14969	-0	7.1
25	1187	3499	2662	2674	3.6	14975	14971	-0	44.6
50	1143	3495	2668	2690	7.1	14962	14970	-1	176.5
74	1150	3495	2666	2700	10.4	14969	14968	-2	384.1
99	1139	3495	2668	2713	13.9	14969	14969	-2	686.3
140	1095	3485	2669	2732	19.6	14958	14967	-3	1369.3
236	1040	3487	2680	2787	32.6	14955	14963	-6	3812.9
284	940	3463	2678	2807	39.0	14923	14959	-8	5463.2
472	835	3453	2687	2901	63.6	14913	14943	-18	14765.5
G147									
0	1199	3502	2663	2663	0.0	14975	14975	0	0.0
10	1197	3503	2664	2668	1.4	14976	14975	-0	7.1
24	1203	3503	2663	2673	3.4	14979	14976	-0	40.9
48	1196	3505	2665	2687	6.8	14982	14979	-1	163.4
73	1194	3504	2665	2698	10.3	14984	14980	-1	376.9
97	1191	3503	2665	2709	13.7	14988	14982	-1	666.8
146	1194	3507	2667	2733	20.7	14997	14985	-1	1511.7
190	1175	3504	2669	2754	26.9	14997	14988	-2	2556.1
288	1043	3476	2671	2801	40.7	14963	14985	-3	5861.0
476	852	3461	2691	2907	65.8	14922	14968	-10	15418.2
G148									
0	1126	3478	2658	2658	0.0	14946	14946	0	0.0
10	1119	3477	2658	2663	1.5	14945	14946	-0	7.3
24	1140	3484	2660	2671	3.5	14955	14948	-1	42.1
48	1179	3502	2666	2688	6.9	14976	14957	-1	165.3
72	1193	3505	2666	2698	10.3	14984	14964	-2	367.3
140	1148	3497	2668	2731	19.9	14979	14973	-3	1380.0
183	1084	3484	2670	2752	25.9	14962	14972	-3	2351.6
260	975	3470	2678	2796	36.4	14934	14965	-6	4679.1
G149									
0	1172	3500	2666	2666	0.0	14965	14965	0	0.0
10	1174	3502	2667	2672	1.4	14968	14966	-0	6.9
24	1172	3500	2666	2677	3.3	14968	14967	-1	39.9
48	1136	3495	2669	2691	6.6	14960	14966	-1	159.5
72	1118	3493	2671	2703	9.9	14956	14963	-2	356.4
96	1119	3493	2671	2714	13.2	14961	14962	-2	631.7
144	1091	3489	2673	2738	19.8	14959	14961	-4	1418.2
160	1075	3486	2673	2745	21.9	14955	14961	-4	1749.2
G150									
0	999	3436	2647	2647	0.0	14895	14895	0	0.0
10	1007	3439	2648	2653	1.6	14900	14898	-1	7.8
25	1162	3492	2662	2673	3.8	14965	14919	-1	47.1
49	1099	3486	2669	2691	7.2	14946	14937	-2	171.9
74	1113	3488	2668	2701	10.6	14956	14941	-3	384.5
98	1100	3490	2672	2716	13.9	14954	14945	-4	668.2
139	1040	3475	2671	2734	19.5	14937	14945	-5	1332.7
296	931	3466	2682	2816	40.6	14922	14937	-12	5902.4
488	836	3460	2693	2914	64.9	14918	14930	-23	15448.6
G151									
0	1115	3467	2651	2651	0.0	14941	14941	0	0.0
10	1115	3467	2651	2656	1.5	14942	14942	-0	7.7
25	1077	3460	2652	2664	3.8	14931	14939	-1	47.8
50	1051	3478	2671	2694	7.4	14927	14934	-2	182.6
75	1038	3476	2672	2706	10.8	14927	14932	-3	393.8
100	994	3471	2676	2721	14.1	14914	14929	-5	686.0
G152									
0	1269	3490	2640	2640	0.0	14997	14997	0	0.0
9	1265	3490	2640	2644	1.5	14997	14997	-0	6.6
23	1277	3491	2639	2649	3.8	15003	14999	-0	43.5
47	1268	3491	2641	2662	7.7	15005	15001	0	181.9
70	1270	3492	2641	2672	11.5	15009	15003	0	403.2
93	1249	3491	2644	2686	15.3	15006	15004	0	709.2
132	1170	3488	2657	2717	21.4	14985	15002	0	1394.9
D745									
0	1326	3393	2553	2553	0.0	15004	15004	0	0.0
15	1280	3417	2581	2588	3.5	14995	14999	-0	26.2
D746									
0	1239	3418	2590	2590	0.0	14978	14978	0	0.0
25	1228	3423	2596	2607	5.2	14979	14979	-0	65.3
50	1190	3440	2616	2639	10.1	14972	14977	-1	249.8
75	1123	3448	2635	2669	14.6	14954	14972	-1	529.4
D747									
0	1243	3463	2624	2624	0.0	14985	14985	0	0.0
25	1179	3460	2634	2645	4.4	14967	14976	-0	54.6
49	1084	3451	2644	2666	8.3	14936	14964	-1	201.5
74	1083	3472	2661	2694	12.2	14943	14956	-2	437.0
99	1046	3471	2667	2711	15.7	14933	14951	-3	746.6
148	985	3466	2673	2740	22.5	14918	14943	-6	1582.0
188	941	3460	2676	2761	27.9	14907	14936	-8	2486.0
266	874	3453	2681	2811	40.8	14897	14925	-14	5552.7
382	816	3447	2685	2859	53.2	14891	14917	-21	9697.0
477	770	3445	2691	2908	65.2	14889	14911	-28	14852.9
665	727	3449	2700	3002	88.2	14903	14907	-41	27939.2
765	693	3449	2705	3052	100.0	14906	14907	-48	36444.3
865	640	3447	2710	3103	111.3	14901	14906	-54	45648.6
D748									
0	1421	3471	2594	2504	0.0	14045	15045	0	0.0
25	1200	3471	2638	2650	4.7	14976	15010	0	58.3
49	1191	3471	2640	2662	8.6	14976	14993	-0	205.2
74	1161	3471	2646	2679	12.7	14970	14987	-1	454.9
98	1072	3469	2660	2705	16.4	14942	14979	-1	771.4
147	994	3466	2672	2738	23.3	14921	14963	-4	1622.0
620	727	3455	2705	2986	82.6	14896	14921	-32	24350.6
852	594	3448	2717	3105	107.9	14881	14912	-50	42987.8
1075	456	3449	2734	3226	129.5	14862	14904	-69	63805.8
1166	411	3451	2741	3274	137.4	14858	14900	-77	72607.4
1283	369	3453	2747	3334	146.8	14860	14897	-88	84198.0
1378	337	3455	2751	3382	154.1	14863	14894	-97	93848.1
D749									
0	1317	3471	2615	2615	0.0	15011	15011	0	0.0
25	1204	3470	2637	2648	4.4	14977	14994	-0	55.4

D	T	S	σ_t	σ_{stp}	ΣΔD	C	C_m	K	ΣΔX
D749 continued									
50	1198	3470	2638	2660	8.6	14978	14986	-0	212.0
75	1170	3470	2643	2677	12.7	14973	14982	-1	469.3
100	1112	3470	2654	2699	16.7	14956	14978	-1	814.1
145	968	3463	2674	2739	23.1	14911	14964	-3	1606.7
284	896	3461	2684	2813	41.4	14907	14937	-12	5522.5
379	822	3454	2690	2862	53.3	14894	14928	-18	9483.7
474	771	3450	2694	2910	65.0	14888	14920	-25	14441.0
571	718	3449	2701	2961	76.5	14884	14915	-33	20445.4
768	613	3447	2714	3064	98.4	14874	14905	-48	35105.7
865	557	3447	2721	3116	108.4	14867	14901	-57	43297.0
955	517	3448	2727	3162	117.2	14866	14898	-65	51341.3
1044	467	3448	2732	3209	125.5	14861	14895	-73	59652.5
1141	417	3450	2739	3261	134.0	14855	14892	-82	68948.1
1240	373	3453	2746	3314	142.1	14855	14889	-92	78540.3
1339	334	3454	2751	3364	149.6	14855	14887	-101	88264.6
1437	314	3456	2754	3412	156.8	14863	14885	-110	98170.4
1620	266	3460	2762	3503	169.3	14872	14883	-127	117287.6
D750									
0	1270	3474	2627	2627	0.0	14995	14995	0	0.0
24	1194	3471	2639	2650	4.1	14972	14984	-0	49.1
48	1195	3470	2638	2660	8.1	14977	14979	-1	192.1
72	1175	3469	2641	2674	12.0	14973	14978	-1	429.8
96	1043	3468	2665	2708	15.7	14931	14971	-2	738.6
144	962	3464	2675	2741	22.3	14909	14954	-4	1531.8
184	946	3464	2678	2762	27.6	14910	14945	-7	2399.2
275	884	3461	2686	2811	39.3	14901	14932	-13	5084.8
364	815	3454	2691	2857	50.3	14888	14922	-19	8612.5
453	755	3450	2697	2903	61.0	14879	14915	-26	12985.3
546	716	3449	2702	2950	71.9	14880	14909	-33	18406.0
638	665	3448	2708	2998	82.3	14874	14904	-41	24549.0
729	599	3447	2716	3048	92.0	14862	14900	-49	31208.8
827	536	3447	2723	3101	101.9	14852	14894	-58	38861.3
915	507	3447	2727	3145	110.3	14855	14891	-67	46208.7
998	484	3448	2730	3186	118.1	14860	14888	-75	53633.7
1096	426	3450	2738	3240	126.7	14853	14885	-84	62730.0
D751									
0	1242	3466	2626	2626	0.0	14985	14985	0	0.0
25	1197	3467	2636	2647	4.3	14974	14980	-0	53.9
49	1138	3470	2649	2671	8.2	14957	14973	-1	197.9
74	1083	3469	2658	2692	12.0	14942	14965	-2	431.6
97	1019	3465	2667	2711	15.3	14922	14957	-3	715.2
146	980	3465	2673	2739	22.1	14916	14944	-5	1536.4
194	952	3465	2678	2766	28.5	14914	14937	-8	2626.2
291	868	3459	2687	2819	41.0	14898	14927	-14	5648.5
386	825	3455	2690	2866	52.8	14895	14919	-21	9647.3
480	759	3450	2696	2915	64.2	14885	14913	-28	14590.6
579	709	3449	2703	2966	75.8	14882	14908	-35	20727.8
777	607	3447	2715	3069	97.6	14873	14900	-52	35528.4
876	567	3447	2720	3119	107.9	14873	14897	-60	44027.6
967	523	3447	2725	3166	117.0	14871	14895	-68	52403.4
1056	481	3448	2731	3213	125.5	14869	14893	-75	60985.5
1156	452	3449	2735	3262	134.6	14873	14891	-84	71105.4
1256	394	3451	2742	3317	143.2	14865	14889	-93	81521.3
1355	375	3452	2745	3364	151.3	14874	14888	-101	92101.2
1453	330	3455	2752	3416	159.0	14871	14887	-110	102805.7
1820	238	3462	2766	3598	184.2	14895	14886	-138	144096.1

D	T	S	σt	σ_{stp}	ΣΔD	C	C_m	K	ΣΔX
D752									
0	1235	3451	2616	2616	0.0	14981	14981	0	0.0
25	1138	3452	2635	2646	4.4	14952	14966	-1	55.5
50	1088	3454	2646	2668	8.5	14938	14955	-1	209.2
75	972	3445	2659	2693	12.4	14899	14943	-3	448.7
100	926	3445	2667	2712	16.0	14886	14930	-5	763.3
149	887	3450	2677	2745	22.6	14880	14915	-8	1593.8
195	887	3451	2678	2766	28.7	14888	14907	-12	2637.2
291	844	3448	2682	2814	41.3	14887	14901	-19	5689.1
384	816	3447	2685	2860	53.2	14891	14898	-26	9734.6
476	796	3446	2688	2904	65.0	14899	14897	-33	14795.9
574	762	3443	2690	2951	77.5	14901	14898	-39	21348.8
772	716	3449	2702	3052	101.9	14916	14901	-51	37786.2
868	618	3448	2714	3109	112.9	14894	14901	-57	46758.6
964	554	3447	2721	3160	123.0	14882	14900	-64	55995.5
1052	510	3448	2727	3207	131.7	14879	14898	-71	64803.8
D753									
0	1355	3414	2564	2465	0.0	15016	15016	0	0.0
10	1279	3411	2576	2581	2.3	14992	15004	0	11.5
20	1230	3419	2592	2601	4.5	14978	14995	-0	44.0
D754									
0	1242	3390	2567	2567	0.0	14975	14975	0	0.0
10	1250	3395	2570	2574	2.3	14980	14978	-0	11.6
20	1247	3400	2574	2583	4.6	14981	14979	-0	45.9
30	1242	3421	2591	2605	6.8	14984	14980	-0	100.5
40	1244	3430	2598	2616	8.9	14987	14982	-0	173.1
D755									
0	1291	3378	2549	2549	0.0	14990	14990	0	0.0
49	1100	3460	2648	2670	10.0	14943	14966	-1	244.5
75	1060	3400	2609	2642	14.2	14924	14956	-2	502.0
97	1034	3457	2658	2702	18.3	14927	14948	-3	852.7
146	1002	3460	2666	2732	25.5	14923	14940	-6	1720.7
190	952	3458	2672	2759	31.6	14911	14935	-8	2753.8
384	888	3457	2682	2856	57.7	14919	14925	-19	10234.4
D756									
0	1283	3450	2606	2606	0.0	14997	14997	0	0.0
25	1189	3452	2626	2637	4.7	14970	14983	-0	58.4
50	1114	3455	2642	2665	8.9	14947	14971	-1	218.2
75	972	3448	2661	2695	12.8	14900	14955	-2	458.8
96	940	3450	2668	2712	15.8	14891	14942	-4	713.7
142	921	3452	2673	2737	22.1	14893	14926	-7	1464.4
289	871	3452	2681	2812	41.6	14898	14910	-17	5680.6
383	828	3448	2684	2858	53.9	14895	14907	-24	9785.5
476	804	3447	2687	2903	65.8	14902	14905	-30	14926.1
573	768	3444	2690	2950	78.2	14904	14905	-36	21421.0
769	715	3449	2702	3050	102.4	14916	14906	-48	37638.6
870	600	3448	2716	3112	113.8	14887	14906	-55	46960.8
963	554	3448	2722	3161	123.4	14882	14904	-62	55774.9
1051	486	3449	2731	3211	131.9	14869	14901	-69	64364.6
1143	472	3449	2732	3254	140.4	14880	14899	-77	73711.4
D757									
0	1313	3471	2616	2616	0.0	15009	15009	0	0.0
18	1246	3470	2629	2637	3.2	14990	15000	-0	29.3
35	1207	3471	2637	2653	6.2	14980	14992	-0	106.3

D	T	S	σ_t	σ_{stp}	$\Sigma\Delta D$	C	C_m	K	$\Sigma\Delta X$
D757 continued									
53	1170	3472	2645	2669	9.1	14969	14986	-0	236.2
71	1075	3473	2663	2695	11.8	14939	14978	-1	405.7
86	1093	3470	2657	2696	14.0	14948	14972	-2	578.0
167	969	3461	2672	2748	25.6	14915	14952	-5	2043.6
259	961	3468	2679	2796	38.0	14927	14941	-10	4683.7
338	910	3465	2685	2838	48.3	14922	14937	-14	7759.0
417	845	3457	2689	2878	58.4	14909	14933	-19	11547.7
573	758	3451	2697	2957	77.6	14901	14925	-28	21051.3
666	706	3448	2702	3005	88.6	14895	14922	-35	27884.6
738	671	3448	2707	3042	96.9	14892	14919	-40	33698.9
837	612	3448	2715	3096	107.8	14885	14915	-47	42274.7
914	570	3448	2720	3136	115.8	14881	14913	-53	49325.0
1004	513	3448	2727	3185	124.8	14872	14909	-61	57898.7
1096	468	3449	2733	3233	133.4	14870	14906	-69	66951.7
1193	415	3451	2740	3286	141.9	14864	14903	-77	76693.4
1283	376	3452	2745	3332	149.3	14863	14900	-85	85851.8
D758									
0	1235	3449	2615	2615	0.0	14980	14980	0	0.0
19	1208	3450	2620	2629	3.5	14974	14977	-0	33.4
53	1089	3456	2647	2671	9.3	14938	14964	-1	241.9
71	972	3457	2668	2701	12.0	14899	14952	-2	407.2
106	936	3459	2676	2724	16.7	14893	14934	-5	825.4
142	917	3458	2678	2743	21.4	14892	14923	-7	1410.5
194	898	3456	2680	2768	28.2	14892	14915	-11	2547.5
252	890	3456	2681	2795	35.7	14899	14910	-15	4228.4
336	887	3457	2682	2835	46.7	14911	14909	-20	7445.3
420	857	3454	2685	2875	57.6	14914	14910	-25	11581.2
573	823	3449	2686	2945	77.6	14926	14912	-33	21520.6
666	767	3444	2690	2992	89.7	14918	14914	-38	29029.1
756	738	3448	2698	3040	101.1	14922	14914	-43	37103.4
840	633	3448	2712	3094	110.9	14895	14914	-48	44921.0
D759									
0	1380	3388	2538	2538	0.0	15021	15021	0	0.0
20	1240	3435	2603	2612	4.6	14983	15002	0	46.0
39	1078	3454	2648	2665	8.0	14932	14981	-1	146.0
59	1058	3458	2654	2681	11.1	14929	14964	-1	297.2
79	1044	3459	2658	2693	14.1	14927	14955	-2	504.3
118	1012	3460	2664	2717	19.8	14922	14945	-4	1065.9
154	1002	3460	2666	2735	24.9	14925	14940	-6	1766.9
247	918	3457	2677	2789	37.8	14908	14931	-11	4342.7
419	861	3452	2682	2872	60.6	14915	14923	-22	11947.3
D760									
0	1266	3442	2603	2603	0.0	14990	14990	0	0.0
22	1118	3450	2637	2647	4.0	14943	14966	-0	44.2
43	1026	3450	2654	2673	7.4	14913	14948	-1	152.8
65	970	3455	2667	2697	10.6	14898	14933	-3	325.6
86	1141	3453	2635	2674	13.8	14963	14933	-4	570.8
130	966	3455	2668	2727	20.6	14906	14933	-6	1307.7
173	927	3458	2677	2755	26.5	14900	14926	-9	2195.8
D761									
0	1331	3365	2531	2531	0.0	15002	15002	0	0.0
23	1145	3451	2633	2644	5.0	14953	14977	-0	58.0
45	1090	3453	2645	2665	8.7	14938	14962	-1	181.7
68	957	3457	2671	2702	12.1	14894	14946	-2	374.0
91	932	3458	2676	2717	15.2	14888	14932	-4	618.5

D	T	S	σ_t	σ_{stp}	$\Sigma\Delta D$	C	C_m	K	$\Sigma\Delta X$
D762									
0	1315	3396	2558	2558	0.0	15001	15001	0	0.0
23	1091	3455	2646	2656	4.6	14934	14967	-1	52.9
45	1020	3461	2663	2684	7.9	14914	14946	-2	165.4
68	986	3460	2668	2699	11.1	14905	14934	-3	347.8
91	974	3460	2670	2712	14.3	14904	14926	-4	599.3
136	960	3460	2673	2734	20.4	14906	14919	-7	1294.7
173	946	3459	2674	2753	25.4	14907	14917	-10	2067.5
266	905	3456	2679	2799	37.9	14906	14913	-15	4797.4
355	875	3452	2680	2841	49.7	14909	14912	-21	8465.0
D763									
0	1285	3320	2505	2505	0.0	14981	14981	0	0.0
6	1207	3425	2601	2604	1.5	14969	14975	-0	4.4
12	1177	3435	2615	2620	2.6	14960	14970	-0	14.9
D764									
0	1140	3449	2632	2632	0.0	14947	14947	0	0.0
23	1041	3447	2649	2659	3.8	14915	14931	-1	43.2
46	944	3449	2667	2688	7.1	14885	14916	-3	160.2
92	933	3456	2674	2716	13.4	14888	14901	-6	592.6
138	917	3457	2677	2740	19.5	14890	14897	-9	1291.5
D765									
0	1257	3467	2624	2624	0.0	14990	14990	0	0.0
22	1232	3467	2629	2639	3.9	14985	14987	-0	42.7
44	1187	3461	2633	2653	7.7	14973	14983	-0	168.3
66	1175	3464	2638	2667	11.4	14973	14980	-1	373.3
88	1064	3463	2657	2697	14.9	14937	14973	-2	641.8
132	967	3459	2671	2731	21.2	14909	14956	-4	1335.6
159	954	3459	2673	2745	24.9	14907	14948	-5	1872.1
251	938	3464	2679	2793	37.2	14918	14935	-11	4393.7
331	879	3459	2685	2835	47.6	14908	14930	-15	7412.0
421	829	3457	2691	2882	58.9	14903	14925	-21	11661.0
470	779	3454	2696	2910	64.8	14892	14922	-24	14308.2
D766									
0	1314	3474	2618	2618	0-0	15010	15010	0	0.0
17	1285	3475	2625	2632	3.1	15004	15007	0	26.2
33	1271	3481	2632	2647	5.9	15001	15005	0	96.3
50	1259	3493	2644	2666	8.7	15002	15004	0	213.8
67	1244	3497	2650	2680	11.4	15001	15003	0	371.5
100	1241	3501	2654	2699	16.5	15005	15003	0	797.5
134	1252	3505	2655	2715	21.7	15015	15005	0	1407.3
187	1175	3494	2661	2745	29.7	14996	15005	1	2691.0
254	1100	3485	2668	2782	39.5	14979	15000	0	4847.3
D767									
0	1285	3477	2626	2626	0.0	15001	15001	0	0.0
18	1278	3477	2628	2536	3.2	15002	15001	0	28.5
35	1238	3473	2633	2648	6.1	14991	14999	-0	106.8
53	1236	3481	2639	2663	9.2	14993	14996	-0	240.4
71	1223	3481	2642	2674	12.1	14991	14995	-0	424.4
106	1148	3471	2648	2696	17.8	14970	14990	-1	923.8
142	1141	3483	2659	2723	23.3	14976	14986	-1	1611.0
244	1013	3471	2672	2783	38.0	14945	14975	-4	4444.7
334	963	3468	2678	2829	50.3	14940	14966	-7	7996.6

D	T	S	σt	σstp	ΣΔD	C	Cm	K	ΣΔX
D768									
0	1131	3447	2633	2633	0.0	14944	14944	0	0.0
17	1085	3445	2639	2647	2.8	14931	14937	-1	24.2
34	1032	3445	2649	2664	5.6	14915	14930	-2	93.7
51	957	3443	2660	2683	8.1	14889	14921	-3	202.8
68	942	3443	2662	2693	10.6	14886	14912	-4	349.2
102	870	3441	2672	2719	15.3	14864	14900	-7	751.9
137	886	3448	2675	2738	20.0	14877	14892	-10	1311.9
193	892	3456	2681	2768	27.4	14890	14890	-14	2521.6
255	894	3458	2682	2798	35.4	14901	14891	-18	4314.4
315	889	3457	2682	2825	43.2	14908	14894	-22	6533.8
370	832	3450	2685	2853	50.3	14896	14895	-26	8967.9
D769									
0	1198	3456	2627	2627	0.0	14968	14968	0	0.0
20	1016	3454	2659	2668	3.2	14907	14938	-1	32.2
40	980	3460	2669	2688	6.1	14898	14920	-2	117.2
60	967	3464	2675	2702	8.7	14897	14912	-4	251.5
80	971	3464	2674	2710	11.4	14901	14909	-5	437.1
D770									
0	1214	3444	2615	2615	0.0	14972	14972	0	0.0
9	1196	3436	2612	2616	1.7	14967	14970	-0	7.7
19	1115	3447	2636	2644	3.5	14941	14961	-0	32.8
D771									
0	1280	3427	2589	2589	0.0	14993	14993	0	0.0
10	1277	3429	2591	2595	2.1	14994	14993	-0	10.6
29	1248	3450	2613	2626	5.9	14990	14992	-0	84.8
48	1108	3459	2646	2668	9.2	14945	14982	-1	212.5
67	1023	3466	2667	2697	12.1	14919	14968	-1	375.7
D772									
0	1203	3454	2625	2625	0.0	14970	14970	0	0.0
14	1182	3454	2629	2635	2.5	14964	14967	-0	17.3
27	1027	3451	2654	2667	4.6	14912	14953	-1	60.7
41	926	3450	2670	2689	6.6	14877	14933	-2	128.8
55	913	3453	2675	2700	8.5	14875	14918	-3	218.5
82	938	3462	2678	2715	12.0	14889	14906	-5	459.9
110	931	3465	2681	2731	15.6	14892	14902	-7	804.0
D773									
0	1126	3440	2628	2628	0.0	14941	14941	0	0.0
24	1097	3441	2634	2645	4.1	14934	14938	-1	49.6
73	901	3444	2670	2703	11.6	14871	14914	-4	413.9
97	875	3446	2676	2720	14.9	14867	14903	-6	687.9
146	905	3456	2679	2745	21.3	14887	14894	-10	1467.4
188	881	3453	2680	2766	26.7	14884	14892	-13	2377.3
291	834	3450	2685	2817	39.9	14884	14889	-21	5536.0
382	797	3447	2688	2862	51.4	14883	14888	-29	9392.5
471	743	3442	2692	2907	62.4	14876	14886	-36	14100.1
D774									
0	1146	3446	2629	2629	0.0	14949	14949	0	0.0
15	1139	3444	2629	2636	2.6	14950	14949	-1	19.6
29	1121	3444	2632	2645	5.0	14945	14948	-1	73.0
44	1057	3445	2644	2664	7.5	14925	14944	-2	163.9
58	975	3450	2662	2689	9.7	14898	14936	-2	272.5

D	T	S	σt	σstp	ΣΔD	C	Cm	K	ΣΔX
D774 continued`									
153	870	3447	2677	2747	22.7	14874	14905	-10	1651.1
238	839	3448	2683	2791	33.7	14876	14894	-17	3805.6
317	817	3447	2685	2830	43.8	14880	14890	-23	6597.2
409	769	3445	2877	2877	55.3	14877	14888	-31	10771.8
D775									
0	1115	3442	2632	2632	0.0	14938	14938	0	0.0
20	1108	3442	2633	2642	3.4	14938	14938	-1	34.2
41	1087	3441	2636	2654	7.0	14934	14937	-2	142.9
61	1018	3440	2647	2675	10.3	14912	14932	-3	309.4
82	944	3446	2664	2702	13.4	14889	14924	-4	534.8
122	875	3447	2676	2732	18.9	14870	14910	-7	1093.4
172	872	3449	2678	2757	25.4	14879	14899	-12	2057.3
267	822	3447	2685	2806	37.7	14874	14891	-19	4740.0
354	789	3446	2689	2850	48.6	14875	14887	-27	8127.6
D776									
0	1119	3443	2632	2632	0.0	14939	14939	0	0.0
25	1105	3443	2634	2646	4.3	14939	14939	-1	53.3
50	1056	3443	2643	2666	8.4	14925	14936	-2	208.7
75	898	3444	2670	2704	12.1	14872	14923	-4	441.8
100	870	3445	2676	2721	15.5	14865	14909	-6	735.2
150	878	3452	2680	2748	22.0	14876	14896	-10	1550.2
195	864	3450	2680	2769	27.8	14879	14892	-14	2552.1
291	819	3448	2686	2818	40.1	14878	14887	-22	5527.7
385	769	3444	2690	2865	51.8	14872	14884	-30	9488.0
D777									
0	1277	3467	2620	2620	0.0	14997	14997	0	00.0
23	1215	3469	2634	2644	4.1	14979	14988	-0	46.6
46	1194	3469	2638	2659	7.9	14977	14983	-1	180.2
69	1084	3470	2659	2690	11.5	14941	14975	-1	387.8
92	1018	3467	2668	2710	14.8	14920	14964	-2	652.6
138	971	3466	2676	2738	21.1	14911	14948	-5	1371.3
184	951	3465	2678	2762	27.2	14912	14939	-8	2350.2
280	907	3464	2685	2812	39.6	14911	14929	-13	5231.4
361	834	3457	2691	2855	49.7	14896	14924	-18	8478.9
450	776	3452	2695	2900	60.5	14887	14917	-25	12857.8
540	733	3452	2702	2947	71.1	14885	14912	-32	18092.8
631	702	3452	2706	2993	81.4	14887	14908	-39	24162.1
724	643	3450	2712	3042	91.7	14880	14905	-46	31094.0
816	608	3449	2716	3088	101.5	14880	14902	-53	38622.0
904	569	3450	2722	3134	110.5	14879	14900	-60	46402.9
979	530	3449	2726	3172	117.9	14876	14898	-66	53391.0
1069	484	3449	2731	3219	126.5	14872	14896	-74	62153.9
1168	428	3450	2738	3272	135.4	14865	14894	-83	72074.2
1271	386	3452	2744	3325	144.0	14865	14892	-92	82594.2
D783									
0	1338	3489	2625	2625	0.0	15020	15020	0	0.0
18	1246	3475	2633	2641	3.1	14990	15005	0	28.3
35	1229	3476	2637	2652	6.0	14988	14997	-0	104.6
53	1217	3478	2640	2664	9.0	14986	14994	-0	236.2
71	1324	3468	2612	2643	12.2	15024	14997	-0	435.5
106	1304	3515	2652	2699	18.3	15029	15007	0	973.9
142	1318	3520	2653	2717	23.9	15041	15014	1	1666.5
302	1126	3495	2671	2807	47.7	14998	15017	3	6941.6
437	939	3464	2679	2877	66.4	14949	15003	1	13871.8

D	T	S	σ_t	σ_{stp}	ΣΔD	C	C_m	K	ΣΔX
D783 continued									
557	827	3461	2695	2947	82.0	14926	14989	-4	21596.6
569	798	3458	2697	2955	83.4	14916	14988	-5	22421.2
619	760	3455	2700	2981	89.1	14909	14981	-8	25980.8
669	741	3453	2701	3005	95.3	14909	14976	-11	29795.7
699	722	3452	2703	3020	98.9	14906	14973	-13	32208.7
739	702	3451	2705	3041	103.5	14905	14969	-15	35550.1
968	531	3447	2724	3165	128.1	14875	14950	-32	56493.8
D784									
0	1396	3480	2606	2606	0.0	15038	15038	0	0.0
24	1362	3482	2615	2625	4.6	15030	15034	1	55.3
49	1346	3483	2619	2641	9.3	15030	15032	1	225.8
73	1331	3484	2622	2655	13.7	15028	15031	2	494.8
98	1214	3477	2640	2684	18.0	14993	15026	2	866.8
146	1091	3471	2659	2724	25.6	14957	15009	1	1790.3
185	1003	3463	2668	2751	31.3	14930	14995	-1	2729.2
374	874	3454	2682	2852	57.1	14912	14958	-11	9940.5
468	843	3456	2688	2900	69.3	14917	14949	-16	15063.7
765	728	3451	2701	3048	106.0	14920	14937	-32	37696.1
864	635	3449	2713	3105	117.3	14899	14934	-38	46956.6
969	548	3447	2722	3163	128.4	14882	14929	-46	57106.1
D785									
0	1379	3478	2608	2608	0.0	15032	15032	0	0.0
22	1359	3478	2612	2622	4.2	15029	15030	0	46.5
44	1332	3479	2618	2638	8.4	15025	15029	1	183.0
66	1335	3480	2619	2648	12.4	15029	15028	1	407.5
87	1306	3481	2625	2664	16.3	15023	15027	2	701.3
151	1128	3472	2653	2712	23.7	14967	15016	1	1504.3
174	804	3463	2700	2779	29.4	14855	14990	-1	2373.3
D786									
0	1319	3473	2616	2616	0.0	15012	15012	0	0.0
25	1199	3455	2626	2637	4.5	14973	14993	-0	56.8
49	1179	3462	2635	2657	8.7	14971	14982	-1	210.7
73	1184	3466	2637	2670	12.8	14976	14979	-1	457.5
98	1132	3462	2644	2688	16.9	14962	14977	-2	810.2
147	1077	3468	2659	2725	24.5	14951	14970	-3	1745.0
196	1051	3473	2667	2756	31.7	14951	14965	-5	2970.6
288	1004	3477	2679	2809	44.3	14949	14960	-8	6042.9
375	942	3472	2685	2855	55.8	14940	14957	-11	9831.6
462	851	3459	2689	2899	66.9	14918	14951	-15	14479.4
549	813	3458	2695	2943	77.7	14918	14946	-20	19958.0
D808									
0	1461	3462	2578	2578	0.0	15057	15057	0	0.0
25	1355	3467	2604	2616	5.3	15028	15042	1	65.7
50	1358	3481	2615	2637	10.1	15034	15036	1	247.1
75	1338	3480	2618	2652	14.8	15032	15035	2	540.6
100	1253	3471	2628	2673	19.3	15005	15031	2	938.9
150	1166	3468	2642	2710	27.9	14983	15019	2	2009.9
200	1125	3475	2655	2745	35.9	14977	15009	1	3405.3
300	989	3466	2672	2808	50.6	14945	14993	-1	7073.1
400	874	3459	2686	2867	64.0	14917	14977	-6	11763.2
D809									
0	1585	3482	2566	2566	0.0	15098	15098	0	0.0
46	1447	3472	2589	2609	10.3	15061	15080	2	236.5
69	1296	3473	2621	2652	14.8	15015	15066	3	498.9

D	T	S	σ_t	σ_{stp}	ΣΔD	C	C_m	K	ΣΔX
D809 continued									
137	1182	3487	2654	2716	26.3	14989	15034	3	1679.5
175	1123	3481	2660	2739	32.0	14974	15023	3	2574.9
261	1017	3470	2671	2789	44.5	14949	15003	0	5282.2
347	939	3463	2679	2835	56.3	14933	14987	-3	8877.3
644	772	3450	2694	2986	94.8	14917	14958	-18	27961.9
890	614	3446	2713	3118	123.6	14895	14944	-33	50064.6
D810									
0	1504	3452	2561	2561	0.0	15069	15069	0	0.0
25	1470	3453	2569	2581	5.9	15063	15066	1	73.4
50	1411	3454	2583	2605	11.5	15048	15061	2	284.7
75	1304	3459	2609	2642	16.7	15018	15051	3	608.8
100	1260	3462	2620	2665	21.5	15006	15042	3	1025.5
D811									
0	1592	3478	2562	2562	0.0	15100	15100	0	0.0
21	1567	3477	2566	2576	5.0	15095	15098	1	52.1
42	1519	3486	2584	2603	9.7	15085	15094	3	201.6
64	1418	3503	2619	2648	14.1	15059	15086	4	436.7
85	1358	3504	2632	2670	17.9	15043	15077	4	717.2
127	1221	3482	2643	2700	25.0	15000	15059	5	1468.3
157	1162	3486	2657	2728	29.7	14985	15046	5	2140.3
312	947	3464	2678	2819	51.9	14931	15002	0	7332.5
389	896	3458	2682	2858	62.1	14924	14987	-3	10933.2
631	783	3451	2694	2979	93.3	14919	14962	-16	26840.3
D812									
0	1662	3488	2553	2553	0.0	15123	15123	0	0.0
25	1536	3483	2578	2589	5.9	15088	15105	2	73.4
49	1369	3479	2611	2633	10.9	15037	15084	3	258.0
74	1341	3477	2615	2648	15.6	15032	15067	3	551.7
98	1288	3476	2625	2669	20.1	15018	15057	4	933.4
D813									
0	1868	3540	2543	2543	0.0	15189	15189	0	0.0
39	1858	3541	2546	2563	10.0	15193	15191	5	194.1
59	1709	3535	2578	2604	14.7	15152	15185	7	428.6
79	1633	3537	2597	2632	19.0	15132	15174	9	726.0
99	1505	3528	2619	2664	23.0	15095	15162	11	1075.4
331	1056	3488	2678	2827	60.3	14977	15073	16	9091.7
418	974	3478	2684	2873	71.8	14960	15051	14	13430.7
634	755	3457	2702	2900	98.6	14910	15012	5	27498.5
D814									
0	1808	3515	2539	2539	0.0	15169	15169	0	0.0
24	1801	3515	2540	2551	6.2	15170	15170	3	74.7
47	1637	3527	2589	2610	11.7	15128	15159	5	267.8
71	1506	3527	2618	2650	16.5	15090	15142	7	550.9
95	1420	3522	2633	2676	20.8	15067	15126	8	908.3
189	1296	3514	2653	2737	36.1	15039	15090	11	3074.7
284	1188	3504	2666	2794	50.6	15017	15069	13	6502.8
D815									
0	1906	3550	2541	2541	0.0	15201	15201	0	0.0
29	1914	3550	2539	2551	7.5	15208	15205	4	109.1
43	1910	3552	2541	2560	11.2	15209	15206	6	240.2
115	1592	3531	2602	2653	27.8	15126	15182	14	1554.2
381	1051	3486	2677	2849	73.1	14983	15092	23	12777.3
575	791	3461	2700	2961	97.8	14915	15044	17	24607.5

D	T	S	σ_t	σ_{stp}	$\Sigma\Delta D$	C	C_m	K	$\Sigma\Delta X$
D816									
0	1898	3552	2544	2544	0.0	15199	15199	0	0.0
57	1893	3553	2546	2571	14.5	15207	15203	8	413.6
77	1886	3552	2547	2581	19.6	15208	15204	10	754.6
115	1460	3529	2630	2681	27.8	15084	15185	14	1540.2
D817									
0	1888	3557	2551	2551	0.0	15197	15197	0	0.0
26	1889	3557	2550	2562	6.5	15202	15199	3	84.2
D818									
0	1958	3562	2536	2536	0.0	15217	15217	0	0.0
19	1954	3563	2538	2546	5.0	15219	15218	3	47.2
38	1957	3563	2537	2554	9.9	15223	15220	6	188.9
77	1960	3562	2536	2570	20.2	15230	15223	11	780.7
115	1712	3556	2593	2644	29.3	15165	15215	16	1650.5
296	1434	3533	2639	2770	64.1	15105	15166	33	8811.8
429	1069	3489	2676	2869	84.9	14998	15130	37	16352.6
577	927	3475	2690	2950	104.8	14968	15092	35	26347.9
687	797	3461	2699	3010	118.6	14935	15069	32	35051.3
D819									
0	2233	3562	2462	2462	0.0	15290	15290	0	0.0
26	2219	3565	2468	2479	8.6	15291	15291	5	111.8
53	1960	3559	2534	2557	16.6	15225	15274	10	429.1
177	1603	3550	2614	2693	45.2	15141	15210	25	3709.6
391	1269	3512	2657	2831	82.8	15064	15151	39	14405.3
525	1015	3468	2670	2905	103.4	14991	15119	42	23808.9
789	755	3458	2703	3060	138.6	14936	15067	35	46982.8
1165	515	3451	2729	3259	179.3	14901	15019	14	86735.4
D820									
0	2020	3561	2519	2519	0.0	15234	15234	0	0.0
15	2018	3561	2520	2526	4.2	15236	15235	2	31.3
45	2023	3562	2519	2539	12.6	15243	15238	7	282.6
60	2024	3562	2519	2545	16.8	15245	15240	10	503.4
90	1794	3549	2568	2608	24.5	15183	15231	14	1083.5
299	1241	3501	2654	2787	65.6	15038	15147	29	9083.2
442	1064	3486	2675	2874	87.0	14997	15105	31	17022.4
557	905	3473	2692	2943	102.4	14956	15078	29	24708.3
647	860	3469	2696	2988	113.7	14953	15061	26	31504.0
789	720	3456	2707	3064	130.7	14922	15039	20	43726.6
D821									
0	1886	3554	2549	2549	0.0	15196	15196	0	0.0
36	1898	3553	2545	2561	9.1	15206	15201	5	163.7
54	1837	3553	2560	2584	13.6	15191	15200	7	364.7
72	1587	3542	2612	2644	17.5	15117	15189	9	610.5
108	1503	3536	2626	2674	24.2	15097	15161	12	1214.1
153	1302	3519	2655	2724	31.7	15037	15133	14	2192.2
283	1164	3502	2669	2796	50.9	15009	15082	16	6389.1
369	1031	3485	2680	2846	62.8	14974	15061	15	10276.7
504	931	3473	2688	2915	80.6	14956	15035	12	18049.1
588	842	3464	2695	2961	91.3	14936	15023	9	23860.3
1415	377	3452	2745	3391	176.5	14884	14957	-41	109218.2
1837	275	3462	2763	3600	208.2	14912	14943	-69	160767.8
D822									
0	1827	3527	2543	2543	0.0	15176	15176	0	0.0
25	1796	3528	2551	2563	6.3	15172	15174	3	78.8
D822 continued									
50	1773	3535	2562	2585	12.4	15169	15172	6	307.3
75	1469	3533	2631	2665	17.6	15081	15156	8	630.0
100	1396	3526	2641	2686	21.8	15060	15135	9	1000.9
150	1310	3518	2653	2720	29.8	15038	15106	11	2002.0
200	1272	3515	2658	2748	37.5	15033	15088	12	3344.4
300	1162	3501	2669	2803	52.2	15011	15066	13	7037.4
391	1065	3488	2676	2852	65.1	14990	15051	13	11476.4
482	947	3471	2683	2901	77.5	14959	15036	12	16871.3
620	814	3456	2693	2973	95.4	14930	15016	6	26730.4
770	702	3447	2702	3051	113.7	14911	14997	-2	39515.7
968	604	3446	2714	3154	136.4	14904	14979	-14	59200.3
1214	453	3446	2732	3286	161.4	14883	14961	-31	86460.1
1445	372	3451	2745	3404	181.8	14887	14949	-49	113537.5
1944	251	3461	2764	3650	219.2	14920	14937	-81	177000.0
D823									
0	1810	3524	2545	2545	0.0	15171	15171	0	0.0
25	1802	3526	2548	2559	6.3	15173	15172	3	79.0
50	1754	3524	2559	2581	12.5	15162	15170	6	310.5
74	1451	3523	2627	2660	17.5	15074	15153	8	623.1
99	1373	3519	2641	2635	21.8	15051	15130	9	994.2
149	1289	3515	2655	2722	29.8	15031	15100	10	1983.0
297	1143	3499	2671	2804	51.6	15003	15058	12	6855.2
495	901	3466	2687	2911	78.5	14944	15024	8	17499.6
642	802	3455	2694	2984	97.3	14930	15004	2	28162.4
791	704	3450	2704	3063	115.4	14915	14989	-6	41140.3
987	566	3443	2717	3166	137.4	14891	14972	-19	60706.3
1237	435	3447	2735	3299	162.1	14879	14954	-38	88185.3
1474	347	3452	2748	3421	182.3	14881	14942	-57	115500.1
1974	255	3461	2764	3662	219.2	14927	14932	-89	179099.3
2457	219	3466	2771	3683	251.9	14994	14938	-102	251536.5
D824									
0	1976	3560	2530	2530	0.0	15222	15222	0	0.0
24	1973	3560	2531	2541	6.4	15224	15223	4	77.2
48	1908	3555	2544	2565	12.7	15210	15220	7	303.8
72	1864	3550	2551	2583	18.8	15200	15215	10	668.8
97	1725	3544	2581	2624	24.7	15164	15207	13	1168.4
145	1517	3537	2624	2688	34.5	15108	15183	18	2347.9
192	1443	3532	2636	2722	42.8	15092	15163	21	3758.7
288	1261	3513	2659	2788	58.5	15043	15131	25	7516.8
387	1134	3498	2672	2845	73.0	15014	15105	27	12414.3
475	1015	3483	2681	2895	85.4	14985	15085	27	17756.3
650	822	3460	2695	2989	108.3	14938	15051	22	30585.5
753	735	3453	2702	3043	120.8	14921	15035	17	39410.1
939	606	3445	2713	3140	142.2	14900	15010	6	57454.0
1181	483	3447	2730	3267	167.1	14890	14986	-11	83912.7
1391	392	3450	2742	3376	186.2	14887	14971	-26	108421.0
1874	263	3461	2763	3617	223.2	14914	14953	-59	168783.6
2346	207	3468	2773	3838	253.8	14969	14951	-77	233449.8
D825									
0	1866	3530	2536	2536	0.0	15187	15187	0	0.0
66	1513	3523	2614	2643	15.0	15092	15140	6	493.6
88	1382	3521	2641	2680	18.9	15053	15123	7	795.1
132	1323	3519	2651	2710	26.0	15041	15097	9	1574.7
175	1283	3517	2658	2736	32.6	15034	15083	10	2591.5
264	1198	3509	2668	2787	45.7	15018	15063	11	5474.9
345	1128	3499	2674	2828	57.2	15005	15051	12	8978.1

D825 continued

D	T	S	σ_t	σ_{stp}	$\Sigma\Delta D$	C	C_m	K	$\Sigma\Delta X$
691	758	3451	2697	3010	102.8	14920	15007	3	32565.9
862	646	3444	2707	3099	123.1	14903	14988	-7	48362.7
1090	512	3444	2724	3220	147.7	14886	14968	-23	72374.1
1319	399	3447	2739	3341	169.2	14878	14953	-41	98314.1
1751	277	3457	2758	3558	203.4	14900	14937	-73	150749.6
2203	235	3463	2767	3767	234.7	14958	14935	-95	212566.4
2635	208	3466	2771	3961	264.1	15019	14944	-98	283702.0

D826

D	T	S	σ_t	σ_{stp}	$\Sigma\Delta D$	C	C_m	K	$\Sigma\Delta X$
0	1931	3541	2527	2527	0.0	15207	15207	0	0.0
24	1892	3541	2537	2548	6.4	15199	15203	3	76.7
48	1838	3537	2548	2569	12.6	15188	15198	6	299.0
72	1538	3531	2614	2646	17.9	15101	15180	9	617.8
97	1462	3531	2631	2674	22.4	15082	15157	10	1003.1
145	1350	3522	2648	2713	30.5	15052	15127	12	1975.5
192	1247	3508	2658	2744	37.8	15024	15105	13	3210.1
288	1158	3501	2670	2799	51.9	15006	15075	14	6603.5
382	1051	3486	2677	2849	65.1	14983	15055	14	11014.3
625	792	3454	2695	2978	96.9	14922	15015	6	27019.8
766	681	3446	2704	3052	113.9	14901	14996	-2	38840.8
956	562	3440	2715	3150	135.3	14885	14975	-16	57231.5
1199	428	3442	2732	3279	159.7	14869	14955	-36	83556.1
1457	345	3450	2747	3412	182.0	14879	14941	-58	113246.4
1924	261	3460	2762	3639	216.9	14921	14931	-89	172203.3
2413	226	3464	2768	3861	250.7	14989	14936	-104	245367.9
2899	193	3470	2776	4080	283.9	15058	14950	-96	333641.1

D827

D	T	S	σ_t	σ_{stp}	$\Sigma\Delta D$	C	C_m	K	$\Sigma\Delta X$
0	1877	3542	2542	2542	0.0	15192	15192	0	0.0
22	1874	3542	2543	2552	5.7	15194	15193	3	62.1
43	1864	3540	2544	2563	11.0	15194	15194	6	237.3
87	1447	3519	2625	2664	20.6	15074	15163	9	861.9
130	1330	3516	2647	2706	28.0	15041	15128	11	1655.7
172	1247	3511	2660	2737	34.5	15021	15104	12	2635.8
257	1161	3503	2671	2786	46.8	15003	15074	13	5280.3
323	1089	3490	2674	2819	56.0	14987	15058	12	7966.0
407	983	3478	2683	2866	67.5	14962	15040	11	12131.0
528	876	3466	2691	2930	83.1	14940	15020	7	19445.0
649	764	3457	2701	2995	97.9	14915	15002	1	28159.6
809	665	3448	2708	3075	116.5	14903	14984	-9	41697.5
1021	533	3445	2722	3187	139.3	14883	14965	-24	62582.0
1230	441	3447	2734	3295	159.5	14881	14951	-40	85275.1
1620	314	3457	2755	3495	191.6	14893	14935	-70	131104.0
2069	233	3464	2768	3710	222.6	14934	14931	-96	188242.0

D828

D	T	S	σ_t	σ_{stp}	$\Sigma\Delta D$	C	C_m	K	$\Sigma\Delta X$
0	1991	3562	2528	2528	0.0	15226	15226	0	0.0
21	1973	3562	2532	2542	5.6	15224	15225	3	59.2
41	1974	3563	2533	2551	11.0	15228	15226	6	224.5
62	1957	3561	2536	2563	16.6	15226	15226	9	511.9
83	1955	3561	2536	2573	22.1	15230	15227	13	915.2
124	1683	3549	2595	2650	31.9	15157	15216	18	1923.8
146	1625	3543	2604	2669	36.4	15142	15206	20	2537.0
216	1462	3533	2633	2729	49.7	15101	15178	26	4940.1
279	1371	3525	2646	2770	60.5	15082	15159	29	7612.2
1094	549	3446	2721	3218	170.6	14903	15034	25	83214.1
1528	345	3454	2750	3447	210.3	14891	14995	-5	135206.4
1789	276	3461	2762	3578	229.4	14906	14981	-23	166923.8

D829

D	T	S	σ_t	σ_{stp}	$\Sigma\Delta D$	C	C_m	K	$\Sigma\Delta X$
0	1991	3562	2528	2528	0.0	15226	15226	0	0.0
25	1974	3562	2532	2543	6.7	15226	15226	4	84.0
49	1936	3562	2542	2564	13.0	15219	15224	7	317.2
74	1930	3558	2541	2573	19.5	15222	15223	11	716.2
98	1769	3557	2580	2624	25.3	15179	15217	14	1215.8
148	1657	3553	2604	2670	36.0	15153	15200	20	2525.6
200	1564	3546	2620	2709	46.1	15131	15185	25	4294.5
300	1400	3528	2642	2776	64.1	15095	15161	32	8779.5
396	1275	3515	2658	2834	79.8	15066	15141	37	14254.7
495	1133	3497	2671	2893	94.9	15032	15123	41	20965.3
674	889	3469	2691	2995	119.6	14969	15090	41	35423.5
822	734	3457	2705	3077	137.9	14933	15065	36	49104.4
1031	577	3449	2720	3188	161.1	14903	15035	24	70629.3
1332	453	3451	2736	3342	190.7	14903	15005	4	105576.4
1483	396	3453	2744	3419	204.1	14904	14994	-5	124371.7
1945	263	3461	2763	3648	239.6	14927	14976	-32	185340.5
2241	225	3464	2768	3786	259.6	14960	14971	-43	227121.9

D830

D	T	S	σ_t	σ_{stp}	$\Sigma\Delta D$	C	C_m	K	$\Sigma\Delta X$
0	2019	3566	2523	2523	0.0	15234	15234	0	0.0
25	2018	3563	2521	2532	6.9	15238	15236	4	86.2
50	1988	3561	2528	2550	13.8	15233	15236	8	343.7
75	1938	3558	2538	2571	20.4	15224	15233	12	761.4
100	1792	3556	2574	2618	26.6	15185	15226	15	1300.0
150	1596	3545	2612	2679	37.2	15133	15204	20	2626.5
200	1464	3530	2630	2719	46.6	15098	15182	24	4261.6
300	1304	3516	2653	2787	63.5	15061	15148	30	8496.2
400	1128	3497	2672	2851	78.6	15015	15120	32	13799.9
500	994	3482	2684	2909	92.5	14981	15095	32	20024.1
631	856	3466	2694	2979	109.4	14948	15068	29	29613.4
783	720	3457	2707	3062	127.7	14921	15042	22	42515.5
875	591	3451	2720	3163	148.7	14901	15016	10	60976.1
1228	471	3451	2734	3293	173.5	14893	14991	-7	88358.8
1479	376	3455	2747	3422	195.3	14896	14975	-25	117782.0
1948	234	3464	2768	3656	229.0	14915	14958	-55	175505.4

D831

D	T	S	σ_t	σ_{stp}	$\Sigma\Delta D$	C	C_m	K	$\Sigma\Delta X$
0	2041	3562	2514	2514	0.0	15240	15240	0	0.0
21	2037	3562	2515	2525	5.9	15242	15241	3	62.4
43	1957	3548	2526	2545	12.1	15221	15236	7	258.1
64	1915	3548	2537	2565	17.7	15215	15230	10	560.0
86	1628	3545	2605	2643	22.8	15134	15216	12	942.5
158	1456	3534	2635	2705	36.2	15090	15168	18	2580.5
237	1333	3521	2651	2757	49.4	15061	15137	22	5179.6
304	1254	3512	2660	2796	59.9	15044	15118	24	8017.6
390	1124	3497	2673	2848	72.6	15012	15098	26	12426.0
512	989	3482	2685	2915	89.4	14981	15074	25	19993.8
640	838	3466	2697	2986	105.7	14943	15051	22	29418.9
818	690	3453	2708	3079	126.8	14915	15024	13	44778.4
974	570	3449	2721	3164	143.7	14891	15005	3	59916.0

D832

D	T	S	σ_t	σ_{stp}	$\Sigma\Delta D$	C	C_m	K	$\Sigma\Delta X$
0	2002	3545	2512	2512	0.0	15227	15227	0	0.0
23	1948	3552	2531	2541	6.4	15216	15222	3	73.1
46	1947	3553	2532	2553	12.5	15221	15220	7	285.5
69	1906	3548	2539	2569	18.6	15212	15219	10	635.5
91	1747	3537	2570	2611	24.0	15168	15212	13	1070.7
138	1551	3538	2617	2678	34.0	15117	15188	17	2207.4
168	1463	3533	2633	2707	39.4	15093	15173	19	3045.9

D832 continued

D	T	S	σ_t	σ_{stp}	ΣΔD	C	C_m	K	ΣΔX
242	1321	3519	2652	2760	51.8	15058	15143	23	5586.1
316	1190	3504	2666	2807	63.2	15023	15119	25	8750.7
390	1100	3494	2675	2850	73.8	15003	15099	26	12505.6
499	970	3479	2686	2911	88.6	14972	15074	25	19087.0
612	841	3466	2696	2973	103.0	14939	15052	21	27065.6
965	569	3449	2721	3160	142.7	14890	15002	1	58403.8

D833

D	T	S	σ_t	σ_{stp}	ΣΔD	C	C_m	K	ΣΔX
0	1935	3542	2527	2527	0.0	15028	15208	0	0.0
18	2052	3544	2498	2506	5.1	15244	15226	3	46.2
50	1777	3543	2568	2590	13.7	15171	15214	7	336.4
67	1655	3536	2591	2621	17.5	15137	15199	9	558.7
100	1527	3538	2622	2667	24.0	15103	15173	12	1102.5
132	1446	3530	2634	2693	29.7	15083	15153	13	1764.5
205	1325	3520	2652	2743	41.8	15053	15123	17	3803.4
253	1226	3508	2662	2775	49.3	15026	15107	18	5494.3
320	1124	3497	2673	2817	58.9	15000	15087	19	8276.4
414	976	3480	2686	2872	71.6	14960	15063	17	12936.9

D834

D	T	S	σ_t	σ_{stp}	ΣΔD	C	C_m	K	ΣΔX
0	1848	3539	2547	2547	0.0	15183	15183	0	0.0
22	1839	3540	2550	2560	5.5	15184	15184	3	60.7
45	1815	3541	2557	2577	11.2	15182	15183	6	251.1
67	1641	3535	2594	2624	16.2	15133	15175	8	530.5
90	1471	3530	2628	2669	20.6	15083	15158	9	879.5
112	1427	3525	2634	2684	24.5	15071	15142	11	1267.9

D835

D	T	S	σ_t	σ_{stp}	ΣΔD	C	C_m	K	ΣΔX
0	1835	3543	2553	2553	0.0	15180	15180	0	0.0
15	1839	3543	2552	2559	3.7	15184	15182	2	27.8
29	1831	3543	2554	2567	7.2	15184	15183	4	103.8
44	1820	3542	2556	2576	10.8	15184	15183	5	238.1
59	1823	3542	2555	2581	14.5	15186	15184	7	427.5
88	1528	3531	2617	2656	20.8	15101	15170	10	890.3
116	1471	3529	2628	2679	25.9	15087	15152	12	1414.5
150	1384	3524	2642	2709	31.8	15063	15135	13	2192.7
193	1303	3518	2654	2741	38.7	15044	15116	15	3375.0

D836

D	T	S	σ_t	σ_{stp}	ΣΔD	C	C_m	K	ΣΔX
0	1918	3552	2539	2539	0.0	15025	15205	0	0.0
16	1921	3552	2538	2545	4.2	15209	15207	2	33.3
31	1925	3552	2537	2551	8.1	15211	15208	4	125.5
47	1920	3552	2539	2559	12.3	15213	15210	7	288.9
63	1904	3548	2540	2567	16.5	15210	15210	9	518.9
94	1648	3541	2597	2639	23.7	15141	15199	12	1089.1
126	1551	3538	2617	2673	30.1	15115	15181	15	1787.4
175	1450	3532	2635	2713	39.0	15091	15159	19	3126.6
220	1356	3523	2647	2746	46.5	15065	15142	21	4621.9
302	1092	3496	2678	2814	58.7	14986	15110	22	7807.7
334	1029	3486	2681	2832	63.0	14967	15097	22	9168.1
452	930	3477	2691	2895	78.2	14949	15061	18	15138.8

D837

D	T	S	σ_t	σ_{stp}	ΣΔD	C	C_m	K	ΣΔX
0	2125	3550	2483	2483	0.0	15261	15261	0	0.0
14	1875	3551	2549	2555	3.9	15194	15227	2	27.6
28	2248	3551	2449	2461	8.1	15297	15236	4	115.3
56	1809	3547	2563	2587	16.3	15183	15238	9	459.4
84	1612	3538	2603	2640	22.5	15128	15210	12	890.7

D837 continued

D	T	S	σ_t	σ_{stp}	ΣΔD	C	C_m	K	ΣΔX
203	1319	3520	2653	2744	43.8	15051	15139	19	3950.6
375	1036	3486	2680	2849	68.9	14976	15081	20	11197.0
472	936	3474	2688	2901	81.6	14954	15057	18	16607.0
780	678	3449	2707	3061	119.1	14903	15006	3	40053.1

D838

D	T	S	σ_t	σ_{stp}	ΣΔD	C	C_m	K	ΣΔX
0	1830	3532	2546	2546	0.0	15177	15177	0	0.0
14	1833	3533	2546	2552	3.5	15180	15179	2	24.8
29	1829	3535	2549	2561	7.3	15182	15180	3	106.2
43	1814	3537	2554	2573	10.8	15180	15180	5	231.7
67	1814	3543	2558	2588	16.7	15185	15181	8	555.2
100	1547	3543	2622	2666	23.7	15110	15170	11	1143.9
134	1498	3539	2629	2689	29.9	15100	15153	14	1863.1
204	1356	3523	2647	2739	41.8	15064	15129	18	3872.7
266	1276	3515	2658	2777	51.6	15046	15111	20	6177.0
333	1207	3507	2665	2814	61.7	15032	15097	21	9215.3
532	934	3471	2686	2925	89.7	14962	15059	21	21304.1
724	710	3448	2702	3030	115.0	14906	15026	13	36564.5
1304	459	3450	2735	3328	175.0	14900	14971	-25	98418.5
1581	334	3456	2752	3474	198.0	14894	14958	-44	132199.4
1833	258	3461	2763	3600	216.0	14905	14050	-61	162904.1

D839

D	T	S	σ_t	σ_{stp}	ΣΔD	C	C_m	K	ΣΔX
0	1846	3550	2556	2556	0.0	15184	15184	0	0.0
29	1841	3552	2559	2571	7.0	15188	15186	4	102.1
52	1810	3555	2569	2592	12.5	15182	15186	6	323.3
76	1711	3549	2588	2622	17.9	15157	15181	9	667.6
100	1563	3542	2617	2662	22.7	15115	15170	11	1093.7
124	1521	3540	2625	2680	27.7	15106	15158	13	1590.4
224	1313	3520	2654	2754	44.1	15052	15123	18	4529.8
318	1204	3507	2665	2808	58.3	15028	15098	21	8404.4
410	1060	3487	2677	2861	71.5	14991	15078	21	13202.5
504	962	3474	2683	2910	84.4	14968	15060	20	19061.4
645	827	3460	2694	2986	102.7	14940	15036	16	29580.5
790	733	3451	2701	3058	120.6	14927	15017	9	42425.0
999	601	3446	2715	3168	144.7	14908	14996	-2	64020.5
1251	482	3449	2731	3300	170.6	14902	14978	-19	93163.7
1510	383	3454	2746	3434	193.8	14903	14965	-35	125136.7
1975	241	3463	2766	3666	228.2	14923	14953	-62	185078.1
2464	202	3468	2774	3890	259.5	14987	14953	-77	254620.2
2767	156	3470	2779	4030	278.2	15019	14958	-77	303475.2

D840

D	T	S	σ_t	σ_{stp}	ΣΔD	C	C_m	K	ΣΔX
0	1825	3525	2542	2542	0.0	15175	15175	0	0.0
24	1797	3524	2548	2559	6.1	15170	15173	3	73.2
48	1794	3524	2549	2570	12.1	15174	15172	6	290.7
72	1611	3521	2590	2622	17.7	15122	15164	8	625.4
96	1387	3510	2631	2674	22.4	15055	15145	9	1016.5
144	1256	3505	2654	2718	30.3	15018	15109	10	1964.5
284	1148	3498	2669	2797	51.1	15003	15060	11	6420.8
373	1045	3485	2678	2846	63.6	14979	15944	11	10512.6
468	935	3470	2685	2896	76.3	14953	15028	9	15872.6
610	830	3459	2693	2969	94.6	14934	15008	3	25737.9
752	730	3452	2702	3043	112.0	14919	14993	-4	37600.8
936	609	3447	2714	3140	133.0	14901	14976	-15	55318.1
1178	471	3447	2731	3268	157.6	14884	14959	-32	81343.2
1425	373	3452	2745	3396	179.4	14884	14949	-51	109695.2
1867	262	3461	2763	3614	212.4	14913	14935	-81	164049.2
2344	212	3466	2771	3835	243.9	14971	14936	-99	230252.5
2831	175	3471	2778	4055	274.9	15039	14948	-98	310537.6

D	T	S	σ_t	σ_{stp}	ΣΔD	C	C_m	K	ΣΔX
D841									
0	1851	3554	2558	2558	0.0	15186	15186	0	0.0
25	1853	3555	2558	2569	6.1	15191	15189	3	75.7
50	1814	3553	2566	2588	12.0	15183	15188	6	299.7
75	1673	3547	2596	2629	17.6	15146	15180	9	646.1
100	1563	3542	2617	2662	22.5	15115	15168	11	1079.6
150	1442	3530	2635	2702	31.6	15083	15145	14	2208.1
198	1346	3521	2648	2736	39.6	15058	15127	17	3604.7
295	1265	3514	2659	2791	54.9	15046	15102	20	7371.1
394	1117	3495	2672	2849	69.5	15009	15083	22	12421.4
490	983	3476	2681	2902	82.9	14974	15065	21	18325.8
634	841	3462	2693	2980	101.7	14944	15041	17	28923.2
779	744	3454	2702	3054	119.6	14930	15022	11	41552.8
981	616	3448	2714	3159	142.9	14911	15001	0	62038.7
1234	456	3448	2733	3296	168.5	14888	14980	-17	90454.2
1496	350	3453	2748	3431	191.1	14888	14963	-36	121209.1
1967	246	3463	2766	3662	225.2	14923	14950	-66	180210.1
D842									
0	1820	3549	2562	2562	0.0	15177	15177	0	0.0
19	1806	3551	2567	2575	4.5	15176	15176	2	42.6
37	1801	3551	2568	2584	8.7	15178	15176	4	160.4
56	1796	3550	2568	2593	13.1	15179	15177	7	366.7
74	1694	3549	2592	2625	17.1	15152	15174	9	626.9
111	1542	3542	2622	2671	24.4	15110	15160	12	1303.4
150	1488	3540	2632	2699	31.4	15099	15145	15	2217.6
224	1312	3518	2653	2753	43.8	15052	15122	18	4521.1
299	1204	3506	2665	2799	55.2	15026	15101	20	7518.9
370	1101	3493	2674	2840	65.5	15000	15084	21	10945.6
600	879	3463	2688	2959	96.7	14952	15042	17	26081.6
753	767	3455	2699	3040	116.1	14934	15022	11	39191.6
959	632	3450	2714	3149	140.1	14914	15001	1	59739.0
1163	528	3448	2725	3254	161.7	14906	14985	-12	82651.0
1547	330	3455	2752	3458	195.7	14888	14963	-38	128754.4
1963	241	3463	2766	3661	224.9	14919	14950	-65	180102.7
D843									
0	1868	3500	2550	2500	0.0	15190	15190	0	0.0
24	1842	3553	2559	2570	5.9	15187	15188	3	70.6
49	1808	3556	2570	2592	11.8	15182	15186	6	286.4
73	1604	3544	2609	2642	16.9	15123	15175	9	598.7
98	1529	3539	2623	2666	21.6	15104	15159	10	1002.6
147	1419	3530	2640	2705	30.2	15076	15136	13	2056.5
196	1345	3522	2649	2737	38.3	15058	15119	16	3437.4
300	1221	3509	2664	2798	54.4	15032	15093	19	7428.5
391	1121	3496	2672	2848	67.6	15010	15076	20	12010.9
487	985	3478	2683	2902	80.9	14975	15060	19	17847.5
632	843	3462	2693	2979	99.9	14945	15037	16	28432.6
774	718	3450	2702	3053	117.3	14917	15017	9	40702.4
972	609	3448	2715	3157	139.9	14906	14996	-3	60433.0
1224	428	3449	2737	3296	164.7	14874	14974	-21	87690.4
1483	330	3457	2754	3431	185.7	14887	14957	-43	116004.7
D844									
0	1717	3506	2554	2554	0.0	15141	15141	0	0.0
18	1719	3507	2554	2562	4.4	15145	15143	2	39.8
36	1717	3507	2555	2571	8.8	15148	15145	3	159.3
54	1652	3507	2570	2594	13.1	15131	15143	5	352.8
72	1469	3524	2624	2656	16.9	15078	15133	6	586.6
108	1406	3521	2635	2684	23.2	15064	15113	8	1156.2
144	1315	3516	2650	2715	29.1	15040	15097	9	1901.3

D	T	S	σ_t	σ_{stp}	ΣΔD	C	C_m	K	ΣΔX
D844 continued									
217	1157	3495	2665	2763	40.2	14994	15070	10	3896.5
280	1063	3485	2674	2801	49.1	14971	15050	9	6110.6
349	943	3467	2681	2839	58.4	14936	15031	7	9039.8
453	866	3462	2689	2895	71.8	14923	15008	2	14430.1
555	803	3457	2695	2947	84.5	14916	14991	-3	20815.1
699	722	3452	2703	3020	101.7	14906	14975	-12	31611.8
888	593	3449	2718	3122	122.6	14887	14958	-25	48199.0
1121	474	3448	2731	3243	145.6	14876	14942	-43	71306.8
D845									
0	1849	3547	2553	2553	0.0	15185	15185	0	0.0
24	1849	3548	2554	2564	5.9	15188	15186	3	71.0
49	1792	3544	2565	2586	12.0	15176	15184	6	291.5
73	1612	3545	2608	2641	17.1	15125	15173	8	608.2
98	1555	3542	2619	2663	21.9	15112	15159	10	1016.8
147	1430	3530	2637	2703	30.7	15079	15138	14	2087.6
200	1313	3519	2653	2743	39.3	15047	15118	16	3590.6
298	1180	3504	2668	2801	54.1	15016	15090	18	7269.0
393	1032	3487	2681	2858	67.3	14978	15067	18	11839.1
492	953	3475	2686	2907	80.4	14963	15047	16	17642.5
642	801	3458	2696	2987	99.5	14930	15024	10	28467.4
785	732	3455	2704	3060	116.8	14925	15006	3	40763.9
986	590	3449	2718	3166	139.3	14902	14987	-8	60671.1
1235	430	3449	2737	3301	163.4	14877	14967	-27	87532.8
1488	344	3456	2751	3431	184.2	14884	14952	-47	115884.8
1958	234	3464	2768	3661	216.9	14916	14940	-78	172173.8
D846									
0	1798	3546	2565	2565	0.0	15170	15170	0	0.0
25	1783	3546	2568	2579	5.8	15170	15170	3	73.0
50	1507	3539	2605	2627	11.2	15120	15158	5	275.0
75	1385	3531	2648	2681	15.7	15053	15134	7	553.8
100	1360	3531	2653	2698	19.6	15048	15113	8	895.8
150	1341	3530	2656	2723	27.3	15050	15092	9	1854.4
200	1328	3529	2658	2747	34.9	15054	15082	11	3187.3
300	1298	3527	2662	2796	50.0	15061	15074	15	6970.3
400	1252	3520	2666	2845	65.0	15060	15070	19	12221.3
500	1182	3506	2669	2892	80.0	15051	15067	22	18945.8
647	943	3470	2683	2974	101.0	14985	15056	24	31024.5
790	838	3459	2691	3047	120.2	14968	15041	22	44833.4
994	659	3450	2710	3160	145.4	14930	15022	15	67282.0
1245	574	3448	2720	3283	173.6	14937	15004	4	98826.3
1500	468	3449	2733	3413	200.1	14936	14993	-7	135182.2
1976	274	3461	2762	3660	240.3	14936	14979	-27	205173.4
2464	220	3466	2771	3885	274.1	14995	14977	-39	280046.0
2961	172	3471	2778	4111	306.9	15059	14985	-30	369217.8
D847									
0	1841	3553	2559	2559	0.0	15183	15183	0	0.0
21	1821	3552	2564	2573	5.0	15180	15182	3	52.6
37	1810	3551	2566	2582	8.8	15180	15181	4	162.2
56	1813	3549	2563	2588	13.3	15184	15181	7	371.5
74	1804	3548	2565	2597	17.6	15185	15182	9	649.8
111	1587	3542	2612	2661	25.6	15124	15173	13	1387.8
146	1507	3538	2627	2692	32.1	15105	15159	15	2229.6
214	1365	3525	2647	2743	43.8	15068	15136	19	4330.9
541	1004	3481	2682	2925	92.8	14991	15071	26	22824.0
670	881	3466	2690	2992	110.0	14964	15053	24	33263.6

D847 continued

D	T	S	σ_t	σ_{stp}	ΣΔD	C	C_m	K	ΣΔX
839	750	3453	2700	3079	131.5	14941	15033	18	49445.5
1017	660	3449	2709	3169	152.8	14935	15016	11	69256.6
1320	488	3450	2731	3331	185.1	14916	14995	-4	107072.3
1649	348	3454	2749	3500	214.4	14911	14979	-23	150498.7
2039	258	3462	2764	3691	243.6	14940	14969	-43	204306.9

D848

D	T	S	σ_t	σ_{stp}	ΣΔD	C	C_m	K	ΣΔX
0	1790	3542	2564	2564	0.0	15167	15167	0	0.0
16	1790	3544	2565	2572	3.8	15170	15169	2	30.2
31	1812	3543	2559	2573	7.3	15178	15171	4	114.2
47	1794	3543	2563	2584	11.2	15176	15173	5	263.8
63	1769	3352	2576	2604	14.9	15172	15174	7	467.9
94	1572	3542	2615	2657	21.3	15118	15164	10	974.1
126	1510	3540	2628	2684	27.2	15103	15150	13	1623.7
203	1345	3522	2649	2740	40.3	15060	15124	17	3775.9
250	1300	3516	2654	2765	47.8	15052	15111	19	5470.1
317	1199	3507	2666	2808	58.0	15026	15096	20	8360.8
383	1092	3491	2674	2846	67.5	14998	15081	21	11682.5
736	804	3459	2697	3029	114.4	14945	15029	14	37924.7
957	681	3450	2707	3140	141.2	14933	15008	5	60615.8
1315	428	3449	2737	3337	178.3	14889	14981	-16	102759.7

D849

D	T	S	σ_t	σ_{stp}	ΣΔD	C	C_m	K	ΣΔX
0	1820	3547	2560	2560	0.0	15176	15176	0	0.0
18	1819	3548	2561	2569	4.3	15179	15178	2	38.8
35	1834	3548	2557	2573	8.4	15187	15180	4	147.5
53	1816	3549	2563	2586	12.7	15183	15182	6	338.4
106	1528	3540	2624	2671	23.9	15105	15163	12	1225.9
140	1486	3536	2630	2692	30.0	15096	15148	14	1978.1
210	1372	3525	2646	2739	42.0	15069	15126	18	4069.8
350	1170	3500	2666	2823	63.8	15022	15094	22	10175.9
456	1054	3487	2678	2883	79.0	14997	15074	22	16292.3
555	921	3469	2686	2936	92.4	14962	15057	21	23073.7
682	823	3459	2694	3002	108.8	14945	15038	17	33237.6
826	744	3452	2700	3073	126.8	14936	15020	11	46786.0
1055	597	3449	2718	3196	153.2	14916	15000	-0	71660.7
1397	414	3451	2740	3377	186.7	14898	14977	-21	112694.9
1777	290	3460	2760	3570	216.8	14909	14961	-46	160385.9
1969	249	3463	2766	3663	229.8	14924	14957	-57	184906.1

D850

D	T	S	σ_t	σ_{stp}	ΣΔD	C	C_m	K	ΣΔX
0	1712	3501	2551	2551	0.0	15139	15139	0	0.0
25	1678	3493	2553	2564	6.2	15133	15136	2	77.3
50	1672	3498	2558	2580	12.3	15135	15135	4	306.9
74	1443	3520	2627	2660	17.4	15071	15124	6	620.1
99	1386	3521	2640	2684	21.7	15056	15109	7	993.0
149	1279	3510	2653	2720	29.7	15027	15086	9	1990.7
200	1205	3501	2661	2750	37.5	15008	15069	9	3345.1
300	1066	3487	2675	2811	51.8	14975	15043	9	6924.1
391	959	3474	2684	2860	64.0	14949	15024	6	11135.5
490	855	3462	2691	2913	76.7	14925	15006	2	16717.3
637	756	3455	2701	2990	94.5	14910	14986	-6	26806.8
777	661	3450	2710	3063	110.6	14895	14971	-15	38162.6
874	515	3446	2725	3170	131.2	14868	14953	-31	56150.9
1214	387	3451	2743	3299	152.6	14856	14935	-53	79605.4
1469	310	3457	2755	3428	172.0	14866	14922	-77	105581.2
1920	232	3464	2768	3644	201.9	14909	14914	-110	156338.7
2404	192	3469	2775	3866	231.5	14973	14919	-129	220302.3

D851

D	T	S	σ_t	σ_{stp}	ΣΔD	C	C_m	K	ΣΔX
0	1675	3498	2558	2558	0.0	15128	15128	0	0.0
15	1672	3498	2558	2565	3.6	15130	15129	1	27.2
31	1679	3500	2558	2572	7.5	15134	15130	3	116.2
46	1722	3481	2533	2554	11.3	15148	15134	4	263.1
53	1275	3481	2631	2655	12.8	15006	15126	4	339.2
106	1125	3479	2659	2706	21.4	14963	15055	4	1017.0
242	983	3469	2676	2785	40.7	14934	14995	-1	4372.1
396	873	3460	2687	2866	60.9	14916	14968	-9	10818.6
483	835	3456	2690	2909	71.9	14915	14958	-13	15671.9
911	589	3447	2717	3131	121.6	14888	14932	-42	50295.6
1512	311	3456	2755	3446	175.1	14873	14911	-89	115095.5
1938	234	3463	2767	3651	204.0	14913	14907	-120	164939.1

D852

D	T	S	σ_t	σ_{stp}	ΣΔD	C	C_m	K	ΣΔX
0	1683	3488	2548	2548	0.0	15129	15129	0	0.0
25	1669	3489	2552	2563	6.2	15130	15129	2	77.9
49	1667	3490	2553	2575	12.2	15132	15130	4	297.8
74	1430	3486	2603	2636	17.8	15062	15119	6	642.2
98	1265	3475	2629	2673	22.3	15010	15099	6	1031.6
147	1208	3486	2648	2714	30.5	15000	15067	7	2040.9
200	1119	3481	2661	2751	38.7	14976	15046	6	3456.0
289	1008	3473	2675	2805	51.4	14951	15021	4	6564.0
388	934	3464	2680	2856	64.8	14939	15001	0	11110.4
484	864	3461	2689	2908	77.4	14927	14988	-4	16578.5
628	791	3454	2695	2979	95.5	14922	14973	-11	26646.6
772	700	3450	2705	3055	112.8	14910	14962	-19	38787.6
962	593	3449	2718	3155	134.0	14898	14951	-31	57102.9
1207	435	3449	2737	3287	157.8	14874	14938	-50	82933.8
1458	347	3454	2750	3416	178.6	14880	14927	-71	110735.3

D853

D	T	S	σ_t	σ_{stp}	ΣΔD	C	C_m	K	ΣΔX
0	1688	3486	2545	2545	0.0	15130	15130	0	0.0
19	1656	3487	2554	2562	4.7	15124	15127	2	45.1
37	1577	3486	2571	2588	9.0	15103	15120	3	165.2
56	1464	3488	2598	2623	13.2	15070	15109	4	357.6
74	1393	3496	2619	2652	16.7	15052	15097	5	586.4
111	1336	3505	2638	2687	23.3	15039	15080	6	1193.1
144	1287	3507	2649	2714	28.7	15029	15069	7	1882.3
206	1159	3492	2662	2755	38.2	14993	15052	7	3544.2
266	1058	3479	2671	2791	46.8	14965	15035	6	5585.9
340	972	3471	2679	2833	57.0	14946	15018	4	8666.5
447	920	3464	2682	2884	71.3	14943	15000	0	14289.4
576	857	3458	2688	2948	88.3	14940	14987	5	22984.5

D854

D	T	S	σ_t	σ_{stp}	ΣΔD	C	C_m	K	ΣΔX
0	1635	3489	2560	2560	0.0	15114	15114	0	0.0
23	1621	3488	2563	2573	5.5	15113	15114	2	63.1
46	1432	3478	2597	2617	10.6	15057	15100	3	239.2
69	1357	3481	2615	2646	15.1	15036	15082	4	500.6
92	1286	3492	2638	2679	19.3	15017	15068	4	831.7
138	1173	3485	2654	2716	26.7	14986	15046	4	1682.6
182	1127	3484	2662	2744	33.3	14978	15030	4	2740.9
276	1033	3477	2673	2798	46.7	14957	15009	2	5812.3
361	948	3466	2679	2843	58.3	14939	14995	-1	9500.5
594	794	3454	2694	2963	88.3	14918	14969	-12	23964.5
721	735	3451	2700	3027	103.8	14916	14960	-19	34052.0
914	603	3449	2717	3132	125.7	14894	14948	-32	51899.9
1397	359	3453	2748	3386	170.4	14875	14926	-69	103560.5
1855	246	3463	2766	3613	203.0	14903	14917	-103	156662.4
2346	197	3468	2774	3839	233.6	14965	14921	-124	220834.9

D	T	S	σt	σstp	ΣΔD	C	Cm	K	ΣΔX
D855									
0	1630	3489	2561	2561	0.0	15113	15113	0	0.0
24	1632	3490	2562	2572	5.7	15117	15115	2	68.7
48	1504	3484	2586	2607	11.2	15081	15107	3	265.4
72	1292	3490	2635	2667	15.8	15016	15087	4	543.9
96	1235	3494	2649	2693	19.8	15002	15068	4	874.0
144	1155	3486	2658	2723	27.1	14981	15042	4	1757.8
196	1037	3471	2668	2757	34.7	14945	15021	3	3044.7
294	916	3461	2681	2814	48.1	14916	14991	-2	6318.6
379	851	3457	2688	2860	59.0	14905	14973	-7	9996.1
473	826	3456	2691	2905	70.8	14910	14960	-13	15015.6
615	763	3453	2698	2977	88.2	14910	14948	-21	24489.8
748	689	3450	2706	3046	103.8	14901	14941	-30	35140.5
930	598	3447	2716	3139	124.0	14895	14932	-42	52079.7
1167	476	3447	2730	3262	148.0	14884	14924	-59	77214.1
1861	242	3462	2765	3615	203.2	14903	14912	-109	160749.8
2340	196	3467	2773	3836	233.2	14965	14917	-130	223800.1
D856									
0	1593	3474	2558	2558	0.0	15100	15100	0	0.0
20	1596	3474	2558	2566	4.8	15104	15102	1	48.4
41	1591	3474	2559	2577	9.9	15106	15103	3	203.6
61	1510	3477	2579	2606	14.6	15084	15100	4	440.9
82	1269	3480	2632	2669	18.7	15008	15087	5	738.8
181	1212	3499	2658	2739	34.8	15009	15044	5	2854.2
257	1055	3478	2670	2786	45.9	14962	15027	5	5286.7
339	962	3467	2678	2831	57.3	14942	15008	2	8659.8
423	897	3461	2684	2875	68.4	14929	14994	-2	12922.3
549	813	3454	2691	2940	84.6	14918	14978	-8	20792.5
681	744	3450	2698	3007	101.0	14913	14966	-16	30826.6
859	645	3446	2709	3099	121.8	14903	14954	-27	46907.7
1103	513	3446	2725	3228	147.8	14890	14941	-44	72394.3
1356	397	3450	2741	3360	171.2	14883	14931	-63	101168.2
D857									
0	1677	3477	2541	2541	0.0	15126	15126	0	0.0
18	1665	3476	2543	2551	4.6	15125	15125	2	41.6
36	1649	3475	2546	2562	9.2	15123	15125	3	165.6
54	1693	3474	2535	2559	13.9	15140	15127	5	375.8
72	1210	3474	2639	2671	17.8	14986	15111	5	620.6
108	1168	3487	2657	2705	23.5	14979	15068	5	1134.2
144	1092	3480	2665	2730	28.8	14958	15043	4	1799.6
280	948	3463	2677	2804	47.6	14926	14994	-1	5801.2
350	877	3458	2685	2843	56.8	14910	14979	-5	8702.5
440	828	3454	2689	2889	68.3	14906	14964	-10	13225.5
528	783	3453	2695	2935	79.2	14903	14954	-16	18497.7
657	716	3451	2703	3002	94.5	14987	14944	-25	27575.9
816	613	3448	2715	3086	112.2	14882	14933	-36	40597.5
979	539	3447	2723	3169	129.0	14879	14924	-49	55710.6
1316	379	3452	2745	3346	159.5	14869	14911	-78	90715.7
D858									
0	1613	3464	2546	2546	0.0	15105	15105	0	0.0
18	1615	3466	2547	2555	4.5	15109	15107	1	40.9
35	1625	3468	2546	2562	8.8	15115	15109	3	155.0
53	1480	3465	2576	2600	13.2	15071	15104	4	344.7
106	1202	3472	2639	2686	23.6	14989	15067	5	1172.8
134	1121	3472	2654	2714	28.1	15966	15048	4	1712.6
184	1042	3475	2670	2754	35.4	14946	15023	3	2876.4
245	1002	3474	2677	2787	43.7	14941	15003	1	4666.2
295	965	3470	2680	2813	50.4	14935	14992	-2	6468.6

D	T	S	σt	σstp	ΣΔD	C	Cm	K	ΣΔX
D858 continued									
384	903	3464	2685	2859	62.1	14926	14978	-6	10418.8
472	805	3456	2694	2908	73.1	14902	14966	-11	15136.8
586	634	3448	2712	2980	86.0	14853	14949	-20	21973.3
998	449	3449	2735	3192	125.6	14846	14908	-61	53335.2
D859									
0	1546	3459	2557	2557	0.0	15083	15083	0	0.0
25	1555	3463	2558	2569	6.1	15091	15087	1	75.6
50	1256	3476	2631	2654	11.2	14999	15066	2	270.2
75	1206	3489	2651	2685	15.3	14988	15042	2	526.6
100	1201	3497	2658	2703	19.1	14991	15029	2	858.8
150	1089	3481	2667	2734	26.4	14957	15010	1	1767.2
200	1012	3472	2673	2764	33.4	14936	14994	-1	2985.6
400	866	3460	2688	2869	59.7	14915	14960	-11	10877.2
500	812	3455	2692	2919	72.2	14909	14950	-17	16511.8
648	710	3450	2703	2998	89.9	14893	14939	-26	26687.1
791	632	3448	2712	3072	106.0	14886	14930	-37	38224.7
990	530	3448	2725	3175	126.6	14878	14920	-52	56568.2
1241	394	3451	2742	3310	149.0	14864	14910	-74	81109.2
1500	311	3457	2755	3442	169.0	14872	14903	-97	108519.2
1982	225	3464	2768	3673	201.0	14916	14901	-131	164498.7
D860									
0	1549	3439	2541	2541	0.0	15082	15082	0	0.0
19	1524	3448	2554	2562	4.8	15078	15080	1	45.4
37	1460	3450	2569	2586	9.1	15061	15075	2	165.9
56	1339	3454	2598	2623	13.2	15025	15064	2	359.1
74	1289	3456	2609	2642	16.8	15012	15053	3	593.1
146	1207	3460	2628	2694	30.3	14996	15029	3	2070.5
212	1050	2461	2658	2754	41.2	14952	15012	2	4018.7
284	942	3458	2674	2803	51.6	14923	14993	-1	6597.8
393	883	3455	2681	2859	66.3	14919	14973	-7	11580.8
492	818	3451	2688	2911	79.2	14910	14961	-13	17284.5
624	751	3447	2695	2978	95.7	14906	14950	-21	26531.5
D861									
0	1571	3465	2556	2556	0.0	15092	15092	0	0.0
22	1564	3468	2560	2570	5.3	15093	15093	1	58.5
41	1532	3470	2569	2587	9.8	15087	15091	2	199.9
43	1373	3464	2598	2618	10.2	15035	15090	3	218.3
61	1244	3465	2625	2653	13.7	14995	15068	3	397.7
160	1008	3461	2665	2738	29.7	14927	15002	0	2161.5
219	983	3465	2673	2772	37.9	14928	14982	-3	3730.1
292	885	3461	2686	2818	47.6	14904	14965	-7	6189.8
406	845	3451	2684	2868	62.2	14905	14948	-14	11289.1
509	787	3446	2689	2920	75.4	14900	14939	-21	17347.3
674	744	3446	2695	3001	96.1	14911	14931	-31	29606.8
D862									
0	1544	3456	2555	2555	0.0	15082	15082	0	0.0
22	1507	3453	2561	2571	5.3	15073	15078	1	58.4
45	1480	3458	2571	2591	10.7	15070	15075	2	239.3
67	1277	3480	2630	2660	15.2	15010	15063	3	488.8
90	1088	3460	2651	2691	19.0	14945	15041	2	787.0
135	1007	3459	2664	2725	25.7	14923	15005	0	1545.5
181	968	3458	2670	2752	32.2	14917	14984	-2	2574.7
348	865	3454	2683	2841	54.7	14905	14949	-12	8514.3
430	841	3453	2686	2881	65.3	14909	14941	-17	12630.0

D	T	S	σt	σstp	ΣΔD	C	C_m	K	ΣΔX
D862 continued									
547	788	3452	2694	2942	80.0	14908	14934	-24	19831.5
666	725	3448	2700	3002	94.5	14902	14929	-32	28608.1
820	652	3449	2710	3083	112.3	14899	14923	-42	41823.6
1037	538	3448	2724	3196	135.2	14889	14917	-57	63143.2
1285	396	3451	2742	3329	158.0	14871	14910	-77	89582.5
D863									
0	1557	3449	2547	2547	0.0	15086	15086	0	0.0
22	1497	3447	2559	2569	5.4	15070	15078	1	59.7
44	1473	3451	2567	2587	10.7	15067	15073	2	232.2
66	1372	3434	2575	2605	15.7	15036	15066	3	511.0
88	1180	3465	2637	2677	20.1	14978	15051	3	845.6
132	1030	3457	2658	2718	27.0	14932	15019	2	1613.7
168	968	3457	2669	2745	32.2	14914	14998	-0	2393.7
254	895	3457	2681	2796	43.8	14901	14967	-6	4841.5
415	827	3450	2686	2874	64.6	14900	14941	-16	11795.0
535	806	3449	2689	2931	80.0	14913	14933	-24	19105.0
654	764	3448	2694	2990	95.1	14916	14930	-31	28072.0
825	655	3449	2710	3085	115.4	14901	14925	-41	43063.2
1053	494	3448	2729	3210	138.9	14873	14917	-58	65168.1
1296	399	3452	2743	3335	160.5	14874	14909	-79	90540.5
1740	264	3460	2762	3557	193.8	14893	14902	-113	141032.0
D864									
0	1599	3482	2563	2563	0.0	15103	15103	0	0.0
25	1557	3479	2570	2581	5.8	15094	15098	2	73.0
49	1457	3471	2586	2608	11.2	15065	15089	3	271.4
74	1384	3473	2603	2636	16.4	15046	15078	4	592.0
123	1193	3469	2638	2693	25.5	14989	15054	4	1483.3
175	1085	3462	2653	2732	33.9	14958	15030	3	2740.0
225	1036	3462	2661	2763	41.5	14949	15013	2	4262.3
319	968	3462	2673	2817	55.0	14940	14992	-2	7945.9
416	873	3456	2684	2872	68.2	14918	14978	-6	12764.9
512	827	3454	2689	2921	80.6	14917	14966	-11	18514.7

APPENDIX III

THE POSSIBILITY OF FORMING EDDIES WHEN MEANDERS MEET A SLOPING BOTTOM TOPOGRAPHY

I would like to examine under what conditions meanders with a southwards phase velocity grow on the northern slope of a bathymetric feature like the Chatham Rise. The occurrence of these growing meanders then would provide a mechanism for forming the small eddies observed on the head of the Hikurangi Trench. Consider a meridional current flowing in a southerly direction with a velocity V, V being negative. For a homogeneous ocean the geostrophic current in this steady flow is given by

$$+ fV = g \frac{\partial \eta}{\partial x}$$

where η is the surface elevation. Now suppose there is a barotropic perturbation having velocity components u, v (u positive to the east and v to the north) and an elevation h in the flow, with the cross-stream change in the perturbed quantities being small compared to the long-stream changes (i.e. the meanders are produced by a pulse which has $\partial/\partial x$ h, u, v, $\doteq$ o). We are going to examine what happens to a meander, which is generated near East Cape, when it meets the decreasing depth of the Chatham Rise; in this simple model the slope of the western side of the Hikurangi Trench will be neglected, i.e. $\partial D/\partial x \doteq$ o. This model is similar to the two-layer model discussed by Stommel (1965), but with the slope of the bottom used as one stability criterion, rather than the surface velocity which, in Stommel's model, was related to the slope of the interface between the two layers (*see* Stommel 1965, p.129, p.196).

The perturbation components of the equations of motion, neglecting friction, may be written in this case as

$$\left(\frac{\partial}{\partial t} + V \frac{\partial}{\partial y}\right) u - f v = 0$$

$$\left(\frac{\partial}{\partial t} + V \frac{\partial}{\partial y}\right) v + fu = - g \frac{\partial h}{\partial y}$$

where it has been assumed that

$$v \frac{\partial V}{\partial y} << V \frac{\partial v}{\partial y}$$

and the perturbation continuity equation is

$$\left(\frac{\partial}{\partial t} + V \frac{\partial}{\partial y}\right) h + v \frac{\partial D}{\partial y} + h \frac{\partial V}{\partial y} + D \frac{\partial v}{\partial y} = 0$$

where D is the depth of the water. Assuming that the perturbed quantities have the form

$$e^{i(\ell y - \omega t)} \qquad \text{e.g. } u = u_0 e^{i(\ell y - \omega t)}$$

the above equations can be written as

$$(-i\omega + Vi\ell)\, u - fv = 0 \tag{26}$$

$$(-i\omega + Vi\ell)\, v + fu = -i g \ell h \tag{27}$$

$$(-i\omega + Vi\ell) h + vK + hJ + Di\ell v = 0 \tag{28}$$

where $K = \partial D/\partial y$, $J = \partial V/\partial y$ and $i = \sqrt{-1}$.

Multiplying equation 26 by $(-i\omega + Vi\ell)$ and adding equation 27 multiplied by f gives

$$u = -\frac{i g f \ell h}{B}$$

where $B = f^2 - \omega^2 - V^2\ell^2 + 2 V \omega \ell$.

Similarly, multiplying equation 27 by $(-i\omega + Vi\ell)$ and subtracting equation 26 multiplied by f, gives

$$v = \frac{g \ell h \ (V\ell - \omega)}{B}$$

Substituting for u and v in equation 28 we have

$$i(V\ell - \omega) h + \frac{g\ell h \ (V\ell-\omega) K}{f^2 - (V\ell-\omega)^2} + hJ + \frac{i g D \ell^2 h \ (V\ell-\omega)}{f^2 - (V\ell-\omega)^2} = 0$$

Now with $\omega = \theta + i\nu$, $V\ell - \theta = \Phi$, $V\ell - \omega = \Phi - i\nu$ the above equation becomes

$$i(\Phi-i\nu) h + \frac{Kg\ell h(\Phi-i\nu)}{f^2-\Phi^2+\nu^2+2i\nu\Phi} + hJ + \frac{igD\ell^2 h(\Phi-i\nu)}{f^2-\Phi^2+\nu^2+2i\nu\Phi} = 0$$

or $i\,(\Phi hA + 2\nu\Phi\ (\nu h + hJ) + g D \ell^2 h \Phi - \nu K g \ell h)$

$$- 2\nu\Phi^2 h + A(\nu h + hJ) + K g \ell h \Phi + g D \ell^2 h \nu = 0$$

$$\text{where } A = f^2 - \Phi^2 + \nu^2$$

For this relationship to be satisfied both the real and imaginary parts must be zero, i.e.

$$\Phi h A + 2 \nu \Phi\ (\nu h + hJ) + g D \ell^2 h \Phi - \nu K g \ell h = 0$$

$$- 2 \nu \Phi^2 h + A(\nu h + hJ) + K g \ell h \Phi + g D \ell^2 h \nu = 0$$

Looking at the imaginary part we have

$$\Phi h(f^2-\Phi^2+\nu^2) + 2\nu\Phi\ (\nu h + hJ) + gD\ell^2\Phi h - \nu K g \ell h = 0$$

and for $h \neq$ o this reduces to

$$3\nu^2\Phi + \nu\,(2\Phi J - Kg\ell) + gD\ell^2\Phi + \Phi\,(f^2 - \Phi^2) = 0$$

which has solutions

$$\nu = \frac{-2\Phi J + Kg\ell \pm \sqrt{4\Phi^2 J^2 + K^2 g^2 \ell^2 - 4Kg\ell\Phi J - 12\Phi(gD\ell^2\Phi + \Phi(f^2-\Phi^2))}}{6\Phi}$$

The continuity equation for steady flow is

$$D\frac{\partial V}{\partial y} + V\frac{\partial D}{\partial y} \hat{=} 0 \quad \text{i.e.} \quad K = -\frac{D}{V}J \tag{29}$$

Substituting for J in the above equation gives

$$\begin{aligned} \nu &= \frac{1}{6\Phi}\left[\frac{KV}{D}\left(2\Phi + \frac{Dg\ell}{V}\right) \pm \sqrt{F^2 - 12\Phi^2\,(gD\ell^2 + f^2 - \Phi^2)}\,\right] \\ &= \frac{1}{6\Phi}\left[F \pm \sqrt{F^2 - 12\Phi^2\,(gD\ell^2 + f^2 - \Phi^2)}\,\right] \end{aligned} \tag{30}$$

$$\text{where } F = \frac{KV}{D}\left(2\Phi + \frac{Dg\ell}{V}\right)$$

For ν positive the meander grows with time. In the region of interest, the head of the Hikurangi Trench, V is negative and K is positive. Taking ℓ negative, (i.e. the meander travelling southward) if $|V\ell| > |\Theta|$

then $\Phi = V\ell - \Theta > 0$

$$F = \frac{KV}{D}\left(2\Phi + \frac{Dg\ell}{V}\right)$$

is negative and equation 30 has the form

$$\nu = a\left(1 \pm \sqrt{1 - \frac{b}{F^2}}\right)$$

$$\text{where } a = \frac{F}{6\Phi} < 0$$

$$b = 12\,\Phi^2\,[f^2 + \ell^2\,(gD - (V - \frac{\Theta}{\ell})^2)]$$

As $|V| > |\frac{\Theta}{\ell}|$ and $gD > V^2$ (i.e. for $g = 10\,\mathrm{m\,s^{-1}}$, and $D = 10^3\,\mathrm{m}$, V would have to be greater than $100\,\mathrm{m\,s^{-1}}$ for this inequality not to hold), b is positive. Therefore any real values of ν are negative and the corresponding meanders decrease in size. The meanders decrease in size if their absolute phase velocity is less than the absolute mean current velocity.

For the case with the absolute phase velocity of the meanders greater than the absolute mean current velocity, Φ is negative,

$$\nu = \frac{F}{6\Phi}\left(1 \pm \sqrt{1 - \frac{b}{F^2}}\right)$$

and at least one value of ν is positive if F is negative, i.e. for K positive the meanders grow if

$$\left|\frac{Dg\ell}{V}\right| > |2\Phi|$$

$$\text{or } \left|\frac{Dg\ell}{V}\right| > 2\,|V - c| \quad \text{where } C = \frac{\Theta}{\ell}$$

For long waves the phase velocity C_0 is given by $C_0{}^2 = g\,D$ and the above condition becomes

$$\left|\frac{C_0{}^2}{V}\right| > |2\,(V - c)|$$

or, as $|c| > |V|$, a condition for the meanders to grow on a bottom sloping upwards in the direction of the meanders is for

$$\left|\frac{C_0{}^2}{V}\right| > 2\,|c|$$

Instead of evaluating equation 30 in detail we will examine the relative magnitude of the term $h\,\partial V/\partial y$ in the perturbed continuity equation to the terms [A] : $V\,\partial h/\partial y$, [B] : $v\,\partial D/\partial y$, [C] : $D\,\partial v/\partial y$.

The relative magnitude of the term $h\,\partial V/\partial y$ to these terms are

$$[A] \quad \frac{hVK}{DV\frac{\partial h}{\partial y}} \hat{=} \frac{K}{\ell D} \hat{=} \frac{10^{-5}}{\ell}$$

$$[B] \quad \frac{hVK}{DvK} \hat{=} \frac{hV}{Dv} \hat{=} \frac{h}{v}\,10^{-3}$$

$$[C] \quad \frac{hVK}{D^2\frac{\partial v}{\partial y}} = \frac{hVK}{D^2\ell v} = \frac{h}{\ell v}\,10^{-8}$$

where extreme values for the region off the east coast of New Zealand of $V = 1\,\mathrm{m\,s^{-1}}$, $D = 10^3\,\mathrm{m}$, $K = 10^{-2}$ have been used to make the term hVK/D large. For the extreme value of $h = 0.5\,\mathrm{m}$, the term $h\,\partial V/\partial y$ is at least as large as one of the others if either

$$\ell \leqslant 10^{-5}\mathrm{m^{-1}} \quad \text{or} \quad v \leqslant 5 \times 10^{-4}\mathrm{m\,s^{-1}}.$$

Of these, the former is the most likely (i.e. ℓ - $10^{-5}\,\mathrm{m^{-1}}$) and then the terms in the perturbation continuity equation have the values

$$h\frac{\partial V}{\partial y} = 5 \times 10^{-6}, \qquad V\frac{\partial h}{\partial y} = -5 \times 10^{-6}$$

$$v\frac{\partial D}{\partial y} = -10^{-2} \times v, \qquad D\frac{\partial V}{\partial y} = -10^{-2}$$

i.e. neither the first or second terms would be significant. Therefore taking

$$\ell \leqslant 10^{-5}\,\mathrm{m}$$

i.e. the scale of the motion must be less than 600 km (approx.) (or this scale is small compared to the scale of the bathymetry), the term $h\,\partial V/\partial y$ can be neglected and the perturbation continuity equation can be written as

$$\left(\frac{\partial}{\partial t} + V\frac{\partial}{\partial y}\right)h + v\frac{\partial D}{\partial y} + D\frac{\partial v}{\partial y} = 0$$

which, for perturbed quantities of the form $e^{i(\ell y - \omega t)}$, reduces to

$$(-i\omega + Vi\ell)h + Kv + i\,\ell\,D\,v = 0$$

Substituting for u, v, (from p.94) in this equation we have

$$i(V\ell - \omega)h + \frac{K\,\ell\,g\,(V\ell - \omega)h}{B} + \frac{i\,\ell^2\,Dg\,(V\ell - \omega)h}{B} = 0$$

where $B = f^2 - \omega^2 - V^2\,\ell^2 + 2\,\omega\,V\,\ell$

If $V\ell \neq \omega$ and $h \neq 0$ we have

$$(f^2 - \omega^2 - V^2\ell^2 + 2V\omega\ell) + \ell^2 Dg - iK\ell g = 0$$

Substituting $\omega = \Theta + i\nu$, $\ell = m + in$

i.e. ω and ℓ are complex, gives

$$f^2 - \Theta^2 + \nu^2 - V^2m^2 + V^2n^2 + 2V\Theta m - 2V\nu n + m^2Dg - n^2Dg + Kng$$

$$+ i(-2\Theta\nu - 2V^2mn + 2V\nu m + 2V\Theta n + 2mnDg - mKg) = 0$$

For this equation to be satisfied, both the real and imaginary parts must be zero, i.e.

$$Kng + f^2 - V^2m^2 - \Theta^2 + \nu^2 + V^2n^2 + 2V\Theta m - 2V\nu n + (m^2 - n^2)Dg = 0 \qquad (31)$$

and

$$2V\nu m + 2V\Theta n + 2mnDg - mKg - 2\Theta\nu - 2V^2mn = 0 \qquad (32)$$

For the case $n = 0$, the above equations reduce to

$$f^2 - V^2m^2 - \Theta^2 + \nu^2 + 2V\Theta m + m^2Dg = 0 \qquad (33)$$

$$-2\nu\Theta + 2V\nu m - Kmg = 0 \qquad (34)$$

From equation 34 we have

$$\nu = \frac{Kgm}{2(Vm-\Theta)} = \frac{Kg}{2(V-c)}$$

i.e. for a meander travelling slower than the mean current, the meander grows with time if the mean current velocity and the slope of the sea bottom have the same signs and decreases with time if they have opposite signs. For a meander travelling faster than the mean current, the meander grows with time if the slope of the sea bottom and the meander velocity have opposite signs (i.e. a meander travelling into shallower water) and decreases with time if they have the same signs. If the sea floor is flat the meanders do not grow with time.

For the case $\nu = 0$, equation 32 reduces to

$$2V\Theta n + 2mnDg - mKg - 2V^2mn = 0$$

$$n = \frac{mKg}{2V\Theta + 2mDg - 2V^2m}$$

$$= \frac{Kg}{2Vc + 2Dg - 2V^2} = \frac{Kg}{2Vc + 2C_0^2 - 2V^2}$$

If the mean current speed is greater than the long wave speed (i.e. in very shallow water) and the phase speed of the meanders is in the opposite direction to the mean current velocity, the meanders decrease in space if they travel into shallower water, and grow in space if they travel into deeper water. For the usual case, where the long wave speed is greater than the mean current speed, and the current and meander velocities are in the same direction, the meanders grow in space if they travel into shallower water and decrease in space if they travel into deeper water. Because the East Cape Current flows southwards into the head of the Hikurangi Trench, where the slope of the bottom is positive, any southwards directed meanders formed will grow with time if the absolute meander velocity is greater than the mean current velocity and the scale of the meanders is such that

$$\left|\frac{K}{\ell D}\right| << 1.$$

In this case, as the meanders are travelling into shallower water and are in the same direction as the mean current, they will also grow in space.

If the scale of the meanders is such that

$$\left|\frac{K}{\ell D}\right| \nless 1,$$

for the case in the Hikurangi Trench, where K is positive and V and ℓ are negative, the meanders will grow with time if the relationship

$$\left|\frac{C_0^2}{V}\right| > 2|C|$$

holds, where V is the mean current velocity, C_0 the long wave phase speed and C the speed of the meanders.

The above analysis shows that one possible mechanism for the formation of the eddies off the east coast of New Zealand is for meanders in the flow generated by an increased transport of water around East Cape to grow in size and form eddies as they travel into shallower water in the head of the Hikurangi Trench. At present there have been no measurements from which the presence, or otherwise, of meanders in the East Cape Current can be shown and until such measurements are made the role, if any, of the above mechanism cannot be evaluated.

A. R. SHEARER, GOVERNMENT PRINTER,
WELLINGTON, NEW ZEALAND—1975